Title

A Gene Encoding an Architectural RNA, *hsrω*, is a Host Genetic Modifier of Cancer Progression in *Drosophila*

Anjali Bajpai[1,2*], Sushmita Kundu[1], Ravi Kant Pandey[1,3], Bushra Ateeq[1,2], Subhash C. Lakhotia[4], Pradip Sinha[1,2]

Running title

***hsrω* arcRNA-dependent cancer resistance**

Keywords

Architectural RNA, Host genetics, Cell homeostasis, Cancer, *Drosophila*

[1]Biological Sciences and Bioengineering, Indian Institute of Technology Kanpur, Kanpur 208016, India.
[2]The Mehta Family Centre for Engineering in Medicine, Indian Institute of Technology Kanpur, Kanpur 208016, India.
[3] Current Address: Biocon Biologics Limited, Bommasandra Industrial Area, Bengaluru 560099, India
[4]Cytogenetics Laboratory, Department of Zoology, Institute of Science, Banaras Hindu University, Varanasi, 221005, India.

* Corresponding author: Anjali Bajpai, anjalii@iitk.ac.in
ORCID:
A. Bajpai: 0000-0002-5645-2466
B. Ateeq: 0000-0003-4682-9773
S. C. Lakhotia: 0000-0003-1842-8411
P. Sinha: 0000-0002-9202-6050

Abstract

Genetic variations among individuals within a population, or host genetics, determine disease susceptibility or resistance. Here we show that heterozygosity of *hsrω*, a gene coding for a long noncoding architectural RNA (arcRNA), displays cancer susceptibility in *Drosophila.* Imaginal epithelia mutant for a null allele of *hsrω, hsrω*^{66} exhibits chronic stress, marked by loss of growth and proteostasis, besides cell death. Imaginal epithelia of larvae heterozygous for *hsrω*^{66} also show cellular stress, but conditionally: for instance, upon heat shock. Somatic clones displaying loss of Lgl tumor suppressor in such stress-sensitive imaginal epithelia of *hsrω*^{66} heterozygotes develop into metastatic tumors, unlike those induced in wild type epithelia wherein these are eliminated by intrinsic tumor suppression. Further, cell-autonomous gain or loss of *hsrω* in *lgl* mutant clones, too, results in their tumor progression. Finally, we note a transcriptional increase in human sat III arcRNA, a functional analog of *Drosophila hsrω,* in cancer cell lines. Loss of sat III decreases the viability of cancer cells under stress. Our findings suggest pervasive roles of arcRNA-coding genes as host genetic modifiers of cancer via their regulation of cell homeostasis.

Summary statement

Heterozygosity for *hsrω,* a gene coding for a long noncoding architectural RNA in *Drosophila,* induces hypersensitivity to physiological stress and promotes cancer progression in oncogenically targeted cells.

Introduction

The genetic etiology of cancers is well-recognized. While many cancer-causing, oncogenic mutations have been identified, a far greater number of cancer-modifying genetic alterations are likely to be present in the human genome (Castro-Giner et al., 2015; Turnbull et al., 2018)—including those of its noncoding components (Elliott and Larsson, 2021). Detection of a cancer-modifying gene is readily resolved when its heterozygosity promotes or suppresses the progression of an oncogenically targeted cell (Chenevix-Trench et al., 2007; Datta et al., 2023; Zeng et al., 2019). Cancer represents failed cellular homeostasis (Green, 2022; Miller and Thorburn, 2021) that renders cell intrinsic tumor suppressive mechanisms defunct, leading to the ready transformation of precancerous cells. Thus, host genetic alterations that perturb cellular homeostasis may double as a cancer-modifying event.

Long noncoding RNAs (lncRNAs) are particularly interesting, given their role in cell and nuclear homeostasis (for review, see Constanty and Shkumatava, 2021; Huarte, 2015; Lakhotia et al., 2020). Some of these lncRNAs provide a physical scaffold for the binding of distinct nuclear proteins, thereby forming specialized membraneless phase-separated bodies and are termed

architectural lncRNAs (arcRNAs) (Luo et al., 2021; Nakagawa et al., 2022). Loss of the arcRNA, therefore, results in disruption of associated nuclear bodies. ArcRNAs associate with distinct sets of proteins; for instance, the arcRNA, Nuclear Paraspeckle Assembly Transcript 1 (NEAT1) houses proteins such as PSPC1, SFPQ, and NONO to form highly ordered nuclear paraspeckles with a ribonucleoprotein core (Clemson et al., 2009) and regulates the availability of associated proteins during development and under stress conditions. ArcRNA-associated nuclear bodies are present at steady-state and respond dynamically to physiological changes, developmental signals, and cellular stresses (Daneshvar et al., 2020; for review, see Luo et al., 2021; Nakagawa et al., 2022)

In *Drosophila*, the lncRNA, the heat shock RNA omega, hsrω, displays hallmarks of an architectural RNA (Lo Piccolo and Yamaguchi, 2017; for review, see Nakagawa et al., 2022). The gene *hsrω* codes for multiple large nuclear and cytoplasmic transcripts (Bendena et al., 1989; Lakhotia et al., 2001), of which the larger nuclear transcripts carrying a long stretch of tandem repeats (Fig. 1A, also see (Lakhotia, 2011)) provide a physical scaffold for binding distinct proteins such as the heterogeneous ribonucleoproteins (hnRNPs) and splicing factors to form nucleoplasmic bodies called as omega speckles (Prasanth et al., 2000). The omega speckles regulate the intranuclear trafficking and availability of multiple RNA-binding proteins, splicing factors, and hnRNPs (Prasanth et al., 2000; Singh and Lakhotia, 2015). These membraneless phase-separated omega speckles are completely disrupted in *hsrω* nullosomics (Prasanth et al., 2000), and their structural integrity is strongly compromised upon loss of chromatin remodeling ATPase ISWI activity (Onorati et al., 2011). Upon stress, the *hsrω* undergoes exaggerated transcription from the 93D locus to form stable RNAs that remain associated with the locus, acting as a temporary sink for omega speckle-associated RNA-binding proteins (Prasanth et al., 2000; Singh and Lakhotia, 2015), thereby controlling housekeeping functions such as transcription and translation under stress conditions. Dysregulation of *hsrω* affects mutant flies' overall life-history parameters and exacerbates stress sensitivity (Lakhotia, 2011; Lakhotia et al., 2020)). Keeping these homeostasis roles of the arcRNA-encoding *hsrω* in mind, we hypothesized that *hsrω* could be a potential host genetic modifier of cancer progression in *Drosophila*.

The human satellite III (sat III) lncRNA is a functional analog of hsrω (for review, see (Jolly and Lakhotia, 2006) and displays shared features as an arcRNA (Nakagawa et al., 2022). Reminiscent of *Drosophila hsrω*, , the sat III arcRNA, too, shows active transcription under stress, with the transcribed RNA remaining associated with the locus (Jolly et al., 2004). The sat III RNAs, akin to *hsrω*, act as a physical scaffold to form phase-separated condensates that house nuclear proteins such as HSF1, RNA-binding proteins, and splicing factors to form a large visible nuclear stress body (Goenka et al., 2016; Jolly et al., 2004) under stress conditions.

Given the homeostatic role of arcRNAs, we have taken advantage of the genetic tractability of *Drosophila* to test if *hsrω* could be a host genetic modifier of cancer. We show that

heterozygosity for *hsrω* provides a tumor-permissive host genetic background, such that, epithelial cells with an oncogenic hit override intrinsic tumor suppression and progress to full-blown metastatic tumors. These findings suggest that nuclear arcRNAs act as host genetic modifiers of cancer.

Results

Loss of hsrω *arcRNA inhibits growth, induces cell stress, and results in loss of proteostasis*

Homozygosity for a near-null allele of the arcRNA *hsrω, hsrω*^{66}, which harbors a 1.6 kb deletion in its promoter, results in a substantial loss of *hsrω* transcripts (Johnson et al., 2011; Ray et al., 2019a). *hsrω*^{66} mutants display high lethality during embryonic life and at different stages of larval development, with only a few escapee adults (Lakhotia and Ray, 1996; Mohler and Pardue, 1984). *hsrω*^{66} larvae are growth compromised; their adult organ primordia, like the wing imaginal discs, for instance, were markedly smaller than their heterozygous siblings (*hsrω*^{66}*/TM6B*, referred to here as *hsrω*^{66}/+, Fig. 1B-D) due to their underproliferation (Fig. 1E-G). Further, *hsrω*^{66} somatic clones were smaller than their wild type twin spot clones, revealing their cell-autonomous underproliferation (Fig. 1H-J).

Minute mutants with compromised organ growth (Kongsuwan et al., 1985) display dysregulated protein homeostasis or proteostasis (Baumgartner et al., 2021). *hsrω*^{66} mutants also display aberrant protein translation (Johnson et al., 2009; Johnson et al., 2011). Not surprisingly, our analysis of previously published transcriptomic data from *hsrω*^{66} mutant embryos (Ray et al., 2019a) using Gene Set Enrichment Analysis (GSEA) (Subramanian et al., 2005) revealed perturbations in gene ontology classes like ribosomal structural proteins, response to unfolded protein, protein refolding, regulation of proteolysis, protein stabilization, protein folding chaperone complex, response to heat stress and mitochondrial translation (Fig. S1A-H and Table S1), thereby suggesting their dysregulated proteostasis. Indeed, *hsrω*^{66} wing epithelium displayed a higher abundance of ubiquitin foci—a marker for proteasomal degradation of proteins (Martínez-Férriz et al., 2022)—in contrast to those of their heterozygous siblings (Fig. 1K, L). Likewise, elevated levels of acidic lysosomes—a hallmark of cytoplasmic clearance of damaged proteins and dysfunctional organelles (Settembre et al., 2013) visualized by hydrophobic and pH-sensitive LysoTracker fluorophore were seen in greater abundance in *hsrω*^{66} wing imaginal discs (Fig. 1M) compared to those of their heterozygous siblings (Fig. 1N) suggesting impaired protein turnover and the likelihood of protein aggregates (Martínez-Férriz et al., 2022). Thus, using the ProteoStat dye that fluoresces upon intercalation with protein aggregate-associated quaternary structures (Baumgartner et al., 2021), we noted that *hsrω*^{66} mutant discs displayed a higher abundance of ProteoStat staining (Fig. 1O) than their *hsrω*^{66}/+ heterozygous counterparts (Fig. 1P). Selective downregulation of *hsrω* in the posterior compartment further confirmed loss of proteostasis (Fig. S2A, B) upon perturbations in *hsrω* levels.

Loss of proteostasis impinges upon the functioning of cell organelles such as the mitochondria, thereby leading to a buildup of mitochondrial redox stress and an increase in reactive oxygen species (ROS) levels (Quiles and Gustafsson, 2020). In agreement, using superoxide sensitive, dihydroethdium (DHE) stain (Owusu-Ansah et al., 2008), we observed elevated levels of ROS in *hsrω*^{66} mutant imaginal discs compared to those of their heterozygous siblings (Fig. S2C-D) or upon a selective downregulation of *hsrω* in the posterior wing compartment (Fig. S2E). The c-Jun N-terminal kinase, JNK, signaling pathway is a primary stress response pathway (Stronach and Perrimon, 1999); using a bio-sensor for JNK-mediated AP-1 signaling (TRE-DsRed, (Chatterjee and Bohmann, 2012), we observed a far stronger signal in *hsrω*^{66} mutant discs (Fig. 1Q) in comparison to their wild type counterparts (Fig. 1R). Finally, we noted abundant cell death in *hsrω*^{66} mutant imaginal discs (Fig. 1S) compared with their heterozygous counterparts (Fig. 1T).

Together, these results reveal that imaginal disc epithelia with loss of *hsrω* arcRNA turn chronically stressed and show loss of proteostasis and dysregulated cellular homeostasis.

An hsrω^{66}/+ genetic background is stress-sensitive and conducive to tumor progression.

Given the critical role of *hrsω arcRNA* in cellular homeostasis (Fig. 1), we further asked if its heterozygosity, as in a *hsrω*^{66}/+ genetic background, leads to cellular stress. *hsrω*^{66}/+ larvae and adults display normal development, suggesting that these do not suffer constitutive dysregulation of cellular homeostasis, unlike their *hsrω*^{66} mutant counterparts (Fig. 1). Next, we asked if *hsrω*^{66}/+ larvae are hypersensitive to environmental stress. To test this possibility, we exposed *hsrω*^{66}/+ larvae to a brief period of heat shock (37°C for 15 minutes). We then compared their ROS levels and cytoplasmic clearance of damaged proteins with their wild type counterparts treated likewise. Compared to their wild type counterparts, we noted that imaginal discs of briefly heat-shocked *hsrω*^{66}/+ larvae displayed elevated ROS (Fig. 2A, B) and acidic lysosomes (Fig. 2C, D). Thus, heterozygosity for *hsrω*^{66} represents a stress-sensitive genetic background with conditional loss of cell homeostasis.

Previously, it was shown that oncogenic lesions, like a homozygous loss of the tumor suppressor Lgl, are extruded by cell death in wild type wing imaginal disc epithelium (Fig. 2E-E'''), thereby revealing intrinsic tumor suppression of the latter (see (Igaki et al., 2009)). By contrast, in *M*/+ genetic background, that displays loss of cell proteostasis (Baumgartner et al., 2021), *lgl* clones survive and undergo neoplastic transformation (Khan et al., 2013). We, therefore, reasoned that a somatic clone of *lgl* induced in the stress-sensitive *hsrω*^{66}/+ might survive and transform, reminiscent of their survival in *M*/+ genetic background. We examined *lgl* MARCM (Lee and Luo, 1999) clones induced in early second instar larvae (48 hours after egg laying, AEL) in wild type or *hsrω*^{66} /+ genetic background. The mosaic wing imaginal discs were examined 96 to 120 hr after clone induction (ACI). We noted that *lgl* clones induced in the *hsrω*^{66}/+ genetic background displayed better survival and growth (Fig. 2F, G) compared to their counterparts induced in wild type larvae (Fig. 2E). Nearly one-third of these *lgl* clones (n=32) displayed

neoplastic transformation by 120 hours ACI (Fig. 2F), as revealed by an increase in nuclear volume (Fig. 2F) and disrupted actin cytoarchitecture (Phalloidin, arrow, Fig. 2F) with accompanying loss of a septate junction protein, Fas III (Fig. S3A). Further, these *lgl* clones in *hsrω*^{66}/+ genetic background exhibited excessive cell proliferation (pH3, Fig. 2H). We noted that *lgl* mutant cells abutting the clone boundaries display exaggerated cell death (Fig. 2I)—implying their elimination by cell competition with the neighboring wild type cells (Khan et al., 2013; for review, see Nagata and Igaki, 2018). Some of these neoplastic *lgl* clones also displayed expression of matrix metalloproteinases, MMP1 (Fig. 2J), suggesting their invasive transformation (Khan et al., 2013; Srivastava et al., 2007). Further, *lgl* cells were seen on larval tracheal tubes (GFP, Fig. 2K, arrow), away from the site of their clonal induction in the imaginal discs (Fig. 2K, star), suggesting their metastatic transformations.

Notably, neoplastic transformation of *lgl* clones in the mosaic wing imaginal disc were restricted to the proximal wing imaginal disc (Fig. 2F) – a hallmark of spatial, domain-specific neoplasia reported earlier (Bajpai and Sinha, 2020; Froldi et al., 2010; Khan et al., 2013; Tamori et al., 2016). Distal *lgl* clones, by contrast, underwent cell death (Fig. S3B) and were marked by cellular stress, like perturbed mitochondrial activity (Fig. S3C) or breakdown of lipid droplets (Fig. S3D).

Our results show that imaginal epithelium with loss of the Lgl tumor suppressor display neoplastic, invasive, and, finally, metastatic transformation in a stress-sensitive *hsrω*^{66} host genetic background (Fig. 2L).

Cell-autonomous perturbations in hsrω arcRNA cooperate for lgl tumor progression

lgl mutant clones induced in *hsrω/+* genetic background are marked by heterozygosity of *hsrω* within the clones and neighboring cells. This scenario does not allow a clear resolution of its cell-autonomous role in tumor progression. We thus generated *lgl* clones expressing a *hsrω-RNAi* transgene (Mallik and Lakhotia, 2009) in a wild type genetic background, which rendered Lgl null clones deficient in *hsrω* RNA. We observed that *lgl UAS-hsrω RNAi* clones displayed improved cell survival (Fig. 3A, B) compared to clones with wild type genetic background (see Fig. 2E). Further, about a third (n=28) of these *hsrω*-compromised *lgl* clones were neoplastically transformed, displaying disrupted F-Actin (Phalloidin, Fig. 3A) and loss of Fas III (Fig. S4A), some of which showed invasive transformation (MMP1, Fig. 3C). We noted elevated cell death along clone boundaries (Fig. 3D, white arrow), besides increase in a transcriptional readout of the *Drosophila inhibitor of apoptosis protein1*, *Diap1* (*th-lacZ* enhancer trap, Fig. 3E), a marker of cell death inhibition in transformed proximal clones. *lgl* clones in the distal wing continued to display cell death (Fig. 3D, yellow arrow) as induced in the wild type wing imaginal discs (see Figs. S3B-D and 2E). Further, consistent with a *hsrω*-dependent omega speckle formation by the ISWI chromatin remodeling complex (Onorati et al., 2011), its cell-autonomous downregulation, too, induced *lgl* tumor progression (*lgl UAS-ISWI-RNAi*, Fig. S4B).

One peculiarity of *hsrω* perturbations is a comparable phenotypic outcome by its gain or loss: for instance, the enhancement of Ras-driven defects in the eye epithelium upon increase or decrease in *hsrω* transcript levels (Ray et al., 2019b). Similar outcomes could be due to disruption of omega speckle biogenesis upon gain or loss of *hsrω* arcRNA (Prasanth et al., 2000; Singh and Lakhotia, 2015), which in turn results in aberrant increase in availability of some of the omega-speckle-associated proteins such as the hnRNPs in the cytoplasm leading to stabilization of cytoplasmic proteins such as DIAP1 (Mallik and Lakhotia, 2009). We further noted that transcriptomes of larval eye epithelium (Ray et al., 2019b) with down- or up-regulation of *hsrω* showed comparable enrichment of protein homeostasis-linked GO classes (Fig. S5A, see Table S2) and also for genes interacting with hsrω RNA-associated hnRNPs (Fig. S5B). These observations suggest that, like loss of *hsrω* in *lgl* clones, its gain, too, may drive *lgl* tumor progression. To test this possibility, we examined somatic clones displaying simultaneous loss of Lgl and gain of *hsrω.* An EP (Rørth et al., 1998) insertion (*EP3037*) in *hsrω,* subsequently referred to as $hsr\omega^{EP3037}$, results in its expression in a Gal4-dependent manner (Mallik and Lakhotia, 2009). We noted that the *lgl* $hsr\omega^{EP3037}$ clones survived well in wild type genetic backgrounds and formed significantly larger clones than their *lgl* counterparts (Fig. 3G, H). Over a tenth of the *lgl* $hsr\omega^{EP3037}$ clones (n=19) showed neoplastic transformations (Fig. 3G), besides varying degrees of cell death (Fig. 3I, yellow arrow).

These results show that cell-autonomous perturbations of *hsrω* transcripts promote clonal progression of *lgl* tumors (Fig. 3F, J).

Perturbations in the levels of human sat III arcRNA, a functional analog of* Drosophila *hsrω, in cancer cell lines

Given the association between *Drosophila hsrω* and cancer progression, we asked if its functional analog in humans, namely, sat III arcRNA (Jolly and Lakhotia, 2006; Nakagawa et al., 2022), is misexpressed in cancers. We ascertained levels of sat III transcripts in a panel of cancer cell lines, namely prostate: 22RV1, PC3, VCaP, LNCaP, breast: MCF7, MDA-MB-231, and cervical: HeLa. We observed an overall increase in sat III transcript levels across the different cell lines (Fig. 4A). We further noted that under stress such as heat shock at 42°C, treatment with genotoxin (doxorubicin at 2.5 µM), or oxidative stress (250µM of H_2O_2), elevates sat III transcript levels, for instance, in MDA-MB-231 cell line (Fig. 4B) with accompanying signatures of cellular stress such as elevated ROS, acidic lysosomes, pJNK, and cell death under stress (Fig. 4C, D). To test if such stress-induced increase in sat III levels conferred a survival advantage, we downregulated expression in cancer cell lines, like PC3 cells, using anti-sense oligos to sat III ((Goenka et al., 2016), also see Fig. S6)) and examined their viability following exposure to a genotoxin, doxorubicin. Indeed, sat III-compromised PC3 cells displayed reduced viability compared to control (Fig. 4E). Together, these results reveal that sat III arcRNA levels are generally elevated in the cancer cells and contribute to their survival under stress.

DISCUSSION

Long noncoding RNAs as host genetic modifiers of cancer is a relatively new and emerging perspective. For instance, nucleotide polymorphisms in a lncRNA, *NEAT1*, also an arcRNA, have been linked to cell fitness and survival in cancer cells (Esposito et al., 2023). Here, we have shown that heterozygosity of *hsrω*, a gene coding for the only known arcRNA in *Drosophila*, is tumor-promoting. Thus, while in a wild type epithelium of the imaginal discs, oncogenically targeted cells are eliminated by intrinsic tumor suppression (Agrawal et al., 1995; Igaki et al., 2009; Jiang et al., 2018; Lowe et al., 2004) those generated in a *hsrω* host genetic background escape cell death and undergo metastatic transformations. We further show that cell-autonomous increase or decrease in expression levels of *hsrω* is also tumor-promoting. *Drosophila*, therefore, offers the prospect of identifying tumor-modifying noncoding genetic loci—reminiscent of those directed at identifying protein-coding genes (Datta et al., 2023).

Earlier studies revealed that lowering the *hsrω* arcRNA levels abrogates TNF/JNK-induced cell death in the larval eye epithelial cells by stabilizing cytoplasmic DIAP1 protein (Mallik and Lakhotia, 2009). It is likely, therefore, that heterozygosity of *hsrω* promotes tumor progression via inhibiting JNK-mediated cell death. Since, either an increase or decrease in *hsrω* RNA levels similarly disrupts the formation of omega speckles (Prasanth et al., 2002), it is not surprising, therefore, that its autonomous gain or knockdown, both drives *lgl* tumor progression with equal propensity, reminiscent of comparable phenotypic outcome, namely, enhancement of Ras-driven differentiation defects of photoreceptors, by either gain or loss of hsrω RNA (Ray et al., 2019b). Finally, housekeeping roles of *hsrω* (Mallik and Lakhotia, 2011) may likely impact tumor progression. For instance, perturbations in *hsrω* arcRNA affect the availability of hnRNPs, such as the Hrb87F, whose loss has been causally linked to increase in telomere length in *Drosophila* (Singh and Lakhotia, 2016), an established hallmark of cancer progression (Hanahan, 2022). Notably, hnRNPA1, the mammalian homolog of *Drosophila* Hrb87F, also regulates telomere lengths (LaBranche et al., 1998).

Human arcRNA, sat III, is a functional analog of *Drosophila hsrω* (Jolly and Lakhotia, 2006). A characteristic feature of *hsrω* is the presence of a long stretch of tandem satellite repeats at its 3-prime end (Johnson et al., 2011; McKechnie et al., 1998) which is reminiscent of sat III repeats seen at the 9q12 heterochromatic region (Jolly and Lakhotia, 2006). Microsatellites are among the most variable loci in the human genome and are prone to display copy number variations and aberrant transcription, often associated with disease conditions (Sonay et al., 2015; Ugarković et al., 2022). For instance, while on one hand the 9q12 locus is frequently deleted in bladder cancers (Hopman et al., 2002; Sauter et al., 1995), on the other increase in sat III levels is seen in cancer cell lines, such as in this study and others ((Chatterjee and Sengupta, 2022), for review see (Ugarković et al., 2022)). Such variations underscores role of sat III in regulating cellular homeostasis, following an oncogenic stress. Given these possibilities, we further speculate that genetic variations in sat III could act as a potent modifier of human cancers.

Our findings find parallels with the seminal seed and soil hypothesis proposed over a century back by Stephen Paget, postulating that successful tumor cell (seed) dispersal (metastasis) depends on the congenial conditions in a distant organ (soil) (Paget, 1989). In the parlance of cancer biology, a congenial soil represents a tumor/tissue microenvironment (for review, see (Fidler, 2003)). The *hsrω* heterozygosity, therefore, likely provides a congenial tissue microenvironment (soil) where the *lgl* mutant clones (seed) survive and proliferate. In essence, *hsrω* arcRNA regulates both tumor cells and tissue microenvironmental homeostasis to underpin host genetics of tumor suppression (Klein, 2009).

Acknowledgement

We acknowledge Bloomington Drosophila Stock Centre (Indiana University) for fly stocks and Developmental Studies Hybridoma Bank (University of Iowa) for antibodies. We thank S. Ganesh, Indian Institute of Technology Kanpur, for the gift of the FK2 anti-ubiquitin antibody. This work was supported by the DBT/ Wellcome Trust India Alliance (IA/E/13/1/501271) and DST/WOS-A/LS-75/2021 to AB. Support by the Science & Engineering Research Board (SERB), Department of Science and Technology, Govt. of India (CO/S5/AB-03/2017) to PS and DBT/ Wellcome Trust India Alliance (IA/S/19/2/504659) to BA is acknowledged. SCL is supported by the Department of Biotechnology, Ministry of Science and Technology (BT/PR32126/BRB/10/1775/2019) and the Science & Engineering Research Board, Govt. of India, as a Distinguished Fellow (SB/DF/009/2019).

The authors declare no competing interests.

Material and Methods

Fly stocks were maintained at 25° C on standard fly food containing corn powder, yeast, and sugar. The following mutant/transgenic lines were used in this study: *w; l(2)gl^{4} FRT40A/CyO* (#36289, BDSC); *w; EP3037/ EP3037* (Mallik and Lakhotia, 2009); *w; UAS-hsrω-RNAi(2x)*(Mallik and Lakhotia, 2009); *w; hsrω^{66}/TM6B* (Johnson et al., 2011)
y w hs-flp, tub-Gal4, UAS-GFP/; tub-Gal80 FRT40A/CyO; w; FRT82B (#86313, BDSC)
y w hs-flp; FRT82B Ubi-GFP (#5188, BDSC); *w; TRE-DsRed;+ (*#59011, BDSC); *w;+;th-lacZ* (Bennett and Harvey, 2006)

Genotypes of clone and method clone induction:

- ***hsrω^{66}* mutant (**non-GFP) and its twin spot (two copies of GFP**,** Fig. 1G): Somatic clones with loss of *hsrω* (Fig. 1G) were generated using the flp/FRT technique (Xu and Rubin, 1993). Larval progeny of the cross: *FRT82B hsrω^{66}/ TM3b* X *y w hs-flp; FRT82B*

Ubi-GFP were subjected to heat shock 48 hours after egg laying (AEL) at 37°C for 30 minutes and incubated at 25°C; non-Tb larvae were selected for dissection at 96 to 120 hours AEL.

- ***lgl⁻* in *hsrω^{66}*/+ genetic background** (Fig. 2)**:** Somatic clones with loss of Lgl in an *hsrω^{66}*/+ genetic background were generated in F1 progeny of the cross: *lgl^{4} FRT40A/Cy-O;hsrω^{66}/ TM3b* and *y w hs-flp tub Gal4 UAS-GFP; tub-Gal80 FRT40A/Cy-O* using MARCM technique (Lee and Luo, 1999). Early second instar larvae (48 hours AEL) were subjected to heat shock at 37°C for 30 minutes and grown further at 25°C till dissection 96 to 120 hours AEL.
- ***lgl⁻ hsrωRNAi*** and ***lgl⁻ lgl^{EP3037}*** (Fig. 3): MARCM clones displaying loss of Lgl and with simultaneous downregulation of *hsrω* (Fig. 3) were generated in F1 progeny of the cross *lgl^{4}UAS-hsrω RNAi (2X) FRT40A;* and *y w hs-flp tub Gal4 UAS-GFP; tub-Gal80 FRT40A/Cy-O*. Likewise, MARCM clones displaying loss of Lgl and with simultaneous gain of *hsrω* (Fig. 3) were generated in F1 progeny of the cross *lgl^{4}FRT40A; hsrω^{EP3037}* and *y w hs-flp tub Gal4 UAS-GFP; tub-Gal80 FRT40A/Cy-O*. In both cases, 48-hour-old (AEL) F1 progeny larvae were heat shocked at 37°C for 30 minutes and grown further at 25° C till 120 hours AEL when the wing imaginal discs were dissected and processed for immunostaining.

Immunofluorescence staining and microscopy

Briefly, larvae of desired genotypes were dissected in 1x Phosphate Buffer Saline (PBS), and imaginal discs were fixed in 4% paraformaldehyde in 1x PBS containing 0.02 % Triton-X-100, and incubated in the desired primary antibody overnight at 4^{0}C, followed by incubation with appropriate fluorescently tagged secondary antibodies for two hours at the room, and counterstained with SYTOX-Green (S33025, Invitrogen) or Alexa Fluor™ 633 Phalloidin (A22284, Invitrogen). The following primary antibodies were used: anti-Caspase-3, rabbit (1:500 dilution, MERK/Sigma Aldrich, C8487), Polyubiquitinylated conjugates monoclonal antibody FK1, mouse (1:500 dilution, Enzo Life Sciences, BML-PW8805-0500), Anti-phospho Histone-3 (pSer^{10}), rabbit (1:500 dilution, MERK /Sigma Aldrich H0412), anti- β Galactosidase, mouse (1:200 dilution, MERK/Sigma Aldrich, G6282). To detect MMP1, we used a cocktail of monoclonal antibodies raised in mice (3A6B4, 3B8D12, 5H7B11, and 3B8D12; 1:1:1:1 ratio at a final dilution of 1:300, Developmental Studies Hybridoma Bank (DSHB), University of Iowa), anti-Fasciclin III, Fas III, mouse, (7G10, DSHB). We used the following secondary antibodies from Invitrogen: Alexa Fluor™ 555 anti-mouse (A32727) and Alexa Fluor 555 anti-rabbit (A32732).

Nuclear labeling was carried out using either SYTOX-Green (Invitrogen #S33025, Fig. 1 B, C, E, F, O-T) at a dilution of 1:300. Corticular F-Actin was labeled using Alexa Fluor™ 633 Phalloidin (#A22284, Invitrogen). After washing, the discs were mounted using a Vectashield anti-fade medium (Vector Laboratories, H-1000). Images were acquired with a Leica-SP5 confocal microscope and processed using the Leica confocal software LAS AF. Images were acquired using a

20x or a 40x (oil immersion) objective. Images of GFP-marked *lgl*; *hsrω*^{66}/+ tumor-bearing larvae were acquired with a Leica M205FA stereomicroscope with epi-fluorescent illumination (excitation filter 480 nm). All images were assembled using Adobe Photoshop CS5 software.

For detecting protein aggregates, the wing imaginal discs were dissected out from larvae of the desired genotype and age in PBS and fixed in 4% formaldehyde in 1× PBS, followed by permeabilization in 0.4% Triton X-100 and 3mM ethylenediaminetetraacetic acid (pH 8.0) in 1× PBS. Fixed imaginal discs were subsequently incubated in ProteoStat detection reagent (1:10,000 dilution, Enzo Life Sciences, #ENZ-51023-KP050), washed in 1XPBS, and the wing imaginal discs were mounted in glycerol-based anti-fade and imaged using Leica-SP5 confocal microscope.
We used LysoTracker® Red DND-99 dye (#L7528, Thermo-Fisher Scientific/Invitrogen) to detect acidic lysosomes and MitoTracker™ Red CMXRos (#M22425, Thermo-Fisher Scientific/Invitrogen). This cell-permeant, red-fluorescent dye stains mitochondria in live cells and is a marker for altered membrane potential. Briefly, larvae of the desired genotype were gently rinsed and dissected in 1x PBS to remove tissues like fat body, gut, etc. The flipped larvae were incubated in freshly prepared 500nM of LysoTracker (in 1X PBS) or 500nM MitoTracker (in 1X PBS) at room temperature in the dark for 15 minutes, followed by a thorough rinse in 1x PBS. Unfixed wing discs were mounted in anti-fade-containing Vectashield (Vector Laboratories, #H-1000), and images were acquired immediately using a Leica-SP5 confocal microscope and processed using Leica confocal software-LAS AF and assembled using Adobe Photoshop.

We used dihydroethidium (#D11347, Invitrogen), a free radical sensitive dye, to detect ROS levels in unfixed larval tissues (Owusu-Ansah et al., 2008). Briefly, larvae of the desired genotype were washed and dissected in 1xPBS. After removing the fat body, gut, and other adherent tissues, the flipped larvae were incubated in freshly made 1:1000 DHE at room temperature in the dark for 15 minutes. The wing imaginal discs were subsequently thoroughly rinsed in 1XPBS, mounted in anti-fade containing Vectashield (Vector Laboratories, #H-1000), and images were acquired with Leica-SP5 confocal microscope and processed using Leica confocal software-LAS AF and AdobePhotoshop CS3.

Quantification of wing disc and clone sizes

The size of wing discs, expressed in arbitrary units (for Fig. 1D), was quantified using ImageJ (http://rsb.info.nih.gov/ij/). Confocal projection images of wing imaginal discs acquired with a Leica-SP5 confocal microscope were projected as a single image and used as the input file. The Freehand selection tool was used to trace the outline of the imaginal discs marked by nuclear fluorescence (SYTOX-Green), and the "Measure" option was used to obtain the area of the wing disc in arbitrary units. The same method was followed to determine the clone sizes depicted in Figs. 2G, 3B, and 3H, wherein the freehand selection tool was used to trace the outline of the nuclear GFP-marked clones in individual discs.

Sizes of *hsrω*^{66} mutant clones (*hsrω*^{66}/*hsrω*^{66}) marked by loss of GFP and their twin spots (*hsr*$^{+}$ *GFP/ hsr*$^{+}$*GFP*) characterized by their brighter GFP fluorescent than their *hsrω*^{66}/+ heterozygous background (Fig. 1J) were calculated using "Analyze Particle" option of Image J platform on confocal projection images. Images were first converted to an 8-bit format; signal thresholds were set to calculate the number of pixels with no signal (non-GFP, *hsrω*^{66}/*hsrω*^{66} clones) and those with double GFP (twin spots, +/+). The measured sizes of discs and clones are presented as box plots (Figs. 1D, 1G, 2G, 3B, 3H) generated with Microsoft Excel.

Quantification of pH3-positive nuclei in wing discs

Confocal projection images of the red channel (pH3) of individual wing imaginal discs were used as input files after converting to 8-bit formats. Image J was used to overlay a grid of uniform unit size, and the Analyze particle option, as discussed above, was used to calculate total fluorescence (red channel) from individual ROI of the grid.

Gene Set Enrichment Analysis (GSEA)

Preprocessed RNAseq data were obtained from earlier publications (Ray et al., 2019a; Ray et al., 2019b). Gene Set Enrichment Analysis (GSEA) is a statistical tool (Subramanian et al., 2005) that provides a quantitative measure of the enrichment of a predefined set of genes between two compared genotypes. A normalized enrichment score (NES) is calculated using running sum statistics. The NES is a positive value if a gene set is positively correlated with the genotype under study (such as *hsrω* misexpression genotypes versus control) and is therefore considered enriched in the former. Predefined gene sets were collated for given Gene Ontology classes from Gene Ontology Resource (http://geneontology.org/). GSEA analyses used the following parameters: genes were ranked based on comparing genotypes: *hsrω* mutant versus control using signal-to-noise metric. The enrichment score was calculated using weighted running sum statistics. Gene-based permutation (n =1000) was used to compute the nominal P value and FDR was computed to correct for multiple-hypothesis testing.

Cancer cell lines, culture conditions, and treatments

22RV1, PC3, VCaP, LNCaP (Prostate cancer cell lines), MCF7, MDA-MB-231 (Breast cancer cell lines), and HeLa (Cervical cancer cell line) were obtained from American Type Culture Collection (ATCC) and were cultured as per the ATCC recommended guidelines. Briefly, the cells were cultured in a growth medium supplemented with 10% fetal bovine serum (FBS) and 0.5% Penicillin-Streptomycin (Gibco, Thermo-Fisher Scientific) in a cell culture incubator (Thermo Fisher Scientific) supplied with 5% CO_2 at 37°C. For the heat-shock treatment, cells were grown in 6-well culture dishes and incubated at 42°C for 1 hour and then at 37°C for 1 hour for recovery. For oxidative stress, cells were treated with 250µM H_2O_2 for 18 hours. Cells were treated with 2.5µM doxorubicin for anticancer drug-induced stress for 18 hours.

Cell viability assay

Cell viability assay using a PC3 cell line was performed by plating 3000 cells per well in a 96-well plate. After 24 hours, cells were treated with 5µM Doxorubicin against DMSO control. After 24 hours, cells were transfected with sat III-antisense constructs along with polyethylenimine (PEI) cellular transfection reagent (CAT# 23966-1, Polyethylenimine, Linear, MW 25000 (6µg/ml)). Cell viability was determined after 48 hours of the drug treatment following incubation with the Cell viability reagent-Resazurin (Cayman), followed by the colorimetric assay as per the manufacturer's protocol. A two-way ANOVA test was used to determine statistical significance for independent samples *$P<0.05$,**$P<0.001$. Error bars represent ±SEM.

RNA isolation and Quantitative PCR (qPCR)

The total RNA was extracted using RNAiso Plus (Takara), and 1µg of total RNA was reverse transcribed into cDNA using First Strand cDNA synthesis kit (PureGene) according to the manufacturer's protocol. Quantitative PCR (qPCR) was performed using cDNA template, primer sets (sat III_FP: TATGAATTCAATCAACCCGAGTGCAATCGAA, sat III_RP: TATGGATCCTTCCATTCCATTCCTGTACTCG; GAPDH_FP: TGCACCACCAACTGCTTAGC, GAPDH_RP: GGCATGGACTGTGGTCATGAG) and SYBR Green PCR Master-Mix (PureGene) on the QuantStudio 5 Real-Time PCR System (Applied Biosystems). Relative sat III expression was calculated for each sample by the $\Delta\Delta C_T$ method. A two-tailed unpaired Student's t-test was applied to determine the statistical significance for independent samples *$P\leq 0.05$ and **$P\leq 0.001$. Error bars represent mean ± SEM.

REFERENCES

Agrawal, N., Kango, M., Mishra, A. and Sinha, P. (1995). Neoplastic transformation and aberrant cell-cell interactions in genetic mosaics of lethal(2)giant larvae (lgl), a tumor suppressor gene of Drosophila. *Dev Biol* **172**, 218–229.

Bajpai, A. and Sinha, P. (2020). Hh signaling from de novo organizers drive lgl neoplasia in Drosophila epithelium. *Dev Biol* **457**, 1–8.

Baumgartner, M. E., Dinan, M. P., Langton, P. F., Kucinski, I. and Piddini, E. (2021). Proteotoxic stress is a driver of the loser status and cell competition. *Nat Cell Biol* **23**, 136–146.

Bendena, W. G., Garbe, J. C., Traverse, K. L., Lakhotia, S. C. and Pardue, M. L. (1989). Multiple inducers of the Drosophila heat shock locus 93D (hsr omega): inducer-specific patterns of the three transcripts. *J Cell Biol* **108**, 2017–2028.

Bennett, F. C. and Harvey, K. F. (2006). Fat Cadherin Modulates Organ Size in Drosophila via the Salvador/Warts/Hippo Signaling Pathway. *Current Biology* **16**, 2101–2110.

Castro-Giner, F., Ratcliffe, P. and Tomlinson, I. (2015). The mini-driver model of polygenic cancer evolution. *Nat Rev Cancer* **15**, 680–685.

Chatterjee, N. and Bohmann, D. (2012). A versatile ΦC31 based reporter system for measuring AP-1 and Nrf2 signaling in Drosophila and in tissue culture. *PLoS One* **7**, e34063.

Chatterjee, M. and Sengupta, S. (2022). Human satellite III long noncoding RNA imparts survival benefits to cancer cells. *Cell Biology International* **46**, 611–627.

Chenevix-Trench, G., Milne, R. L., Antoniou, A. C., Couch, F. J., Easton, D. F., Goldgar, D. E., and CIMBA (2007). An international initiative to identify genetic modifiers of cancer risk in BRCA1 and BRCA2 mutation carriers: the Consortium of Investigators of Modifiers of BRCA1 and BRCA2 (CIMBA). *Breast Cancer Research* **9**, 104.

Clemson, C. M., Hutchinson, J. N., Sara, S. A., Ensminger, A. W., Fox, A. H., Chess, A. and Lawrence, J. B. (2009). An architectural role for a nuclear noncoding RNA: NEAT1 RNA is essential for the structure of paraspeckles. *Mol Cell* **33**, 717–726.

Constanty, F. and Shkumatava, A. (2021). lncRNAs in development and differentiation: from sequence motifs to functional characterization. *Development* **148**, dev182741.

Daneshvar, K., Ardehali, M. B., Klein, I. A., Hsieh, F.-K., Kratkiewicz, A. J., Mahpour, A., Cancelliere, S. O. L., Zhou, C., Cook, B. M., Li, W., et al. (2020). lncRNA DIGIT and BRD3 protein form phase-separated condensates to regulate endoderm differentiation. *Nat Cell Biol* **22**, 1211–1222.

Datta, I., Vassel, T., Linkous, B., Odum, T., Drew, C., Taylor, A. and Bangi, E. (2023). A targeted genetic modifier screen in Drosophila uncovers vulnerabilities in a genetically complex model of colon cancer. *G3 (Bethesda)* **13**, jkad053.

Elliott, K. and Larsson, E. (2021). Non-coding driver mutations in human cancer. *Nat Rev Cancer* **21**, 500–509.

Fidler, I. J. (2003). The pathogenesis of cancer metastasis: the "seed and soil" hypothesis revisited. *Nat Rev Cancer* **3**, 453–458.

Froldi, F., Ziosi, M., Garoia, F., Pession, A., Grzeschik, N. A., Bellosta, P., Strand, D., Richardson, H. E., Pession, A. and Grifoni, D. (2010). The lethal giant larvae tumour suppressor mutation requires dMyc oncoprotein to promote clonal malignancy. *BMC Biol* **8**, 33.

Goenka, A., Sengupta, S., Pandey, R., Parihar, R., Mohanta, G. C., Mukerji, M. and Ganesh, S. (2016). Human satellite-III non-coding RNAs modulate heat-shock-induced transcriptional repression. *J Cell Sci* **129**, 3541–3552.

Green, D. R. (2022). A Matter of Life and Death. *Cold Spring Harb Perspect Biol* **14**, a041004.

Hanahan, D. (2022). Hallmarks of Cancer: New Dimensions. *Cancer Discovery* **12**, 31–46.

Hopman, A. H. N., Kamps, M. A. F., Speel, E. J. M., Schapers, R. F. M., Sauter, G. and Ramaekers, F. C. S. (2002). Identification of chromosome 9 alterations and p53 accumulation in isolated carcinoma in situ of the urinary bladder versus carcinoma in situ associated with carcinoma. *Am J Pathol* **161**, 1119–1125.

Huarte, M. (2015). The emerging role of lncRNAs in cancer. *Nat Med* **21**, 1253–1261.

Igaki, T., Pastor-Pareja, J. C., Aonuma, H., Miura, M. and Xu, T. (2009). Intrinsic tumor suppression and epithelial maintenance by endocytic activation of Eiger/TNF signaling in Drosophila. *Dev Cell* **16**, 458–465.

Jiang, Y., Seimiya, M., Schlumpf, T. B. and Paro, R. (2018). An intrinsic tumour eviction mechanism in Drosophila mediated by steroid hormone signalling. *Nat Commun* **9**, 3293.

Johnson, T. K., Carrington, L. B., Hallas, R. J. and McKechnie, S. W. (2009). Protein synthesis rates in Drosophila associate with levels of the hsr-omega nuclear transcript. *Cell Stress Chaperones* **14**, 569–577.

Johnson, T. K., Cockerell, F. E. and McKechnie, S. W. (2011). Transcripts from the Drosophila heat-shock gene hsr-omega influence rates of protein synthesis but hardly affect resistance to heat knockdown. *Mol Genet Genomics* **285**, 313–323.

Jolly, C. and Lakhotia, S. C. (2006). Human sat III and Drosophila hsrω transcripts: a common paradigm for regulation of nuclear RNA processing in stressed cells. *Nucleic Acids Research* **34**, 5508–5514.

Jolly, C., Metz, A., Govin, J., Vigneron, M., Turner, B. M., Khochbin, S. and Vourc'h, C. (2004). Stress-induced transcription of satellite III repeats. *J Cell Biol* **164**, 25–33.

Khan, S. J., Bajpai, A., Alam, M. A., Gupta, R. P., Harsh, S., Pandey, R. K., Goel-Bhattacharya, S., Nigam, A., Mishra, A. and Sinha, P. (2013). Epithelial neoplasia in Drosophila entails switch to primitive cell states. *Proc Natl Acad Sci U S A* **110**, E2163-2172.

Klein, G. (2009). Toward a genetics of cancer resistance. *Proceedings of the National Academy of Sciences* **106**, 859–863.

Kongsuwan, K., Yu, Q., Vincent, A., Frisardi, M. C., Rosbash, M., Lengyel, J. A. and Merriam, J. (1985). A Drosophila Minute gene encodes a ribosomal protein. *Nature* **317**, 555–558.

LaBranche, H., Dupuis, S., Ben-David, Y., Bani, M.-R., Wellinger, R. J. and Chabot, B. (1998). Telomere elongation by hnRNP A1 and a derivative that interacts with telomeric repeats and telomerase. *Nat Genet* **19**, 199–202.

Lakhotia, S. C. (2011). Forty years of the 93D puff of Drosophila melanogaster. *J Biosci* **36**, 399–423.

Lakhotia, S. C. and Ray, P. (1996). hsp 83 mutation is a dominant enhancer of lethality associated with absence of the non-protein codinghsrω locus inDrosophila melanogaster. *J Biosci* **21**, 207–219.

Lakhotia, S. C., Rajendra, T. K. and Prasanth, K. V. (2001). Developmental regulation and complex organization of the promoter of the non-coding hsr(omega) gene of Drosophila melanogaster. *J Biosci* **26**, 25–38.

Lakhotia, S. C., Mallick, B. and Roy, J. (2020). Chapter 2 - Non-coding RNAs: ever-expanding diversity of types and functions. In *Rna-Based Regulation in Human Health and Disease* (ed. Pandey, R.), pp. 5–57. Academic Press.

Lee, T. and Luo, L. (1999). Mosaic analysis with a repressible cell marker for studies of gene function in neuronal morphogenesis. *Neuron* **22**, 451–461.

Lo Piccolo, L. and Yamaguchi, M. (2017). RNAi of arcRNA hsrω affects sub-cellular localization of Drosophila FUS to drive neurodiseases. *Experimental Neurology* **292**, 125–134.

Lowe, S. W., Cepero, E. and Evan, G. (2004). Intrinsic tumour suppression. *Nature* **432**, 307–315.

Luo, J., Qu, L., Gao, F., Lin, J., Liu, J. and Lin, A. (2021). LncRNAs: Architectural Scaffolds or More Potential Roles in Phase Separation. *Front Genet* **12**, 626234.

Mallik, M. and Lakhotia, S. C. (2009). The developmentally active and stress-inducible noncoding hsromega gene is a novel regulator of apoptosis in Drosophila. *Genetics* **183**, 831–852.

Mallik, M. and Lakhotia, S. C. (2011). Pleiotropic consequences of misexpression of the developmentally active and stress-inducible non-coding hsrω gene in Drosophila. *J Biosci* **36**, 265–280.

Martínez-Férriz, A., Ferrando, A., Fathinajafabadi, A. and Farràs, R. (2022). Ubiquitin-mediated mechanisms of translational control. *Semin Cell Dev Biol* **132**, 146–154.

McKechnie, S. W., Halford, M. M., McColl, G. and Hoffmann, A. A. (1998). Both allelic variation and expression of nuclear and cytoplasmic transcripts of Hsr-omega are closely associated with thermal phenotype in Drosophila. *Proc Natl Acad Sci U S A* **95**, 2423–2428.

Miller, D. R. and Thorburn, A. (2021). Autophagy and organelle homeostasis in cancer. *Developmental Cell* **56**, 906–918.

Mohler, J. and Pardue, M. L. (1984). Mutational Analysis of the Region Surrounding the 93d Heat Shock Locus of DROSOPHILA MELANOGASTER. *Genetics* **106**, 249–265.

Nagata, R. and Igaki, T. (2018). Cell competition: Emerging mechanisms to eliminate neighbors. *Dev Growth Differ* **60**, 522–530.

Nakagawa, S., Yamazaki, T., Mannen, T. and Hirose, T. (2022). ArcRNAs and the formation of nuclear bodies. *Mamm Genome* **33**, 382–401.

Onorati, M. C., Lazzaro, S., Mallik, M., Ingrassia, A. M. R., Carreca, A. P., Singh, A. K., Chaturvedi, D. P., Lakhotia, S. C. and Corona, D. F. V. (2011). The ISWI chromatin remodeler organizes the hsrω ncRNA-containing omega speckle nuclear compartments. *PLoS Genet* **7**, e1002096.

Owusu-Ansah, E., Yavari, A., Mandal, S. and Banerjee, U. (2008). Distinct mitochondrial retrograde signals control the G1-S cell cycle checkpoint. *Nat Genet* **40**, 356–361.

Paget, S. (1989). The distribution of secondary growths in cancer of the breast. 1889. *Cancer Metastasis Rev* **8**, 98–101.

Prasanth, K. V., Rajendra, T. K., Lal, A. K. and Lakhotia, S. C. (2000). Omega speckles - a novel class of nuclear speckles containing hnRNPs associated with noncoding hsr-omega RNA in Drosophila. *J Cell Sci* **113 Pt 19**, 3485–3497.

Quiles, J. M. and Gustafsson, Å. B. (2020). Mitochondrial Quality Control and Cellular Proteostasis: Two Sides of the Same Coin. *Front Physiol* **11**, 515.

Ray, M., Acharya, S., Shambhavi, S. and Lakhotia, S. C. (2019a). Over-expression of Hsp83 in grossly depleted hsrω lncRNA background causes synthetic lethality and l(2)gl phenocopy in Drosophila. *J Biosci* **44**, 36.

Ray, M., Singh, G. and Lakhotia, S. C. (2019b). Altered levels of hsromega lncRNAs further enhance Ras signaling during ectopically activated Ras induced R7 differentiation in Drosophila. *Gene Expr Patterns* **33**, 20–36.

Rørth, P., Szabo, K., Bailey, A., Laverty, T., Rehm, J., Rubin, G. M., Weigmann, K., Milán, M., Benes, V., Ansorge, W., et al. (1998). Systematic gain-of-function genetics in Drosophila. *Development* **125**, 1049–1057.

Sauter, G., Moch, H., Carroll, P., Kerschmann, R., Mihatsch, M. J. and Waldman, F. M. (1995). Chromosome-9 loss detected by fluorescence in situ hybridization in bladder cancer. *Int J Cancer* **64**, 99–103.

Settembre, C., Fraldi, A., Medina, D. L. and Ballabio, A. (2013). Signals for the lysosome: a control center for cellular clearance and energy metabolism. *Nat Rev Mol Cell Biol* **14**, 283–296.

Singh, A. K. and Lakhotia, S. C. (2015). Dynamics of hnRNPs and omega speckles in normal and heat shocked live cell nuclei of Drosophila melanogaster. *Chromosoma* **124**, 367–383.

Singh, A. K. and Lakhotia, S. C. (2016). The hnRNP A1 homolog Hrb87F/Hrp36 is important for telomere maintenance in Drosophila melanogaster. *Chromosoma* **125**, 373–388.

Sonay, T. B., Koletou, M. and Wagner, A. (2015). A survey of tandem repeat instabilities and associated gene expression changes in 35 colorectal cancers. *BMC Genomics* **16**, 702.

Srivastava, A., Pastor-Pareja, J. C., Igaki, T., Pagliarini, R. and Xu, T. (2007). Basement membrane remodeling is essential for Drosophila disc eversion and tumor invasion. *Proc Natl Acad Sci U S A* **104**, 2721–2726.

Stronach, B. E. and Perrimon, N. (1999). Stress signaling in Drosophila. *Oncogene* **18**, 6172–6182.

Subramanian, A., Tamayo, P., Mootha, V. K., Mukherjee, S., Ebert, B. L., Gillette, M. A., Paulovich, A., Pomeroy, S. L., Golub, T. R., Lander, E. S., et al. (2005). Gene set enrichment analysis: a knowledge-based approach for interpreting genome-wide expression profiles. *Proc Natl Acad Sci U S A* **102**, 15545–15550.

Tamori, Y., Suzuki, E. and Deng, W.-M. (2016). Epithelial Tumors Originate in Tumor Hotspots, a Tissue-Intrinsic Microenvironment. *PLoS Biol* **14**, e1002537.

Turnbull, C., Sud, A. and Houlston, R. S. (2018). Cancer genetics, precision prevention and a call to action. *Nat Genet* **50**, 1212–1218.

Ugarković, Đ., Sermek, A., Ljubić, S. and Feliciello, I. (2022). Satellite DNAs in Health and Disease. *Genes (Basel)* **13**, 1154.

Xu, T. and Rubin, G. M. (1993). Analysis of genetic mosaics in developing and adult Drosophila tissues. *Development* **117**, 1223–1237.

Zeng, H., Castillo-Cabrera, J., Manser, M., Lu, B., Yang, Z., Strande, V., Begue, D., Zamponi, R., Qiu, S., Sigoillot, F., et al. (2019). Genome-wide CRISPR screening reveals genetic modifiers of mutant EGFR dependence in human NSCLC. *Elife* **8**, e50223.

Figure Legend

Fig. 1 Loss of *hsrω* arcRNA disrupts cell homeostasis in *Drosophila* larval imaginal discs

(A) Schematic representation of *hsrω* gene organization and its multiple transcripts (RA-RF) (Lakhotia et al., 2020). (B-C) Wing imaginal discs from $hsr\omega^{66}$ heterozygous (B) and $hsr\omega^{66}$ homozygous (C) larvae of comparable age. (D) Comparison of wing disc areas (Y-axis) of $hsr\omega^{66}$ hetero- and homozygous (X-axis) larvae. (E-G) Mitotically dividing cells marked by phospho-Histone (pH3) in wing discs of $hsr\omega^{66}$ heterozygous (E) and homozygous (F) larvae; and their quantification (G). (H-J) Mosaic wing imaginal discs carrying $hsr\omega^{66}$ homozygous somatic clones ($hsr\omega^{66}/hsr\omega^{66}$ non-GFP, H) and their respective wild type twin clones ($hsr\omega^{+}$ GFP/ $hsr\omega^{+}$ GFP, H); a schematic representation of the $hsr\omega^{66}$twin clones (I), and quantification of the twin clone areas from mosaic discs (J). Wing imaginal discs showing Ubiquitin-positive foci (anti-FK1); acidic lysosomes (LysoTracker); protein aggregates (ProteoStat);JNK signaling (TRE-Ds Red); Caspase (anti-Caspase-3) from $hsr\omega^{66}$ homozygous (M, O, Q and S) and $hsr\omega^{66}$ heterozygous (N, P, R and T) larvae. Wing imaginal discs in B, C, E, F, O, P, Q-T are counterstained with nucleic acid specific SYTOX Green. Boxed areas in K and M; or O and P are shown at higher magnification along, or the right, respectively. Scale bars represent 100µm. ** in D and G represent $p<0.01$, Student's t-test.

Fig. 2 Neoplastic transformation of *lgl* clones in *hsrω* heterozygous genetic background

(A-D) Wing imaginal discs displaying ROS (DHE, A, B), and acidic Lysosomes (LysoTracker, C, D) from wild type (A, C) and $hsr\omega^{66}$ heterozygous (B, D) larvae subjected to 15 minutes heat shock at 37°C. (E) Wing disc carrying somatic *lgl* clones (GFP, green) exhibiting cell death (Caspase-3); the wing epithelium displays intact F-actin (grey, E'). Projections of select apical (E, E') and basal (E'', E''') optical sections, note basal localization of dying *lgl* clones (GFP, E''') displaying Caspase (Red). (F-J) wing disc from $hsr\omega^{66}$/+ heterozygous larva carrying *lgl* clones (green, *lgl GFP;*$hsr\omega^{66}$/+) showing disrupted F-Actin (grey, yellow arrow). Pink dotted line marks the distal wing pouch. (G) Comparison of *lgl* clone sizes in WT or $hsr\omega^{66}$/+ genetic background. (H-K) *lgl* clones (green) in $hsr\omega^{66}$ heterozygous genetic background immunostained for phospho-Histone (pH3, H), Caspase-3 (I), and MMP1 (J); H, I and J also show F-actin staining with Phalloidin (grey). (K) $hsr\omega^{66}$ heterozygous larva bearing *lgl* clones (GFP) in imaginal discs (marked *) also seen away from the imaginal disc. Magnified view of the boxed area in K is shown on the right. (L) Schema displaying fate of *lgl* clones generated in WT (left) or $hsr\omega^{66}$/+heterozygous genetic background. Scale bars represent 100µm.

Fig. 3 Cell autonomous perturbation in *hsrω* levels results in the transformation of *lgl* clones

(A) *lgl* clones with downregulation of *hsrω* (*lgl UAS hsrω RNAi GFP,* green) displaying disrupted F-Actin (grey, A, arrow) and characteristic large, dispersed nuclei (GFP). (B) Comparison of clone sizes (Y-axis) of *lgl* and *lgl UAS-hsrω RNAi* clones (X-axis). (C-E) *lgl UAS hsrω RNAi GFP* clones (green) displaying MMP1 (C, arrow), Caspase-3 (D, proximal clone: white arrow, distal clone: yellow arrow), and *th-lacZ* (E, β-Gal). (F) Schema indicating fate of *lgl* clones on cell autonomous down-regulation of *hsrω.* (G) *lgl* clones with over-expression of *hsrω* (*lgl* $hsr\omega^{EP3037}$) displaying large nuclei and disrupted cyto-architecture (F-Actin, grey). (H) Comparison of clone sizes (Y axis) of *lgl* and *lgl* $hsr\omega^{EP3037}$ somatic

clones (X-axis). (I) *lgl hsrω*^{EP3037} clones displaying cell death (Caspase-3). (J) Schema displaying fate of *lgl* clones upon cell autonomous up-regulation of *hsrω.* Scale bars represent 100µm.

Fig. 4 Downregulation of sat III expressions in cancer cell lines

(A) Endogenous *sat III* transcript levels in immortalized prostate epithelial cells (benign line: PNT2) and in Prostate (22RV1, PC3, VCaP, LNCaP), Cervical (HeLa) and Breast (MCF7, MDA-MB-231) cancer cell lines determined by Q-PCR. (B) Elevated levels of *sat III* in HeLa, MDA-MB-231and PC3 cells under conditions of heat shock (42℃ for 1 hour, HS), Doxorubicin (2.5µM, Doxo) and Hydrogen peroxide (250µM, H_2O_2) treatment, compared to control (without any treatment), as determined by Q-PCR. (C-D) MDA-MB-231 cells displaying signatures of cell stress: ROS (DHE), acidic lysosomes (LysoTracker), pJNK, and cell death (Caspase-3) in control (C) and upon heat shock (D). (E) Decrease in viability of PC3 cells treated with Doxorubicin (but not DMSO) following transfection with anti-sense sat III oligos. Control (CTL) represents cells not transfected with anti-sense sat III oligo. Error bars represent mean ± SEM. *P<0.01, **P<0.001 for two-way ANOVA.

Figure 1

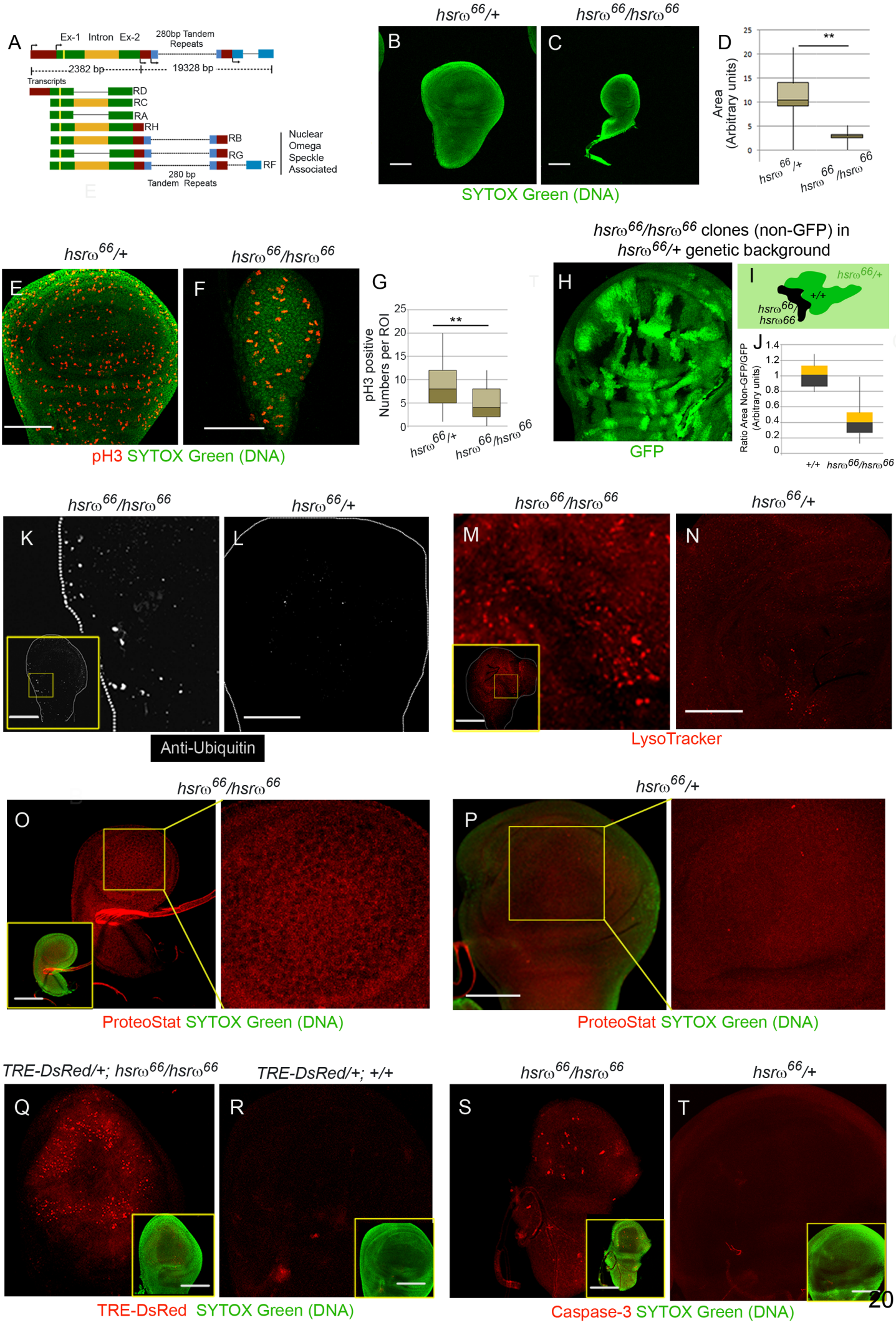
A
Ex-1
Intron
Ex-2
280bp Tandem Repeats
2382 bp
19328 bp
Transcripts
RD
RC
RA
RH
RB
RG
RF
280 bp Tandem Repeats
Nuclear Omega Speckle Associated
hsrω66/+
hsrω66/hsrω66
B
C
SYTOX Green (DNA)
D
Area (Arbitrary units)
**
hsrω66/+
hsrω66/hsrω66
E
F
pH3 SYTOX Green (DNA)
G
pH3 positive Numbers per ROI
**
hsrω66/+
hsrω66/hsrω66
hsrω66/hsrω66 clones (non-GFP) in hsrω66/+ genetic background
H
GFP
I
hsrω66/+
+/+
hsrω66/hsrω66
J
Ratio Area Non-GFP/GFP (Arbitrary units)
+/+
hsrω66/hsrω66
K
L
Anti-Ubiquitin
M
N
LysoTracker
O
P
ProteoStat SYTOX Green (DNA)
TRE-DsRed/+; hsrω66/hsrω66
TRE-DsRed/+; +/+
Q
R
TRE-DsRed SYTOX Green (DNA)
S
T
Caspase-3 SYTOX Green (DNA)

Figure 2

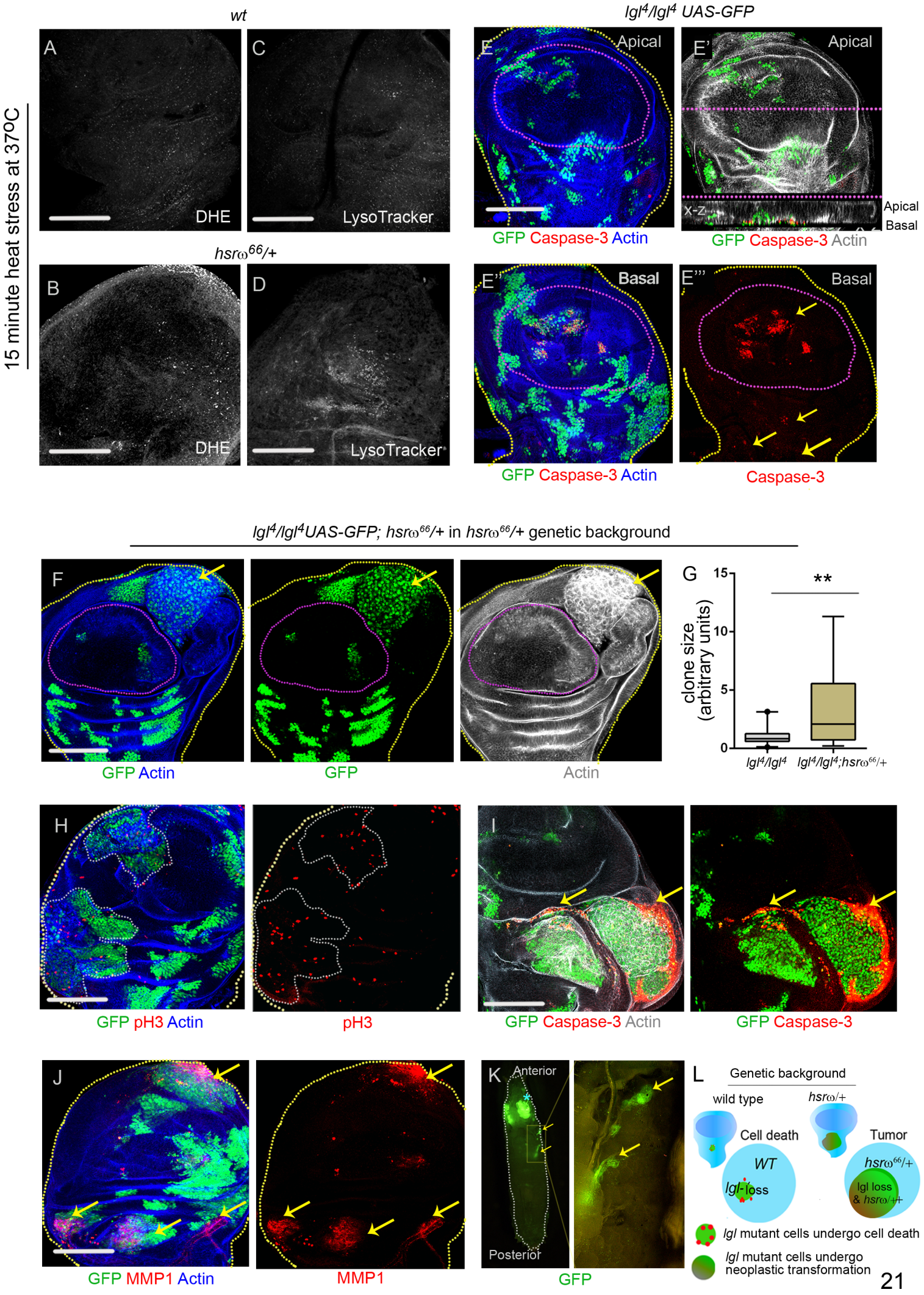
wt
lgl4/lgl4 UAS-GFP
15 minute heat stress at 37°C
A
DHE
C
LysoTracker
hsrω66/+
B
DHE
D
LysoTracker
E
Apical
GFP Caspase-3 Actin
E'
Apical
x-z
Apical
Basal
GFP Caspase-3 Actin
E''
Basal
GFP Caspase-3 Actin
E'''
Basal
Caspase-3
lgl4/lgl4UAS-GFP; hsrω66/+ in hsrω66/+ genetic background
F
GFP Actin
GFP
Actin
G
clone size (arbitrary units)
15
10
5
0
**
lgl4/lgl4
lgl4/lgl4;hsrω66/+
H
GFP pH3 Actin
pH3
I
GFP Caspase-3 Actin
GFP Caspase-3
J
GFP MMP1 Actin
MMP1
K
Anterior
Posterior
GFP
L
Genetic background
wild type
hsrω/+
Cell death
Tumor
WT
lgl-loss
hsrω66/+
lgl loss & hsrω/++
lgl mutant cells undergo cell death
lgl mutant cells undergo neoplastic transformation

Figure 3

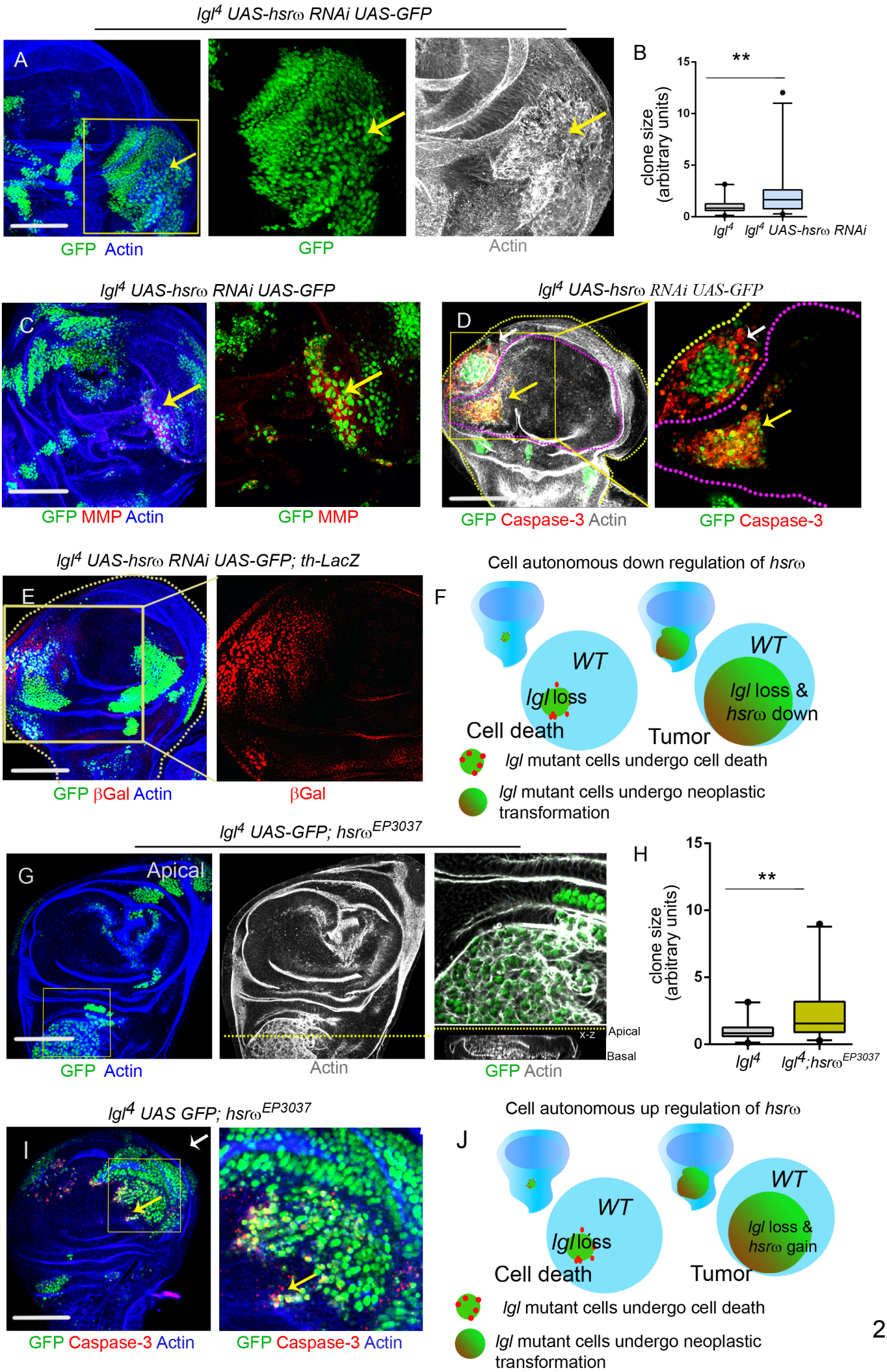
lgl4 UAS-hsrω RNAi UAS-GFP
A
GFP Actin
GFP
Actin
B
**
clone size (arbitrary units)
15
10
5
0
lgl4
lgl4 UAS-hsrω RNAi
lgl4 UAS-hsrω RNAi UAS-GFP
C
GFP MMP Actin
GFP MMP
lgl4 UAS-hsrω RNAi UAS-GFP
D
GFP Caspase-3 Actin
GFP Caspase-3
lgl4 UAS-hsrω RNAi UAS-GFP; th-LacZ
E
GFP βGal Actin
βGal
Cell autonomous down regulation of hsrω
F
WT
lgl loss
Cell death
WT
lgl loss &
hsrω down
Tumor
lgl mutant cells undergo cell death
lgl mutant cells undergo neoplastic transformation
lgl4 UAS-GFP; hsrωEP3037
G
Apical
GFP Actin
Actin
X-Z
Apical
Basal
GFP Actin
H
**
clone size (arbitrary units)
15
10
5
0
lgl4
lgl4;hsrωEP3037
lgl4 UAS GFP; hsrωEP3037
I
GFP Caspase-3 Actin
GFP Caspase-3 Actin
Cell autonomous up regulation of hsrω
J
WT
lgl loss
Cell death
WT
lgl loss &
hsrω gain
Tumor
lgl mutant cells undergo cell death
lgl mutant cells undergo neoplastic transformation

Figure 4

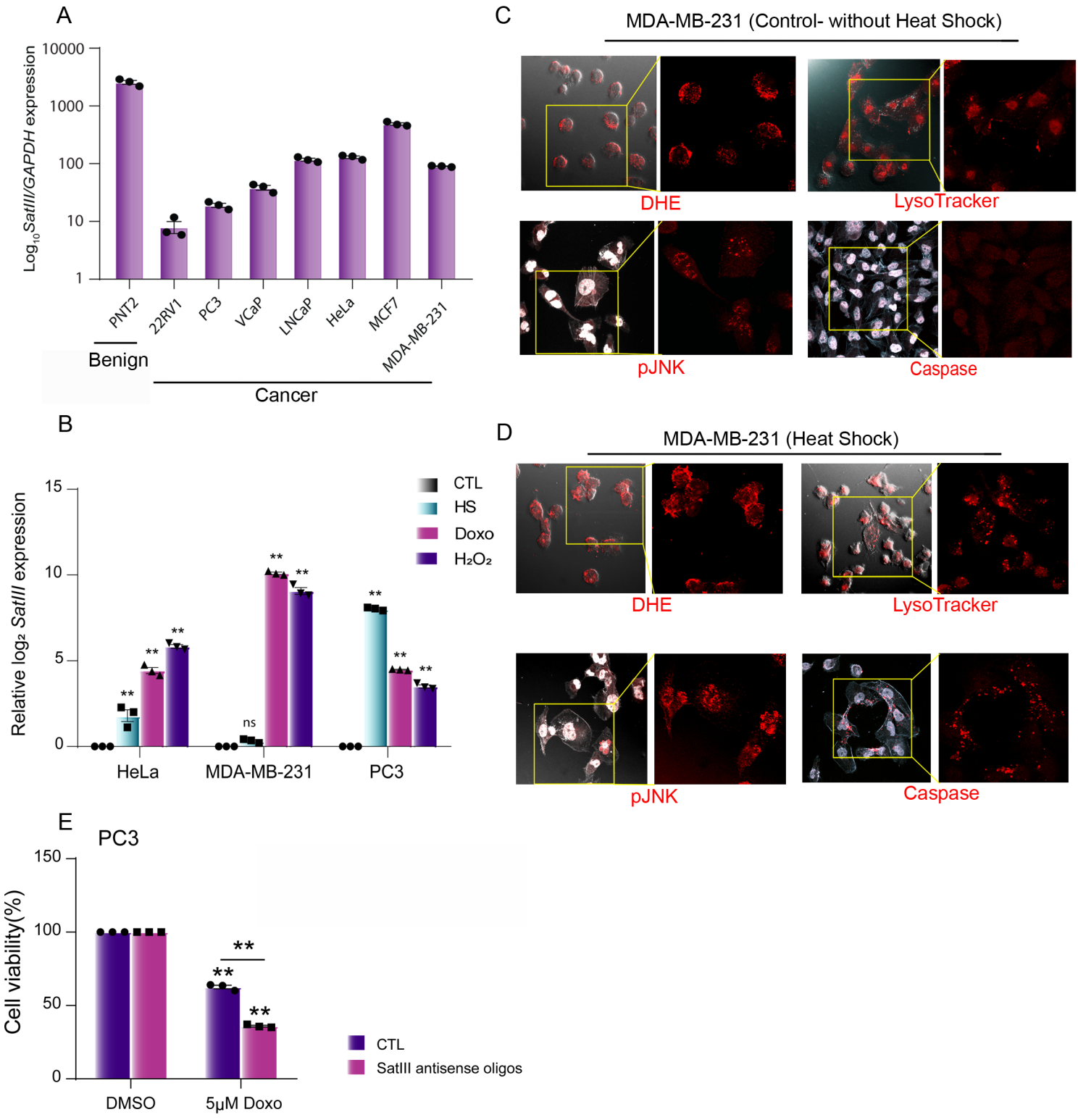
A
Log10 SatIII/GAPDH expression
10000
1000
100
10
1
PNT2
22RV1
PC3
VCaP
LNCaP
HeLa
MCF7
MDA-MB-231
Benign
Cancer
B
Relative log2 SatIII expression
15
10
5
0
CTL
HS
Doxo
H2O2
HeLa
MDA-MB-231
PC3
ns
C
MDA-MB-231 (Control- without Heat Shock)
DHE
LysoTracker
pJNK
Caspase
D
MDA-MB-231 (Heat Shock)
DHE
LysoTracker
pJNK
Caspase
E
PC3
Cell viability(%)
150
100
50
0
DMSO
5μM Doxo
CTL
SatIII antisense oligos

SUPPLEMENTARY DATA

Fig. S1: Gene Set Enrichment Analysis (GSEA) of *hsrω*^{66} mutant transcriptome

(A-I) Gene Set Enrichment Analysis (GSEA) plots displaying enrichment of gene ontology classes in *hsrω*^{66} (A-D), or wild type (E-H) transcriptomes, in *hsrω*^{66} versus wild type comparison. The X-axis represent ranked gene lists in descending order of expression (red is high, blue is low). Black bars mark the position of genes being queried (see Table S1 for gene list pertaining to the different GO classes). NES: Normalized Enrichment Score; p value is the Nominal p-value. The GSEA plots were generated using preprocessed data from previously published transcriptomes (Ray et al., 2019a).

Fig. S2: Loss of lncRNA *hsrω* disrupts cell homeostasis (A-B) Wing imaginal discs exhibiting enhanced staining for LysoTracker (A) and ProteoStat (B) in posterior compartment upon selective downregulation of *hsrω* (*en> UAS hsrω* RNAi GFP). (C-E) ROS levels (DHE) in wing imaginal discs from *hsrω*^{66} homozygous (C), *hsrω*^{66} heterozygous (D), and *en> UAS hsrω* RNAi GFP (E) larvae. Scale bars represent 100µm.

Fig. S3: *lgl* clones in *hsrω* heterozygous genetic background display neoplastic transformation

(A-D) wing disc from *hsrω*^{66}/+heterozygous larva carrying *lgl* clones (green, *lgl GFP;hsrω*^{66}/+), showing loss of junction protein Fas III (A). Clones in the distal (marked by pink broken line) wing display abundant cell death (Caspase-3, B); increase stain for MitoTracker (C), and, display non-uniform lipid droplets (Nile red, arrow). Scale bars represent 100µm.

Fig. S4: *lgl* clones with cell autonomous loss of *hsrω* (A) *lgl* clones with downregulation of *hsrω* (*lgl UAS hsrω RNAi GFP,* green) displaying loss of junctional protein Fas III (A, arrow). (B) *lgl* clones with downregulation of *ISWI* (*lgl UAS ISWI RNAi GFP,* green) exhibiting neoplastic transformation (disrupted F-Actin, B, arrow).

Fig. S5: Gene Set Enrichment Analysis (GSEA) of GO classes from transcriptomes of eye imaginal discs with up- or down-regulation of *hsrω*. (A, B) GSEA plots, displaying enrichment (top panels, A) or absence of enrichment (bottom panels, A) of gene ontology classes associated with protein homeostasis in *sev-Gal4> UAS-hsrω RNAi* vs *sev-Gal4*, and *sev-Gal4>EP3037* vs *sev-Gal4* transcriptomic data published earlier (Ray et al., 2019b). (B) GSEA pots displaying comparable trends in expression of genes interacting with different hnRNPs in larval eye discs with loss (top panel) or gain (lower panel) of *hsrω* activity based on the earlier published RNAseq profiles of larval eye discs (Ray et al., 2019b). The x-axis represents ranked gene lists in descending order of expression (red is high, blue is low). Black bars mark the position of genes being queried (see Table S3).

Fig. S6. Decrease in mRNA levels of sat III, as determined by Q-PCR, in Doxorubicin (5.0µM) treated PC3 cells. Error bars represent mean ± SEM. **P<0.001 for two-way ANOVA.

Tables S1. GSEA-list and ranking of genes in *hsrω*^{66} mutant vs wild type (Ray et al., 2019a)

Table displaying Gene Set Enrichment Analysis (GSEA) output containing list and ranking of genes (columns 2, 3, 4) in the transcriptome of *hsrω*^{66} mutant *vs* wild type (Ray et al., 2019a) for predefined gene sets belonging to different Gene Ontology classes pertaining to Fig. S1. The genes are ranked by their correlation to the phenotype under study, such that genes are that are positively correlated (up-regulated) in *hsrω*^{66} mutant transcriptome are ranked higher to genes are that are negatively correlated (down-regulated) in *hsrω*^{66} mutant. The genes are listed in descending order of their ranking. The degree of enrichment of a gene class is calculated using a cumulative running sum statistics, which provides an enrichment score (ES) (Columns, 5, 6). The ES is a positive score, when positively correlated with the *hsrω*^{66} phenotype; or a negative score when negatively correlated with the *hsrω*^{66} phenotype. Set of genes that contribute to the enrichment score form the core enrichment gene set. These are labelled as "yes" (column 7).

,

Tables S2 . GSEA- list and ranking of genes correlated with gain (*EP3037*) or loss (*UAS-hsrω RNAi*) of hsrω in the eye epithelium (Ray et al., 2019b).

Table displaying Gene Set Enrichment Analysis (GSEA) output containing list and ranking of genes (columns 2, 3, 4) in the transcriptome comparison of *sev-Gal4>UAS- hsrω RNAi vs sev-Gal4* (Ray et al., 2019b) and *sev-Gal4>EP3037 vs sev-Gal4* (Ray et al., 2019b)for predefined gene sets belonging to different Gene Ontology classes pertaining to Fig. S5A. The genes are ranked by their correlation to the phenotype under study, such that genes are that are positively correlated (up-regulated) in gain/or loss of *hsrω* are ranked higher to genes are that are negatively correlated (down-regulated) in gain/or loss of *hsrω*. The genes are listed in descending order of their ranking. The degree of enrichment of a gene class is calculated using a cumulative running sum statistics, which provides an enrichment score (ES) (Columns, 5, 6). The ES is a positive score, when positively correlated with the phenotype; or a negative score when negatively correlated with the phenotype. Set of genes that contribute to the enrichment score form the core enrichment gene set. These are labelled as "yes" (column 7).

Tables S3. GSEA- list and ranking of genes correlated with gain (*EP3037*) or loss (*UAS-hsrω RNAi*) of hsrω in the eye epithelium (Ray et al., 2019b)

Table displaying Gene Set Enrichment Analysis (GSEA) output containing list and ranking of genes (columns 2, 3, 4) in the transcriptome comparison of *sev-Gal4>UAS- hsrω RNAi vs sev-Gal4* (Ray et al., 2019b) and *sev-Gal4>EP3037 vs sev-Gal4* (Ray et al., 2019b)for predefined gene sets belonging to different Gene Ontology classes pertaining to Fig. S5B. The genes are ranked by their correlation to the phenotype under study, such that genes are that are positively correlated (up-regulated) in gain/or loss of *hsrω* transcriptome are ranked higher to genes are that are negatively correlated (down-regulated) in gain/or loss of *hsrω*. The genes are listed in descending order of their ranking. The degree of enrichment of a gene class is calculated using a cumulative running sum statistics, which provides an enrichment score (ES) (Columns, 5, 6).

The ES is a positive score, when positively correlated with the *hsrω*^{66} phenotype; or a negative score when negatively correlated with the *hsrω*^{66} phenotype. Set of genes that contributes to the enrichment score form the core enrichment gene set. These are labelled as "yes" (column 7).

Ray, M., Acharya, S., Shambhavi, S. and Lakhotia, S. C. (2019a). Over-expression of Hsp83 in grossly depleted hsrω lncRNA background causes synthetic lethality and l(2)gl phenocopy in Drosophila. *J Biosci* **44**, 36.

Ray, M., Singh, G. and Lakhotia, S. C. (2019b). Altered levels of hsromega lncRNAs further enhance Ras signaling during ectopically activated Ras induced R7 differentiation in Drosophila. *Gene Expr Patterns* **33**, 20–36.

Figure S1

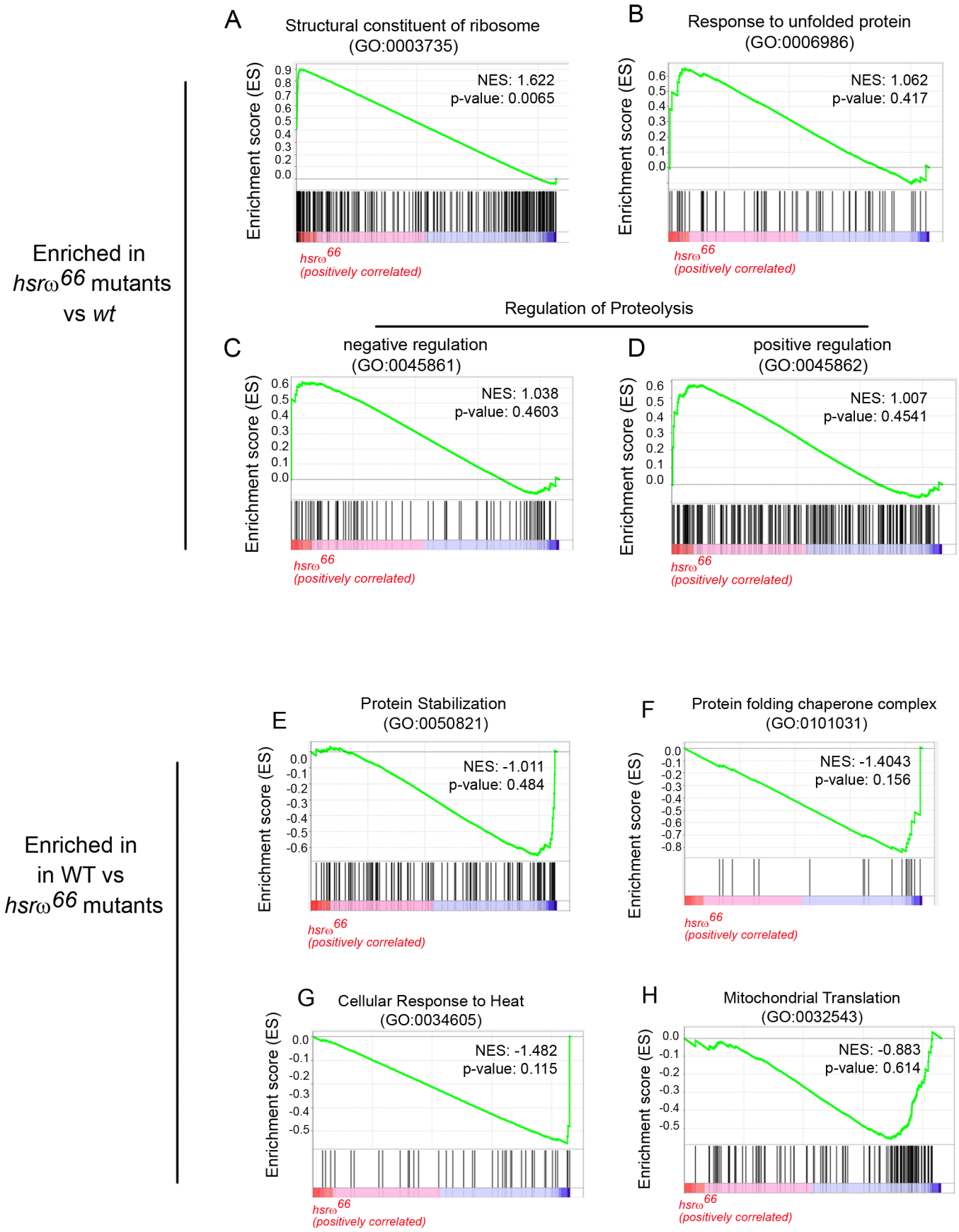
Enriched in
hsrω66 mutants
vs wt
A
Structural constituent of ribosome
(GO:0003735)
NES: 1.622
p-value: 0.0065
B
Response to unfolded protein
(GO:0006986)
NES: 1.062
p-value: 0.417
Regulation of Proteolysis
C
negative regulation
(GO:0045861)
NES: 1.038
p-value: 0.4603
D
positive regulation
(GO:0045862)
NES: 1.007
p-value: 0.4541
Enriched in
in WT vs
hsrω66 mutants
E
Protein Stabilization
(GO:0050821)
NES: -1.011
p-value: 0.484
F
Protein folding chaperone complex
(GO:0101031)
NES: -1.4043
p-value: 0.156
G
Cellular Response to Heat
(GO:0034605)
NES: -1.482
p-value: 0.115
H
Mitochondrial Translation
(GO:0032543)
NES: -0.883
p-value: 0.614
Enrichment score (ES)
hsrω66
(positively correlated)

Figure S2

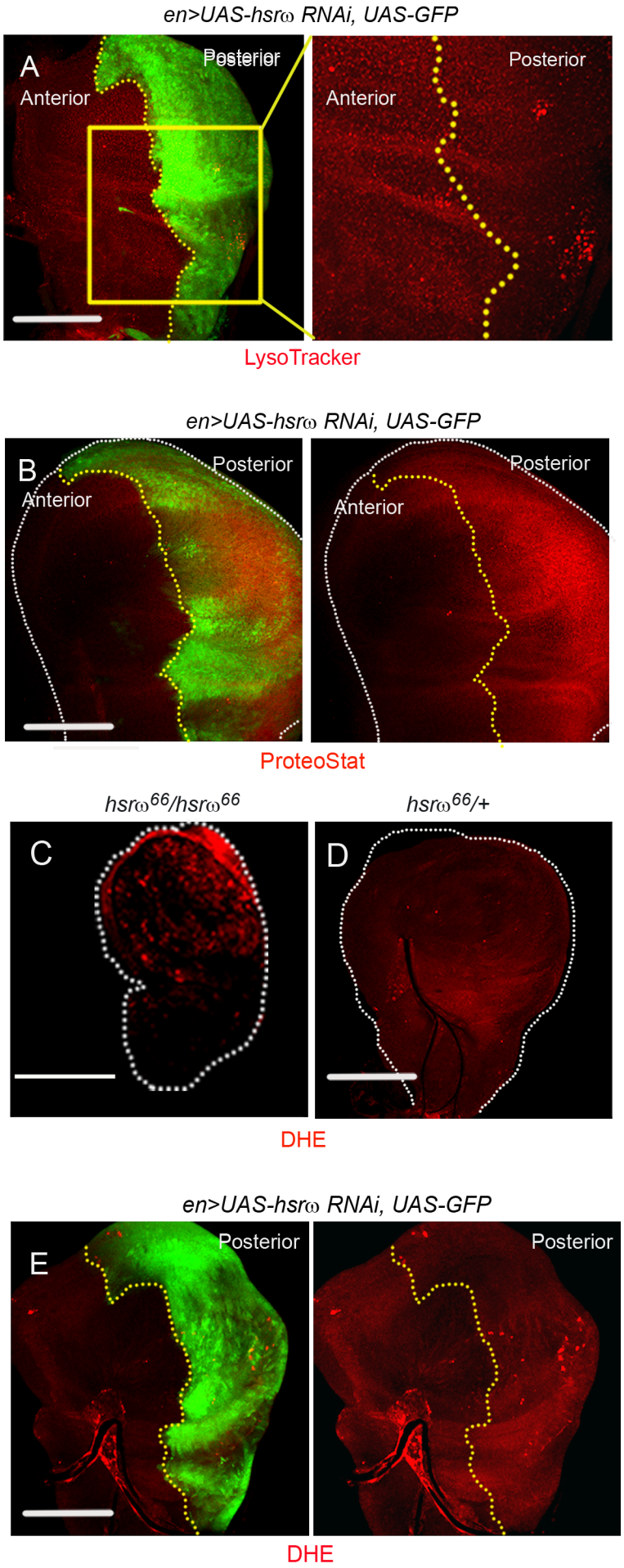
en>UAS-hsrω RNAi, UAS-GFP
A
Anterior
Posterior
Anterior
Posterior
LysoTracker
en>UAS-hsrω RNAi, UAS-GFP
B
Anterior
Posterior
Anterior
Posterior
ProteoStat
hsrω66/hsrω66
hsrω66/+
C
D
DHE
en>UAS-hsrω RNAi, UAS-GFP
E
Posterior
Posterior
DHE

Figure S3

lgl^{4}/*lgl*^{4}*UAS-GFP; hsr*ω^{66}/+ in *hsr*ω^{66}/+ genetic background

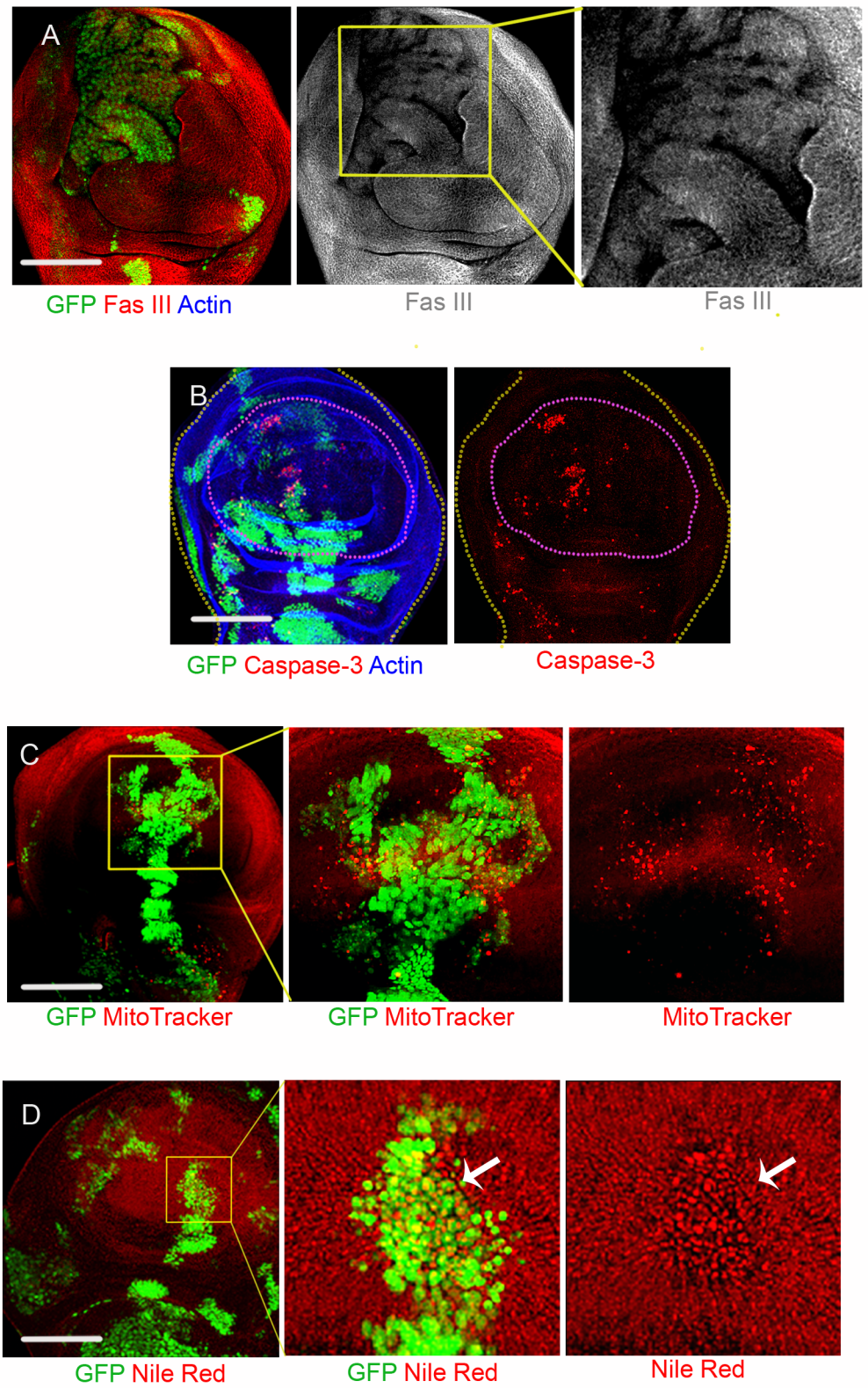

Figure S4

lgl UAS-GFP; UAS-hsrω RNAi

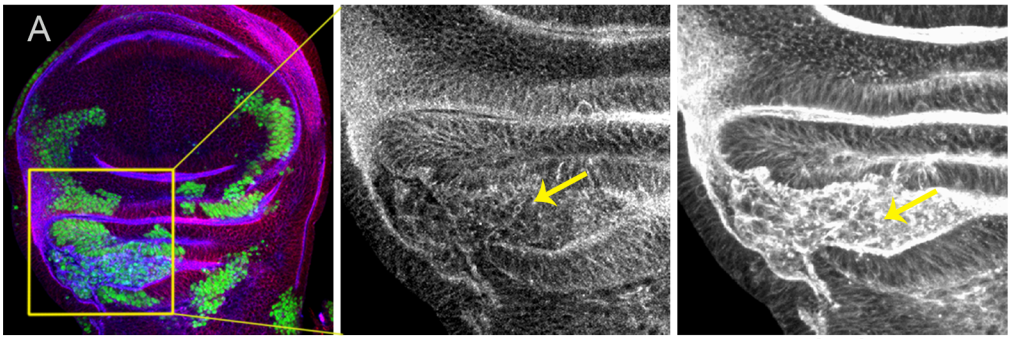

GFP Fas III Actin Fas III Actin

lgl UAS-GFP; UAS-ISWI RNAi

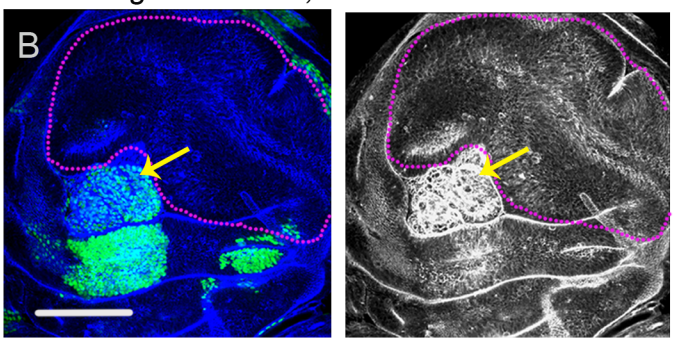

GFP Actin Actin

Figure S5

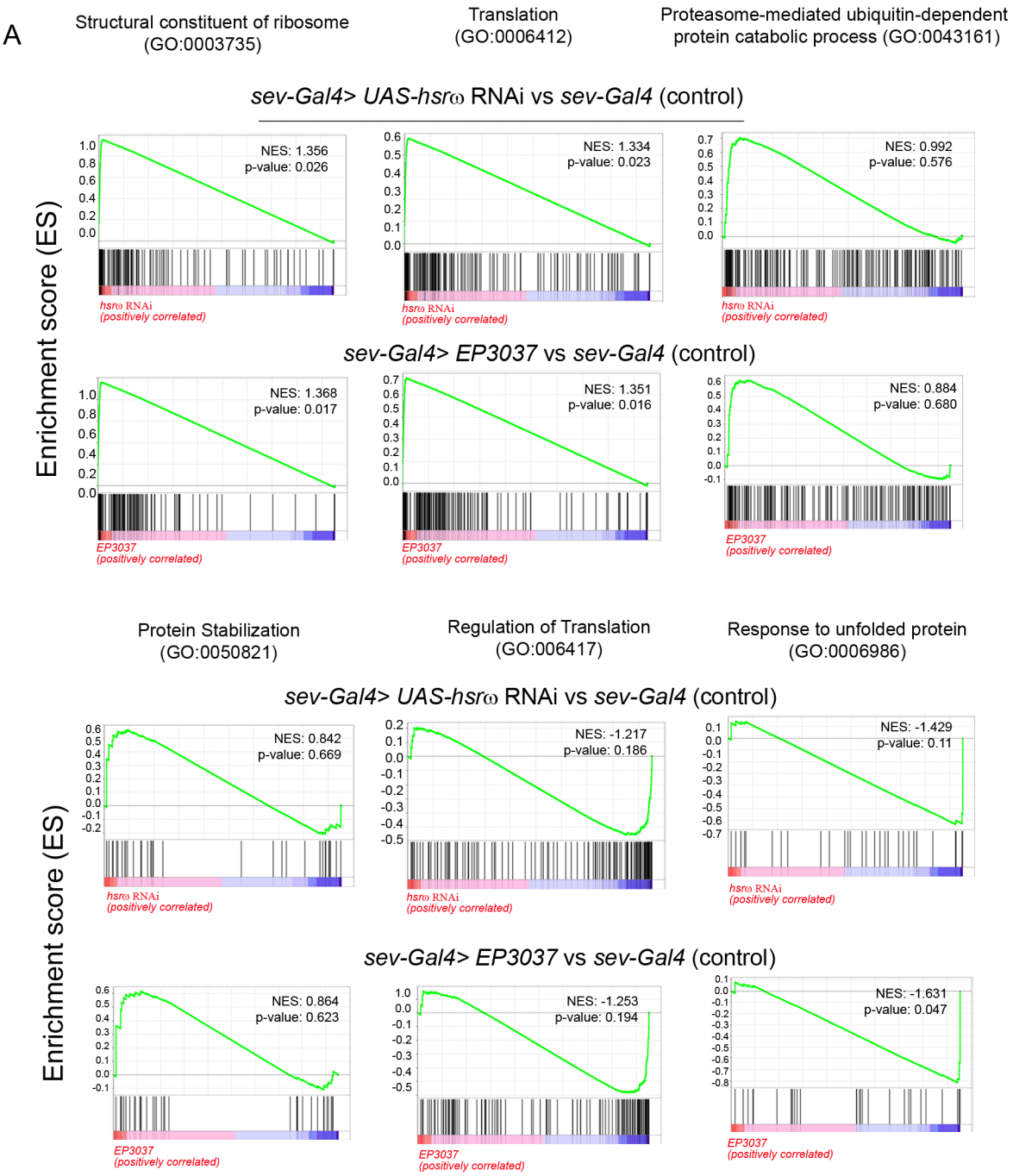
A
Structural constituent of ribosome (GO:0003735)
Translation (GO:0006412)
Proteasome-mediated ubiquitin-dependent protein catabolic process (GO:0043161)
sev-Gal4> UAS-hsrω RNAi vs sev-Gal4 (control)
NES: 1.356
p-value: 0.026
NES: 1.334
p-value: 0.023
NES: 0.992
p-value: 0.576
hsrω RNAi (positively correlated)
sev-Gal4> EP3037 vs sev-Gal4 (control)
NES: 1.368
p-value: 0.017
NES: 1.351
p-value: 0.016
NES: 0.884
p-value: 0.680
EP3037 (positively correlated)
Enrichment score (ES)
Protein Stabilization (GO:0050821)
Regulation of Translation (GO:006417)
Response to unfolded protein (GO:0006986)
sev-Gal4> UAS-hsrω RNAi vs sev-Gal4 (control)
NES: 0.842
p-value: 0.669
NES: -1.217
p-value: 0.186
NES: -1.429
p-value: 0.11
hsrω RNAi (positively correlated)
sev-Gal4> EP3037 vs sev-Gal4 (control)
NES: 0.864
p-value: 0.623
NES: -1.253
p-value: 0.194
NES: -1.631
p-value: 0.047
EP3037 (positively correlated)
Enrichment score (ES)

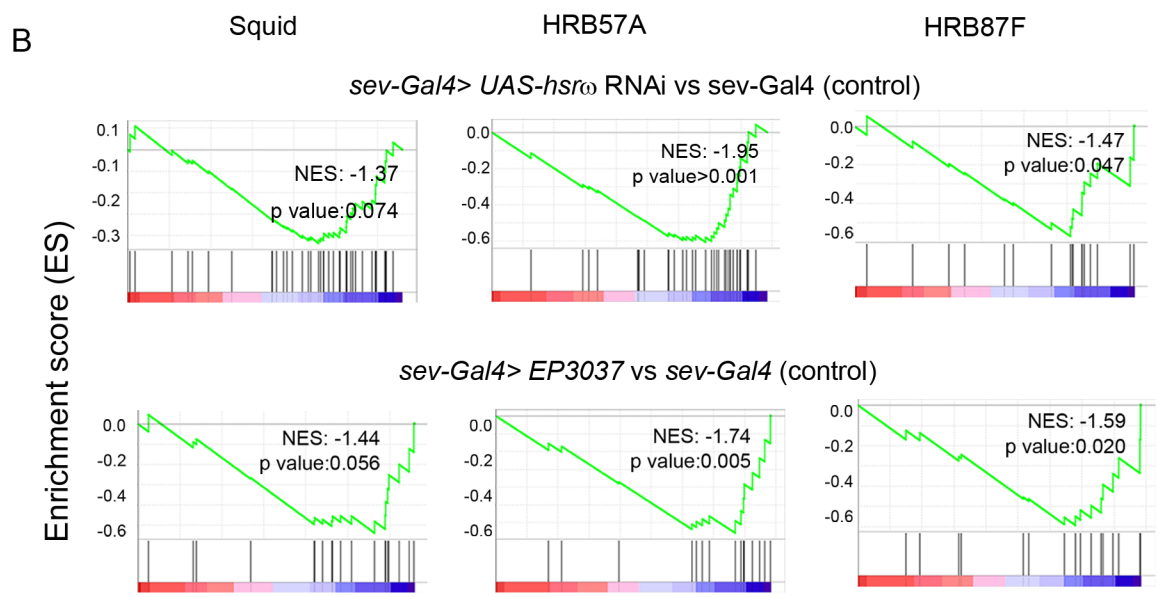
B
Squid
HRB57A
HRB87F
sev-Gal4> UAS-hsrω RNAi vs sev-Gal4 (control)
NES: -1.37
p value:0.074
NES: -1.95
p value>0.001
NES: -1.47
p value:0.047
sev-Gal4> EP3037 vs sev-Gal4 (control)
NES: -1.44
p value:0.056
NES: -1.74
p value:0.005
NES: -1.59
p value:0.020
Enrichment score (ES)

Figure S6

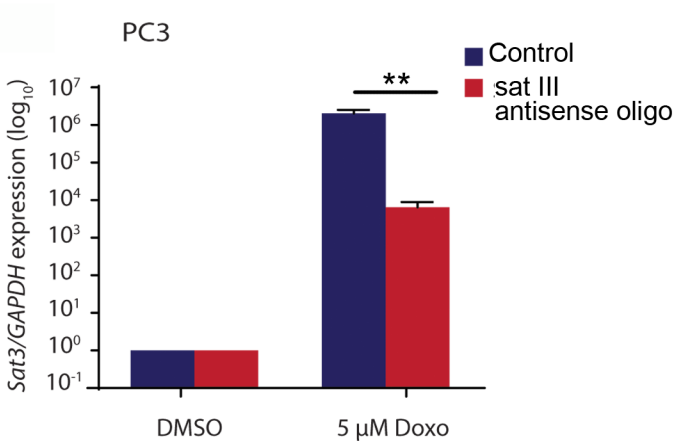
PC3
Control
sat III
antisense oligo
**
Sat3/GAPDH expression (log10)
10^7
10^6
10^5
10^4
10^3
10^2
10^1
10^0
10^-1
DMSO
5 µM Doxo

Table S1

GO 0003735 Structural Constituent of ribosome						
Sp/CyO; hsrω^{66} vs Oregon R+ (WT)						
NAME	SYMBOL	TITLE	RANK IN GENE LIST	RANK METRIC SCORE	RUNNING ES	CORE ENRICHMENT
row_0	TCONS_00039981	mt:lrRNA	0	11328.000	0.412	Yes
row_1	TCONS_00000138	RpLP1	42	495.160	0.428	Yes
row_2	TCONS_00019088	RpL15	47	440.140	0.444	Yes
row_3	TCONS_00024060	RpL3	52	422.370	0.459	Yes
row_4	TCONS_00015113	RpL39	64	346.110	0.471	Yes
row_5	TCONS_00010624	RpS16	65	338.850	0.483	Yes
row_6	TCONS_00018298	RpL26	66	330.960	0.495	Yes
row_7	TCONS_00017545	RpS4	69	324.440	0.507	Yes
row_8	TCONS_00027131	RpS8	70	323.530	0.519	Yes
row_9	TCONS_00039004	RpS5a	71	323.110	0.531	Yes
row_10	TCONS_00013257	RpS23	72	318.530	0.542	Yes
row_11	TCONS_00004515	RpL27A	75	309.980	0.553	Yes
row_12	TCONS_00031992	RpL6	77	302.448	0.564	Yes
row_13	TCONS_00008187	RpL31	79	295.240	0.575	Yes
row_14	TCONS_00031790	RpS7	81	284.130	0.585	Yes
row_15	TCONS_00023197	RpL13A	85	277.150	0.595	Yes
row_16	TCONS_00010698	RpL23	86	276.920	0.605	Yes
row_17	TCONS_00000905	RpL37A	87	266.120	0.615	Yes
row_18	TCONS_00016818	RpL14	90	255.600	0.624	Yes
row_19	TCONS_00037308	RpS6	91	253.600	0.633	Yes
row_20	TCONS_00020333	RpL18	94	244.750	0.642	Yes
row_21	TCONS_00036282	RpL36	95	242.844	0.651	Yes
row_22	TCONS_00007368	RpL21	96	240.980	0.660	Yes
row_23	TCONS_00009471	RpLP2	97	240.300	0.669	Yes
row_24	TCONS_00001834	RpL13	102	232.040	0.677	Yes
row_25	TCONS_00020782	RpS17	103	230.700	0.685	Yes
row_26	TCONS_00015286	RpL19	104	226.010	0.693	Yes
row_27	TCONS_00010110	RpL11	109	215.450	0.701	Yes
row_28	TCONS_00036296	RpL22	112	212.074	0.709	Yes
row_29	TCONS_00035388	RpS19a	114	206.900	0.716	Yes
row_30	TCONS_00036395	sta	116	200.880	0.723	Yes
row_31	TCONS_00015800	RpL8	119	196.510	0.730	Yes
row_32	TCONS_00025590	RpS30	120	196.100	0.738	Yes
row_33	TCONS_00011251	RpL38	125	181.760	0.744	Yes
row_34	TCONS_00037103	RpL7A	132	176.640	0.750	Yes
row_35	TCONS_00033879	RpS14a	134	175.230	0.756	Yes
row_36	TCONS_00010955	RpL12	136	173.200	0.763	Yes
row_37	TCONS_00020806	RpS9	142	164.770	0.769	Yes
row_38	TCONS_00028799	RpS25	143	163.390	0.774	Yes
row_39	TCONS_00010219	RpS18	145	160.242	0.780	Yes
row_40	TCONS_00022857	RpL10	146	159.610	0.786	Yes
row_41	TCONS_00019710	RpL28	148	157.239	0.792	Yes
row_42	TCONS_00001859	RpL7	149	155.450	0.797	Yes
row_43	TCONS_00031760	RpL32	151	153.820	0.803	Yes
row_44	TCONS_00028454	RpL34b	152	153.068	0.808	Yes
row_45	TCONS_00000511	RpS21	154	150.710	0.814	Yes
row_46	TCONS_00018834	RpLP0	155	148.530	0.819	Yes
row_47	TCONS_00006207	RpL24	156	145.070	0.825	Yes
row_48	TCONS_00026854	RpL4	169	130.213	0.829	Yes
row_49	TCONS_00031090	RpS27	172	126.590	0.833	Yes
row_50	TCONS_00037133	RpL17	173	126.546	0.838	Yes
row_51	TCONS_00013710	RpS15	180	122.190	0.842	Yes
row_52	TCONS_00005600	RpS2	181	121.549	0.846	Yes
row_53	TCONS_00010217	RpS18	182	121.480	0.851	Yes
row_54	TCONS_00033540	RpL35	183	120.852	0.855	Yes
row_55	TCONS_00033881	RpS14b	190	114.691	0.859	Yes
row_56	TCONS_00006884	RpL30	196	107.730	0.863	Yes

row_57	TCONS_00032365	RpS3A	206	102.460	0.866	Yes
row_58	TCONS_00023897	RpS29	211	98.510	0.870	Yes
row_59	TCONS_00026061	RpS3	230	80.280	0.872	Yes
row_60	TCONS_00005866	RpL9	232	79.250	0.874	Yes
row_61	TCONS_00010414	RpL29	233	78.730	0.877	Yes
row_62	TCONS_00014803	RpS24	259	64.690	0.878	Yes
row_63	TCONS_00000510	RpS21	265	62.328	0.880	Yes
row_64	TCONS_00017540	RpS12	280	57.030	0.882	Yes
row_65	TCONS_00013915	RpL18A	282	55.970	0.884	Yes
row_66	TCONS_00005289	RpL36A	285	54.380	0.886	Yes
row_67	TCONS_00031169	RpL27	293	53.680	0.887	Yes
row_68	TCONS_00020331	RpL18	307	49.731	0.889	Yes
row_69	TCONS_00012798	RpS11	314	48.860	0.890	Yes
row_70	TCONS_00037105	RpL7A	334	44.628	0.891	Yes
row_71	TCONS_00038213	RpS15Aa	346	42.720	0.892	Yes
row_72	TCONS_00026062	RpS3	347	42.528	0.893	Yes
row_73	TCONS_00017367	RpL10Ab	358	39.080	0.894	Yes
row_74	TCONS_00025578	RpS20	361	38.630	0.896	Yes
row_75	TCONS_00027781	RpL35A	364	37.700	0.897	Yes
row_76	TCONS_00005288	RpL36A	398	32.815	0.897	No
row_77	TCONS_00038212	RpS15Aa	493	23.970	0.893	No
row_78	TCONS_00005864	RpL9	525	21.978	0.892	No
row_79	TCONS_00005393	RpS13	589	18.447	0.890	No
row_80	TCONS_00028826	RpL24-like	592	18.408	0.891	No
row_81	TCONS_00034161	RpS28b	610	17.439	0.890	No
row_82	TCONS_00033539	RpL35	614	17.320	0.891	No
row_83	TCONS_00035831	RpS10b	621	17.006	0.891	No
row_84	TCONS_00023896	RpS29	662	15.769	0.890	No
row_85	TCONS_00027132	RpS8	690	14.920	0.889	No
row_86	TCONS_00037131	RpL17	847	11.381	0.882	No
row_87	TCONS_00038209	RpS15Aa	915	10.020	0.879	No
row_88	TCONS_00020804	RpS9	935	9.695	0.879	No
row_89	TCONS_00031168	RpL27	1048	8.199	0.874	No
row_90	TCONS_00019083	RpL15	1055	8.156	0.874	No
row_91	TCONS_00013256	RpS23	1057	8.148	0.874	No
row_92	TCONS_00028451	RpL34b	1073	7.922	0.874	No
row_93	TCONS_00000514	RpS21	1115	7.544	0.872	No
row_94	TCONS_00001835	RpL13	1159	7.261	0.870	No
row_95	TCONS_00032366	RpS3A	1413	5.581	0.859	No
row_96	TCONS_00010111	RpL11	1421	5.535	0.859	No
row_97	TCONS_00022856	RpL10	1471	5.288	0.856	No
row_98	TCONS_00031791	RpS7	1487	5.244	0.856	No
row_99	TCONS_00014892	RpL37b	1513	5.091	0.855	No
row_100	TCONS_00038459	RpL37a	1527	5.031	0.854	No
row_101	TCONS_00006780	RpS26	1598	4.750	0.851	No
row_102	TCONS_00006206	RpL24	1718	4.427	0.846	No
row_103	TCONS_00011250	RpL38	1775	4.265	0.843	No
row_104	TCONS_00015285	RpL19	1889	3.981	0.838	No
row_105	TCONS_00019085	RpL15	1902	3.949	0.838	No
row_106	TCONS_00025589	RpS30	2009	3.683	0.833	No
row_107	TCONS_00016174	mRpS6	2089	3.511	0.829	No
row_108	TCONS_00017993	mRpS34	2126	3.444	0.828	No
row_109	TCONS_00006778	RpS26	2199	3.305	0.825	No
row_110	TCONS_00025828	mRpL35	2479	2.842	0.811	No
row_111	TCONS_00012800	RpS11	2547	2.752	0.808	No
row_112	TCONS_00006781	RpS26	2585	2.697	0.807	No
row_113	TCONS_00035153	mRpS30	2589	2.692	0.807	No
row_114	TCONS_00000139	RpLP1	2596	2.682	0.807	No
row_115	TCONS_00006208	RpL24	2636	2.612	0.805	No
row_116	TCONS_00022244	mRpL21	2648	2.601	0.804	No
row_117	TCONS_00010957	RpL12	2712	2.523	0.801	No
row_118	TCONS_00019706	RpL28	2731	2.506	0.801	No
row_119	TCONS_00034698	mRpL49	2756	2.483	0.800	No

row_120	TCONS_00017368	RpL10Ab	2765	2.475	0.799	No
row_121	TCONS_00036393	sta	2824	2.417	0.797	No
row_122	TCONS_00020807	RpS9	2953	2.259	0.791	No
row_123	TCONS_00006539	mRpL4	3097	2.123	0.784	No
row_124	TCONS_00035391	RpS19a	3296	1.962	0.775	No
row_125	TCONS_00033538	RpL35	3377	1.896	0.771	No
row_126	TCONS_00019032	mRpS5	3635	1.740	0.759	No
row_127	TCONS_00000860	mRpL28	3712	1.697	0.756	No
row_128	TCONS_00037132	RpL17	3740	1.681	0.754	No
row_129	TCONS_00023626	mRpL1	3754	1.672	0.754	No
row_130	TCONS_00031761	RpL32	3809	1.646	0.751	No
row_131	TCONS_00000513	RpS21	3991	1.548	0.743	No
row_132	TCONS_00018297	RpL26	4052	1.515	0.740	No
row_133	TCONS_00011866	mRpL52	4246	1.414	0.731	No
row_134	TCONS_00032960	mRpL16	4271	1.403	0.730	No
row_135	TCONS_00037101	RpL7A	4316	1.385	0.728	No
row_136	TCONS_00010356	mRpL54	4346	1.369	0.727	No
row_137	TCONS_00029402	RpS5b	4643	1.244	0.713	No
row_138	TCONS_00031254	RpL34a	4781	1.197	0.706	No
row_139	TCONS_00038210	RpS15Aa	4791	1.194	0.706	No
row_140	TCONS_00025968	mRpL45	4899	1.155	0.701	No
row_141	TCONS_00018299	RpL26	5003	1.124	0.696	No
row_142	TCONS_00000904	RpL37A	5094	1.095	0.692	No
row_143	TCONS_00014781	mRpS29	5177	1.066	0.688	No
row_144	TCONS_00027129	RpS8	5207	1.057	0.687	No
row_145	TCONS_00039005	RpS5a	5717	0.917	0.663	No
row_146	TCONS_00010623	RpS16	5744	0.911	0.662	No
row_147	TCONS_00035390	RpS19a	5946	0.858	0.652	No
row_148	TCONS_00006777	RpS26	6091	0.824	0.645	No
row_149	TCONS_00019705	RpL28	6224	0.794	0.639	No
row_150	TCONS_00027227	mRpS18C	6227	0.793	0.639	No
row_151	TCONS_00006883	RpL30	6249	0.790	0.638	No
row_152	TCONS_00000906	RpL37A	6264	0.787	0.638	No
row_153	TCONS_00000324	mRpL48	6338	0.772	0.634	No
row_154	TCONS_00000323	mRpL48	6465	0.746	0.628	No
row_155	TCONS_00007369	RpL21	6669	0.702	0.619	No
row_156	TCONS_00026191	cav	6675	0.699	0.618	No
row_157	TCONS_00015801	RpL8	7085	0.612	0.599	No
row_158	TCONS_00026830	RpS10a	7304	0.575	0.589	No
row_159	TCONS_00019090	RpL15	7370	0.562	0.586	No
row_160	TCONS_00004520	mRpL27	8007	0.449	0.556	No
row_161	TCONS_00039339	mRpS14	8111	0.430	0.551	No
row_162	TCONS_00028453	RpL34b	8383	0.385	0.538	No
row_163	TCONS_00039340	mRpS14	8456	0.373	0.535	No
row_164	TCONS_00013434	mRpL41	8924	0.289	0.513	No
row_165	TCONS_00026189	cav	8964	0.284	0.511	No
row_166	TCONS_00019033	mRpS5	9356	0.223	0.493	No
row_167	TCONS_00008189	RpL31	9651	0.174	0.479	No
row_168	TCONS_00036473	CG14817	9868	0.139	0.469	No
row_169	TCONS_00005601	RpS2	9919	0.131	0.466	No
row_170	TCONS_00031091	RpS27	10072	0.106	0.459	No
row_171	TCONS_00017547	RpS4	10136	0.095	0.456	No
row_172	TCONS_00008188	RpL31	10153	0.091	0.455	No
row_173	TCONS_00007076	mRpS18B	10314	0.064	0.448	No
row_174	TCONS_00037135	RpL17	10352	0.057	0.446	No
row_175	TCONS_00001750	RpS28-like	10650	0.013	0.432	No
row_176	TCONS_00023198	RpL13A	10750	-0.005	0.427	No
row_177	TCONS_00020334	mRpL50	10828	-0.019	0.424	No
row_178	TCONS_00035833	RpS10b	10846	-0.022	0.423	No
row_179	TCONS_00037309	RpS6	10908	-0.033	0.420	No
row_180	TCONS_00025012	mRpS11	10919	-0.035	0.420	No
row_181	TCONS_00030580	CG31156	11365	-0.105	0.399	No
row_182	TCONS_00024059	RpL3	11373	-0.106	0.398	No

row_183	TCONS_00028285	mRpS18A	11444	-0.115	0.395	No
row_184	TCONS_00014907	RpL22-like	11641	-0.148	0.386	No
row_185	TCONS_00032363	RpS3A	11702	-0.156	0.383	No
row_186	TCONS_00004519	mRpL27	11934	-0.189	0.372	No
row_187	TCONS_00015398	mRpL17	11937	-0.189	0.372	No
row_188	TCONS_00013711	RpS15	12056	-0.205	0.366	No
row_189	TCONS_00001917	mRpS7	12255	-0.239	0.357	No
row_190	TCONS_00023196	RpL13A	12310	-0.247	0.355	No
row_191	TCONS_00024625	mRpS10	12766	-0.322	0.333	No
row_192	TCONS_00024062	RpL3	12871	-0.341	0.328	No
row_193	TCONS_00000859	mRpL28	13264	-0.409	0.310	No
row_194	TCONS_00036630	tko	13349	-0.420	0.306	No
row_195	TCONS_00026192	cav	13534	-0.450	0.297	No
row_196	TCONS_00019086	RpL15	13770	-0.493	0.286	No
row_197	TCONS_00019708	RpL28	14222	-0.564	0.265	No
row_198	TCONS_00019089	RpL15	14267	-0.572	0.263	No
row_199	TCONS_00031789	RpS7	14330	-0.584	0.260	No
row_200	TCONS_00039006	RpS5a	14478	-0.612	0.253	No
row_201	TCONS_00006882	RpL30	14519	-0.619	0.251	No
row_202	TCONS_00026190	cav	14550	-0.627	0.250	No
row_203	TCONS_00017546	RpS4	14902	-0.699	0.233	No
row_204	TCONS_00000095	mRpL10	15067	-0.733	0.226	No
row_205	TCONS_00020525	mRpL36	15521	-0.831	0.204	No
row_206	TCONS_00004603	mRpS2	15563	-0.844	0.202	No
row_207	TCONS_00007367	RpL21	15576	-0.847	0.202	No
row_208	TCONS_00000746	RpL40	15742	-0.882	0.194	No
row_209	TCONS_00006852	CG10602	15906	-0.925	0.186	No
row_210	TCONS_00017889	mRpS31	15957	-0.937	0.184	No
row_211	TCONS_00005392	RpS13	16123	-0.979	0.176	No
row_212	TCONS_00010852	mRpL43	16326	-1.040	0.167	No
row_213	TCONS_00015685	mRpL46	16399	-1.062	0.163	No
row_214	TCONS_00018223	mRpS26	16403	-1.063	0.163	No
row_215	TCONS_00037104	RpL7A	16520	-1.098	0.158	No
row_216	TCONS_00030833	RpS19b	16718	-1.165	0.149	No
row_217	TCONS_00018833	RpLP0	16782	-1.183	0.146	No
row_218	TCONS_00036472	CG14817	16990	-1.256	0.136	No
row_219	TCONS_00036285	RpL36	17024	-1.266	0.135	No
row_220	TCONS_00031758	RpL32	17215	-1.338	0.126	No
row_221	TCONS_00038361	mRpS25	17259	-1.359	0.124	No
row_222	TCONS_00031255	RpL34a	17343	-1.396	0.120	No
row_223	TCONS_00028746	mRpL37	17351	-1.399	0.119	No
row_224	TCONS_00015397	mRpL17	17399	-1.417	0.117	No
row_225	TCONS_00010956	RpL12	17425	-1.428	0.116	No
row_226	TCONS_00036607	mRpL14	17458	-1.445	0.115	No
row_227	TCONS_00030070	mRpL55	17603	-1.518	0.108	No
row_228	TCONS_00021319	mRpL20	17631	-1.534	0.107	No
row_229	TCONS_00030904	mRpS24	17785	-1.622	0.100	No
row_230	TCONS_00021548	mRpL39	17831	-1.644	0.098	No
row_231	TCONS_00029165	mRpS21	17871	-1.666	0.096	No
row_232	TCONS_00024688	mRpL9	17935	-1.705	0.093	No
row_233	TCONS_00036284	RpL36	18059	-1.781	0.087	No
row_234	TCONS_00036629	tko	18103	-1.801	0.085	No
row_235	TCONS_00035832	RpS10b	18140	-1.829	0.084	No
row_236	TCONS_00024093	mRpL40	18142	-1.830	0.084	No
row_237	TCONS_00007077	mRpS18B	18177	-1.858	0.082	No
row_238	TCONS_00010416	RpL29	18213	-1.883	0.080	No
row_239	TCONS_00008979	mRpL53	18219	-1.890	0.080	No
row_240	TCONS_00028178	mRpS9	18240	-1.910	0.079	No
row_241	TCONS_00034947	mRpL38	18348	-1.996	0.074	No
row_242	TCONS_00024546	mRpL11	18406	-2.050	0.072	No
row_243	TCONS_00023673	mRpL19	18473	-2.101	0.069	No
row_244	TCONS_00000512	RpS21	18481	-2.112	0.069	No
row_245	TCONS_00024604	RpL10Aa	18527	-2.157	0.066	No

row_246	TCONS_00022498	mRpL15	18666	-2.295	0.060	No
row_247	TCONS_00019551	mRpL23	18720	-2.370	0.058	No
row_248	TCONS_00033880	RpS14a	18750	-2.400	0.056	No
row_249	TCONS_00004628	mRpL24	18821	-2.486	0.053	No
row_250	TCONS_00032959	mRpL16	18836	-2.501	0.053	No
row_251	TCONS_00008810	mRpL18	18856	-2.518	0.052	No
row_252	TCONS_00036606	mRpL14	18926	-2.589	0.049	No
row_253	TCONS_00016175	mRpS6	18947	-2.619	0.048	No
row_254	TCONS_00015832	mRpS35	18994	-2.690	0.046	No
row_255	TCONS_00004521	mRpL27	19037	-2.757	0.044	No
row_256	TCONS_00027352	mRpL32	19057	-2.782	0.043	No
row_257	TCONS_00035152	mRpS30	19062	-2.796	0.043	No
row_258	TCONS_00035147	mRpL3	19075	-2.811	0.042	No
row_259	TCONS_00035424	mRpL22	19086	-2.832	0.042	No
row_260	TCONS_00025591	RpS30	19098	-2.845	0.042	No
row_261	TCONS_00017254	mRpL2	19101	-2.847	0.042	No
row_262	TCONS_00009354	mRpL34	19116	-2.859	0.041	No
row_263	TCONS_00008473	RpS15Ab	19138	-2.917	0.040	No
row_264	TCONS_00027782	mRpL44	19174	-2.977	0.039	No
row_265	TCONS_00026853	mRpS22	19260	-3.123	0.035	No
row_266	TCONS_00035389	RpS19a	19286	-3.182	0.034	No
row_267	TCONS_00029166	mRpS21	19315	-3.218	0.033	No
row_268	TCONS_00037134	RpL17	19337	-3.274	0.032	No
row_269	TCONS_00012400	RpLP0-like	19404	-3.391	0.029	No
row_270	TCONS_00006254	mRpS23	19492	-3.595	0.025	No
row_271	TCONS_00010637	bonsai	19516	-3.638	0.024	No
row_272	TCONS_00036392	sta	19580	-3.811	0.021	No
row_273	TCONS_00028478	mRpL47	19656	-4.012	0.018	No
row_274	TCONS_00001833	RpL13	19708	-4.135	0.015	No
row_275	TCONS_00022245	mRpL21	19868	-4.668	0.008	No
row_276	TCONS_00006853	mRpL13	19910	-4.829	0.006	No
row_277	TCONS_00037074	CG11700	20034	-5.268	0.001	No
row_278	TCONS_00036394	sta	20099	-5.556	-0.002	No
row_279	TCONS_00001916	mRpS7	20107	-5.607	-0.002	No
row_280	TCONS_00008272	mRpL42	20129	-5.732	-0.003	No
row_281	TCONS_00001858	RpL7	20174	-5.935	-0.005	No
row_282	TCONS_00015134	mRpS17	20178	-5.962	-0.005	No
row_283	TCONS_00024624	mRpS10	20214	-6.189	-0.006	No
row_284	TCONS_00020332	RpL18	20265	-6.506	-0.008	No
row_285	TCONS_00006851	CG10602	20333	-6.918	-0.011	No
row_286	TCONS_00024061	RpL3	20364	-7.174	-0.012	No
row_287	TCONS_00028798	RpS25	20412	-7.548	-0.014	No
row_288	TCONS_00038460	RpL37a	20416	-7.590	-0.014	No
row_289	TCONS_00033411	mRpL30	20440	-7.742	-0.015	No
row_290	TCONS_00029648	mRpS33	20441	-7.743	-0.015	No
row_291	TCONS_00004517	RpL27A	20466	-8.043	-0.016	No
row_292	TCONS_00036286	RpL36	20477	-8.170	-0.016	No
row_293	TCONS_00005434	mRpL51	20484	-8.238	-0.016	No
row_294	TCONS_00013253	mRpS16	20488	-8.271	-0.016	No
row_295	TCONS_00007373	RpL5	20497	-8.333	-0.016	No
row_296	TCONS_00006850	CG10602	20548	-8.866	-0.018	No
row_297	TCONS_00031788	RpS7	20553	-8.946	-0.018	No
row_298	TCONS_00014065	mRpS28	20673	-10.600	-0.023	No
row_299	TCONS_00007372	RpL5	20693	-10.979	-0.023	No
row_300	TCONS_00016879	mRpL12	20739	-11.904	-0.025	No
row_301	TCONS_00036841	mRpL33	20782	-12.581	-0.027	No
row_302	TCONS_00031253	RpL34a	20796	-12.789	-0.027	No
row_303	TCONS_00019084	RpL15	20898	-15.640	-0.031	No
row_304	TCONS_00022858	RpL10	20899	-15.839	-0.030	No
row_305	TCONS_00005865	RpL9	20911	-16.370	-0.030	No
row_306	TCONS_00019409	RpL23A	20929	-16.857	-0.030	No
row_307	TCONS_00031171	RpL27	20996	-19.052	-0.033	No
row_308	TCONS_00031991	RpL6	21044	-21.124	-0.034	No

row_309	TCONS_00034160	RpS28b	21081	-23.850	-0.035	No
row_310	TCONS_00036283	RpL36	21095	-25.010	-0.035	No
row_311	TCONS_00010415	RpL29	21100	-25.356	-0.034	No
row_312	TCONS_00027130	RpS8	21128	-28.239	-0.034	No
row_313	TCONS_00005602	RpS2	21203	-36.331	-0.037	No
row_314	TCONS_00004516	RpL27A	21225	-39.068	-0.036	No
row_315	TCONS_00001944	RpS27A	21234	-40.490	-0.035	No
row_316	TCONS_00005394	RpS13	21292	-59.010	-0.036	No
row_317	TCONS_00000745	RpL40	21313	-68.730	-0.034	No
row_318	TCONS_00007374	RpL5	21456	-372.880	-0.027	No
row_319	TCONS_00015256	RpL41	21492	-837.649	0.002	No
GO:0006986 Response to unfolded protein						
Sp/CyO; hsrω^{66} *vs* Oregon R+ (WT)						
NAME	**SYMBOL**	**TITLE**	**RANK IN GENE LIST**	**RANK METRIC SCORE**	**RUNNING ES**	**CORE ENRICHMENT**
row_0	TCONS_00024627	Hsc70-4	139	168.630	0.384	Yes
row_1	TCONS_00003542	crc	304	50.387	0.493	Yes
row_2	TCONS_00030872	Hsp68	765	13.189	0.502	Yes
row_3	TCONS_00037988	Hsc70-3	778	12.852	0.531	Yes
row_4	TCONS_00003918	Spp	779	12.837	0.561	Yes
row_5	TCONS_00037985	Hsc70-3	897	10.296	0.580	Yes
row_6	TCONS_00005237	Herp	906	10.156	0.603	Yes
row_7	TCONS_00010378	Xbp1	983	9.041	0.620	Yes
row_8	TCONS_00027429	sip3	1136	7.374	0.630	Yes
row_9	TCONS_00010377	Xbp1	1147	7.319	0.647	Yes
row_10	TCONS_00024354	Hsc70-2	1386	5.689	0.649	Yes
row_11	TCONS_00026084	Gba1a	1750	4.322	0.642	No
row_12	TCONS_00036498	Edem1	2721	2.513	0.602	No
row_13	TCONS_00002372	Edem2	2773	2.466	0.606	No
row_14	TCONS_00037986	Hsc70-3	2835	2.404	0.608	No
row_15	TCONS_00030983	REPTOR	2906	2.316	0.611	No
row_16	TCONS_00030991	REPTOR	2911	2.313	0.616	No
row_17	TCONS_00030589	wfs1	3201	2.038	0.607	No
row_18	TCONS_00020568	CG7182	3926	1.584	0.577	No
row_19	TCONS_00029660	Der-2	3948	1.572	0.580	No
row_20	TCONS_00037987	Hsc70-3	4625	1.255	0.551	No
row_21	TCONS_00027780	PEK	6284	0.782	0.476	No
row_22	TCONS_00036492	Edem1	7102	0.610	0.439	No
row_23	TCONS_00005236	Herp	7320	0.572	0.430	No
row_24	TCONS_00007487	Atf6	7393	0.557	0.428	No
row_25	TCONS_00003544	crc	7403	0.555	0.429	No
row_26	TCONS_00030150	Ire1	7704	0.501	0.416	No
row_27	TCONS_00007489	Atf6	7900	0.469	0.408	No
row_28	TCONS_00011391	Trap1	7987	0.452	0.405	No
row_29	TCONS_00002371	Edem2	8083	0.435	0.402	No
row_30	TCONS_00020569	CG7182	9190	0.250	0.351	No
row_31	TCONS_00024632	Hsc70-4	9222	0.245	0.350	No
row_32	TCONS_00024628	Hsc70-4	9602	0.182	0.333	No
row_33	TCONS_00030992	REPTOR	10243	0.075	0.303	No
row_34	TCONS_00011392	Trap1	10544	0.028	0.289	No
row_35	TCONS_00027779	PEK	10654	0.012	0.284	No
row_36	TCONS_00000179	Hsp60B	11439	-0.114	0.248	No
row_37	TCONS_00006219	Hsp60D	11543	-0.130	0.243	No
row_38	TCONS_00007488	Atf6	12229	-0.235	0.212	No
row_39	TCONS_00024694	CG5038	12402	-0.263	0.204	No
row_40	TCONS_00017640	Hsc70-1	12521	-0.283	0.200	No
row_41	TCONS_00013268	Hsc70-5	12551	-0.289	0.199	No
row_42	TCONS_00003543	crc	12752	-0.320	0.190	No
row_43	TCONS_00034357	Hsp60A	13554	-0.455	0.154	No
row_44	TCONS_00009443	Parp16	14459	-0.609	0.113	No
row_45	TCONS_00036495	Edem1	14939	-0.706	0.093	No
row_46	TCONS_00000356	Der-1	14941	-0.707	0.094	No
row_47	TCONS_00006035	CG6766	14973	-0.715	0.095	No

row_48	TCONS_00016249	CG4603	15444	-0.812	0.075	No
row_49	TCONS_00020561	BI-1	15491	-0.824	0.074	No
row_50	TCONS_00001028	Hsp60C	16276	-1.027	0.040	No
row_51	TCONS_00030588	wfs1	16524	-1.099	0.031	No
row_52	TCONS_00032023	CG2126	16560	-1.109	0.032	No
row_53	TCONS_00034358	Hsp60A	16655	-1.140	0.030	No
row_54	TCONS_00013269	Hsc70-5	16858	-1.207	0.024	No
row_55	TCONS_00036497	Edem1	17445	-1.436	0.000	No
row_56	TCONS_00026086	Gba1b	17689	-1.565	-0.008	No
row_57	TCONS_00001029	Hsp60C	17884	-1.676	-0.013	No
row_58	TCONS_00037984	Hsc70-3	18449	-2.086	-0.035	No
row_59	TCONS_00019696	CG32276	18613	-2.236	-0.037	No
row_60	TCONS_00024633	Hsc70-4	20073	-5.440	-0.092	No
row_61	TCONS_00000357	Der-1	20203	-6.105	-0.084	No
row_62	TCONS_00027428	sip3	20374	-7.289	-0.075	No
row_63	TCONS_00020560	BI-1	20802	-13.002	-0.065	No
row_64	TCONS_00019697	CG32276	21244	-42.662	0.013	No
GO:0045861 Negative regulation of proteolysis						
Sp/CyO; hsrω^{66} *vs* Oregon R+ (WT)						
NAME	**SYMBOL**	**TITLE**	**RANK IN GENE LIST**	**RANK METRIC SCORE**	**RUNNING ES**	**CORE ENRICHMENT**
row_0	TCONS_00014183	cer	53	421.314	0.524	Yes
row_1	TCONS_00004684	eIF3h	363	37.720	0.556	Yes
row_2	TCONS_00006016	CG44008	471	25.290	0.583	Yes
row_3	TCONS_00021743	Diap1	505	23.070	0.610	Yes
row_4	TCONS_00036461	CG14812	663	15.756	0.623	Yes
row_5	TCONS_00009811	Spn55B	889	10.494	0.625	Yes
row_6	TCONS_00014989	sigmar	925	9.872	0.636	Yes
row_7	TCONS_00011469	Spn42Da	1207	6.910	0.631	No
row_8	TCONS_00004970	Spn27A	1414	5.575	0.629	No
row_9	TCONS_00013578	Diap2	1578	4.809	0.627	No
row_10	TCONS_00016322	Usp47	1594	4.754	0.632	No
row_11	TCONS_00007716	Spn43Aa	1708	4.448	0.633	No
row_12	TCONS_00016952	CG32039	1861	4.041	0.631	No
row_13	TCONS_00014216	hpo	2131	3.435	0.622	No
row_14	TCONS_00014990	sigmar	2184	3.335	0.624	No
row_15	TCONS_00026218	crb	2263	3.202	0.624	No
row_16	TCONS_00021742	Diap1	2347	3.067	0.624	No
row_17	TCONS_00018985	CkIIalpha	2390	2.995	0.626	No
row_18	TCONS_00016323	Usp47	2492	2.829	0.625	No
row_19	TCONS_00012965	CG17019	3013	2.210	0.604	No
row_20	TCONS_00016320	Usp47	3032	2.191	0.605	No
row_21	TCONS_00012834	DUBAI	3614	1.751	0.581	No
row_22	TCONS_00012835	DUBAI	3719	1.695	0.578	No
row_23	TCONS_00013626	casp	3721	1.695	0.580	No
row_24	TCONS_00011461	Spn42Da	3771	1.664	0.580	No
row_25	TCONS_00013579	Diap2	3794	1.655	0.581	No
row_26	TCONS_00024929	CSN5	4232	1.420	0.562	No
row_27	TCONS_00011463	Spn42Da	4406	1.344	0.556	No
row_28	TCONS_00028684	Timp	4653	1.240	0.546	No
row_29	TCONS_00005281	Spn28Dc	4851	1.174	0.538	No
row_30	TCONS_00030658	hh	5063	1.108	0.530	No
row_31	TCONS_00007869	CSN4	5129	1.084	0.528	No
row_32	TCONS_00018476	Spn77Ba	5250	1.043	0.524	No
row_33	TCONS_00014987	sigmar	5365	1.010	0.520	No
row_34	TCONS_00006017	CG44008	5366	1.009	0.521	No
row_35	TCONS_00026222	crb	5681	0.926	0.507	No
row_36	TCONS_00002166	CG42486	5811	0.893	0.502	No
row_37	TCONS_00007663	Spn42Dc	6117	0.818	0.489	No
row_38	TCONS_00011471	Spn42Db	6553	0.724	0.470	No
row_39	TCONS_00007665	Spn42Dd	6924	0.643	0.453	No
row_40	TCONS_00007666	Spn42De	7644	0.511	0.421	No
row_41	TCONS_00021741	Diap1	8126	0.427	0.399	No

row_42	TCONS_00004685	eIF3h	8957	0.285	0.360	No
row_43	TCONS_00018988	CkIIalpha	9626	0.177	0.329	No
row_44	TCONS_00011464	Spn42Da	11030	-0.052	0.264	No
row_45	TCONS_00021549	Reck	11433	-0.113	0.245	No
row_46	TCONS_00021744	Diap1	12353	-0.253	0.203	No
row_47	TCONS_00007667	Spn42De	12457	-0.271	0.198	No
row_48	TCONS_00002353	Tor	12511	-0.281	0.196	No
row_49	TCONS_00021550	Reck	13526	-0.449	0.150	No
row_50	TCONS_00004359	Sfp23F	13674	-0.477	0.143	No
row_51	TCONS_00013624	casp	14880	-0.696	0.088	No
row_52	TCONS_00018145	CG32176	14977	-0.715	0.084	No
row_53	TCONS_00015828	Acp62F	15718	-0.877	0.051	No
row_54	TCONS_00002352	Tor	15743	-0.882	0.051	No
row_55	TCONS_00011462	Spn42Da	15748	-0.884	0.052	No
row_56	TCONS_00011470	Spn42Db	16068	-0.963	0.038	No
row_57	TCONS_00011467	Spn42Da	16300	-1.032	0.029	No
row_58	TCONS_00011466	Spn42Da	16826	-1.196	0.006	No
row_59	TCONS_00007664	Spn42Dc	17578	-1.507	-0.027	No
row_60	TCONS_00011468	Spn42Da	18088	-1.792	-0.049	No
row_61	TCONS_00018474	Spn77Ba	18440	-2.082	-0.063	No
row_62	TCONS_00012966	CG17019	18743	-2.396	-0.074	No
row_63	TCONS_00013623	casp	18918	-2.580	-0.079	No
row_64	TCONS_00011465	Spn42Da	18948	-2.625	-0.077	No
row_65	TCONS_00029455	Spn88Ea	19186	-3.005	-0.084	No
row_66	TCONS_00002167	CG42486	19214	-3.044	-0.081	No
row_67	TCONS_00011459	Spn42Da	19353	-3.303	-0.084	No
row_68	TCONS_00021745	Diap1	19514	-3.634	-0.087	No
row_69	TCONS_00018986	CkIIalpha	19635	-3.975	-0.087	No
row_70	TCONS_00014217	hpo	19761	-4.255	-0.088	No
row_71	TCONS_00007662	Spn42Dc	19800	-4.399	-0.084	No
row_72	TCONS_00018475	Spn77Ba	19831	-4.507	-0.080	No
row_73	TCONS_00018984	CkIIalpha	19914	-4.844	-0.078	No
row_74	TCONS_00007870	CSN4	20006	-5.173	-0.075	No
row_75	TCONS_00036462	CG14812	20103	-5.582	-0.073	No
row_76	TCONS_00018987	CkIIalpha	20147	-5.803	-0.068	No
row_77	TCONS_00016951	CG32039	20296	-6.661	-0.066	No
row_78	TCONS_00029454	Spn88Ea	20336	-6.966	-0.059	No
row_79	TCONS_00024928	CSN5	20371	-7.268	-0.052	No
row_80	TCONS_00011542	nec	20759	-12.248	-0.055	No
row_81	TCONS_00016660	CG8209	20790	-12.682	-0.040	No
row_82	TCONS_00011460	Spn42Da	20835	-13.860	-0.025	No
row_83	TCONS_00029456	Spn88Eb	21255	-45.863	0.013	No
GO 0045862 Positive regulation of proteolys						
Sp/CyO; hsrω^{66} *vs* Oregon R+ (WT)						
NAME	**SYMBOL**	**TITLE**	**RANK IN GENE LIST**	**RANK METRIC SCORE**	**RUNNING ES**	**CORE ENRICHMENT**
row_0	TCONS_00001086	eIF4A	98	238.752	0.216	Yes
row_1	TCONS_00008982	Cp1	164	136.963	0.340	Yes
row_2	TCONS_00005247	Rack1	219	91.640	0.422	Yes
row_3	TCONS_00034360	Rpt3	470	25.294	0.433	Yes
row_4	TCONS_00017122	Dronc	478	24.927	0.456	Yes
row_5	TCONS_00001090	eIF4A	483	24.334	0.479	Yes
row_6	TCONS_00013249	eIF3m	541	20.816	0.495	Yes
row_7	TCONS_00001088	eIF4A	586	18.748	0.510	Yes
row_8	TCONS_00032723	SkpA	641	16.444	0.523	Yes
row_9	TCONS_00001091	eIF4A	929	9.802	0.519	Yes
row_10	TCONS_00010378	Xbp1	983	9.041	0.524	Yes
row_11	TCONS_00028387	Kcmf1	1054	8.158	0.529	Yes
row_12	TCONS_00017645	26-29-p	1118	7.495	0.533	Yes
row_13	TCONS_00027429	sip3	1136	7.374	0.539	Yes
row_14	TCONS_00010377	Xbp1	1147	7.319	0.545	Yes
row_15	TCONS_00030343	slmb	1204	6.926	0.549	Yes
row_16	TCONS_00033131	sgg	1229	6.696	0.554	Yes

row_17	TCONS_00030831	Rpt2	1241	6.608	0.559	Yes
row_18	TCONS_00007853	Cul1	1273	6.355	0.564	Yes
row_19	TCONS_00038577	CG8974	1331	6.017	0.567	Yes
row_20	TCONS_00023720	skap	1345	5.927	0.572	Yes
row_21	TCONS_00037353	UbcE2H	1458	5.327	0.571	Yes
row_22	TCONS_00016326	scny	1475	5.275	0.575	Yes
row_23	TCONS_00005249	Rack1	1626	4.661	0.573	Yes
row_24	TCONS_00012551	CG33144	1669	4.558	0.575	Yes
row_25	TCONS_00028388	Kcmf1	1764	4.282	0.574	Yes
row_26	TCONS_00008389	RanBPM	1777	4.262	0.578	Yes
row_27	TCONS_00037351	UbcE2H	2049	3.607	0.568	No
row_28	TCONS_00014541	CG3295	2074	3.539	0.571	No
row_29	TCONS_00014216	hpo	2131	3.435	0.571	No
row_30	TCONS_00028567	Rpt3R	2153	3.393	0.573	No
row_31	TCONS_00023724	skap	2225	3.256	0.573	No
row_32	TCONS_00008390	RanBPM	2248	3.224	0.575	No
row_33	TCONS_00012750	PI31	2314	3.126	0.575	No
row_34	TCONS_00039179	ari-1	2362	3.038	0.575	No
row_35	TCONS_00031413	pll	2389	2.996	0.577	No
row_36	TCONS_00002431	CG31855	2456	2.891	0.576	No
row_37	TCONS_00018074	CG9951	2916	2.305	0.557	No
row_38	TCONS_00023149	7B2	3024	2.202	0.554	No
row_39	TCONS_00022490	trbl	3108	2.111	0.552	No
row_40	TCONS_00012758	RnrS	3272	1.975	0.546	No
row_41	TCONS_00019684	Usp5	3423	1.864	0.541	No
row_42	TCONS_00031161	Tnks	3908	1.592	0.520	No
row_43	TCONS_00013250	eIF3m	3922	1.586	0.521	No
row_44	TCONS_00005291	poe	3954	1.569	0.521	No
row_45	TCONS_00012627	Fbl6	3967	1.562	0.521	No
row_46	TCONS_00030344	slmb	4033	1.525	0.520	No
row_47	TCONS_00031932	dco	4130	1.476	0.517	No
row_48	TCONS_00006416	Cul3	4336	1.375	0.508	No
row_49	TCONS_00008985	Cp1	4402	1.346	0.507	No
row_50	TCONS_00016329	scny	4776	1.198	0.490	No
row_51	TCONS_00030642	p53	4809	1.189	0.490	No
row_52	TCONS_00009352	CG8405	4910	1.152	0.486	No
row_53	TCONS_00006418	Cul3	4912	1.152	0.487	No
row_54	TCONS_00031089	bam	4997	1.126	0.484	No
row_55	TCONS_00037352	UbcE2H	5071	1.104	0.482	No
row_56	TCONS_00006414	Cul3	5284	1.035	0.473	No
row_57	TCONS_00016330	scny	5304	1.028	0.473	No
row_58	TCONS_00003302	lok	5375	1.006	0.471	No
row_59	TCONS_00022125	rpr	5444	0.987	0.468	No
row_60	TCONS_00039178	ari-1	5504	0.968	0.466	No
row_61	TCONS_00012550	CG33144	5787	0.898	0.454	No
row_62	TCONS_00027171	Axn	5871	0.877	0.451	No
row_63	TCONS_00003641	Cul2	6122	0.817	0.440	No
row_64	TCONS_00023150	7B2	6191	0.799	0.437	No
row_65	TCONS_00031933	dco	6297	0.779	0.433	No
row_66	TCONS_00018070	sina	6377	0.765	0.430	No
row_67	TCONS_00033121	sgg	6558	0.722	0.422	No
row_68	TCONS_00005548	Pka-C1	6635	0.710	0.420	No
row_69	TCONS_00022330	CG8786	6723	0.689	0.416	No
row_70	TCONS_00031931	dco	6727	0.689	0.417	No
row_71	TCONS_00036015	Rpt6	6922	0.643	0.408	No
row_72	TCONS_00030832	Rpt2	6968	0.636	0.407	No
row_73	TCONS_00000137	ebi	7059	0.617	0.403	No
row_74	TCONS_00007847	Cul1	7097	0.610	0.402	No
row_75	TCONS_00008391	RanBPM	7173	0.596	0.399	No
row_76	TCONS_00028384	Kcmf1	7174	0.596	0.399	No
row_77	TCONS_00022614	park	7243	0.584	0.397	No
row_78	TCONS_00009353	CG8405	7730	0.495	0.374	No
row_79	TCONS_00031934	dco	7825	0.480	0.370	No

row_80	TCONS_00012749	PI31	7840	0.477	0.370	No
row_81	TCONS_00022329	CG8786	7908	0.467	0.367	No
row_82	TCONS_00012882	muskelin	8010	0.448	0.363	No
row_83	TCONS_00029337	HtrA2	8015	0.447	0.363	No
row_84	TCONS_00022261	pip	8256	0.406	0.352	No
row_85	TCONS_00032726	SkpA	8264	0.405	0.352	No
row_86	TCONS_00009748	Dlish	8285	0.401	0.352	No
row_87	TCONS_00012748	PI31	8319	0.396	0.351	No
row_88	TCONS_00011862	Rpt1	8502	0.364	0.342	No
row_89	TCONS_00005248	Rack1	8529	0.358	0.342	No
row_90	TCONS_00033090	wds	8613	0.342	0.338	No
row_91	TCONS_00009707	POSH	8669	0.330	0.336	No
row_92	TCONS_00023722	skap	8942	0.287	0.323	No
row_93	TCONS_00011860	Rpt1	9095	0.264	0.316	No
row_94	TCONS_00022123	grim	9266	0.237	0.309	No
row_95	TCONS_00039177	ari-1	9326	0.228	0.306	No
row_96	TCONS_00017158	CG12362	9345	0.225	0.305	No
row_97	TCONS_00009842	pen-2	9432	0.210	0.302	No
row_98	TCONS_00034624	CG2577	9758	0.159	0.286	No
row_99	TCONS_00030883	CG13605	9828	0.146	0.283	No
row_100	TCONS_00036076	Usp2	9856	0.141	0.282	No
row_101	TCONS_00009576	Dark	9947	0.128	0.278	No
row_102	TCONS_00000142	ex	10085	0.104	0.272	No
row_103	TCONS_00015862	Jafrac2	10161	0.090	0.268	No
row_104	TCONS_00039661	CG1724	10306	0.065	0.262	No
row_105	TCONS_00039173	ari-1	10724	-0.001	0.242	No
row_106	TCONS_00003300	lok	10788	-0.012	0.239	No
row_107	TCONS_00017384	Rpt4R	10793	-0.013	0.239	No
row_108	TCONS_00027651	Ubc6	10884	-0.028	0.235	No
row_109	TCONS_00036082	Usp2	11075	-0.060	0.226	No
row_110	TCONS_00022115	hid	11191	-0.079	0.220	No
row_111	TCONS_00005292	poe	11306	-0.095	0.215	No
row_112	TCONS_00003299	lok	11324	-0.098	0.215	No
row_113	TCONS_00032725	SkpA	11343	-0.101	0.214	No
row_114	TCONS_00022328	CG8786	11393	-0.108	0.212	No
row_115	TCONS_00008986	Cp1	11417	-0.111	0.211	No
row_116	TCONS_00003401	IKKepsilon	11489	-0.121	0.207	No
row_117	TCONS_00005856	abo	11612	-0.142	0.202	No
row_118	TCONS_00036085	Usp2	11741	-0.161	0.196	No
row_119	TCONS_00033126	sgg	11812	-0.172	0.193	No
row_120	TCONS_00033099	sgg	11840	-0.176	0.192	No
row_121	TCONS_00008392	RanBPM	11896	-0.184	0.189	No
row_122	TCONS_00004214	CG9962	12048	-0.204	0.182	No
row_123	TCONS_00038355	CG13404	12049	-0.204	0.183	No
row_124	TCONS_00026180	Apc2	12136	-0.220	0.179	No
row_125	TCONS_00010571	ari-2	12254	-0.239	0.173	No
row_126	TCONS_00032591	klhl10	12274	-0.241	0.173	No
row_127	TCONS_00034755	REG	12340	-0.251	0.170	No
row_128	TCONS_00001089	eIF4A	12345	-0.252	0.170	No
row_129	TCONS_00033127	sgg	12444	-0.269	0.166	No
row_130	TCONS_00038574	CG8974	12587	-0.295	0.159	No
row_131	TCONS_00010920	fzr2	12715	-0.315	0.154	No
row_132	TCONS_00032719	Roc1a	12722	-0.316	0.154	No
row_133	TCONS_00012879	muskelin	12762	-0.321	0.152	No
row_134	TCONS_00006417	Cul3	12769	-0.323	0.152	No
row_135	TCONS_00034675	CkIalpha	12876	-0.342	0.147	No
row_136	TCONS_00022270	pip	12913	-0.348	0.146	No
row_137	TCONS_00032721	SkpA	13048	-0.371	0.140	No
row_138	TCONS_00033106	sgg	13321	-0.416	0.128	No
row_139	TCONS_00002432	CG31855	13339	-0.418	0.127	No
row_140	TCONS_00030643	p53	13545	-0.453	0.118	No
row_141	TCONS_00033116	sgg	13580	-0.458	0.117	No
row_142	TCONS_00007851	Cul1	13812	-0.500	0.107	No

row_143	TCONS_00012626	Fbl6	13854	-0.505	0.105	No
row_144	TCONS_00019686	Usp5	13907	-0.513	0.103	No
row_145	TCONS_00016327	scny	13946	-0.519	0.102	No
row_146	TCONS_00036701	ttm50	14104	-0.546	0.095	No
row_147	TCONS_00023725	skap	14154	-0.553	0.093	No
row_148	TCONS_00027170	Axn	14177	-0.558	0.093	No
row_149	TCONS_00031935	dco	14190	-0.560	0.093	No
row_150	TCONS_00027777	CG12147	14229	-0.565	0.091	No
row_151	TCONS_00013285	phyl	14421	-0.602	0.083	No
row_152	TCONS_00015864	Jafrac2	14853	-0.689	0.063	No
row_153	TCONS_00018068	sina	14924	-0.703	0.061	No
row_154	TCONS_00036878	fzr	14934	-0.705	0.061	No
row_155	TCONS_00036079	Usp2	14972	-0.715	0.060	No
row_156	TCONS_00036290	Dredd	15101	-0.739	0.055	No
row_157	TCONS_00012628	Fbl6	15236	-0.767	0.049	No
row_158	TCONS_00034670	Cklalpha	15265	-0.776	0.048	No
row_159	TCONS_00016328	scny	15278	-0.779	0.049	No
row_160	TCONS_00016333	scny	15308	-0.783	0.048	No
row_161	TCONS_00036081	Usp2	15445	-0.812	0.042	No
row_162	TCONS_00033089	wds	15525	-0.834	0.039	No
row_163	TCONS_00036288	Dredd	15738	-0.881	0.030	No
row_164	TCONS_00019776	ntc	15773	-0.891	0.029	No
row_165	TCONS_00022272	pip	16015	-0.951	0.019	No
row_166	TCONS_00015863	Jafrac2	16460	-1.080	-0.001	No
row_167	TCONS_00038578	CG8974	16495	-1.090	-0.001	No
row_168	TCONS_00006415	Cul3	16509	-1.094	-0.001	No
row_169	TCONS_00005549	Pka-C1	16528	-1.100	-0.001	No
row_170	TCONS_00032727	SkpA	16646	-1.138	-0.005	No
row_171	TCONS_00021015	Ufd1-like	16660	-1.142	-0.005	No
row_172	TCONS_00036289	Dredd	16717	-1.165	-0.006	No
row_173	TCONS_00002785	fzy	16795	-1.187	-0.009	No
row_174	TCONS_00022331	CG8786	16847	-1.203	-0.010	No
row_175	TCONS_00038575	CG8974	16904	-1.225	-0.012	No
row_176	TCONS_00022615	park	17191	-1.328	-0.024	No
row_177	TCONS_00012751	PI31	17195	-1.329	-0.023	No
row_178	TCONS_00017157	CG12362	17331	-1.391	-0.028	No
row_179	TCONS_00036877	fzr	17377	-1.409	-0.029	No
row_180	TCONS_00022332	CG8786	17434	-1.432	-0.030	No
row_181	TCONS_00039180	ari-1	17464	-1.448	-0.030	No
row_182	TCONS_00023721	skap	17628	-1.531	-0.036	No
row_183	TCONS_00030268	EloB	17645	-1.539	-0.036	No
row_184	TCONS_00033104	sgg	17677	-1.559	-0.036	No
row_185	TCONS_00036700	ttm50	17894	-1.680	-0.044	No
row_186	TCONS_00029336	HtrA2	17901	-1.686	-0.043	No
row_187	TCONS_00019685	Usp5	17937	-1.705	-0.043	No
row_188	TCONS_00032115	krz	17956	-1.714	-0.042	No
row_189	TCONS_00032718	Roc1a	17968	-1.723	-0.041	No
row_190	TCONS_00001959	STUB1	18181	-1.858	-0.049	No
row_191	TCONS_00036077	Usp2	18196	-1.871	-0.048	No
row_192	TCONS_00012752	PI31	18255	-1.920	-0.049	No
row_193	TCONS_00032720	Roc1a	18286	-1.947	-0.049	No
row_194	TCONS_00032114	krz	18295	-1.957	-0.047	No
row_195	TCONS_00034672	Cklalpha	18322	-1.979	-0.047	No
row_196	TCONS_00025833	Fadd	18365	-2.008	-0.047	No
row_197	TCONS_00033117	sgg	18374	-2.015	-0.046	No
row_198	TCONS_00002835	Cyt-c-d	18411	-2.055	-0.045	No
row_199	TCONS_00002688	Tim17b2	18584	-2.211	-0.051	No
row_200	TCONS_00009841	pen-2	18589	-2.214	-0.049	No
row_201	TCONS_00007852	Cul1	18654	-2.285	-0.050	No
row_202	TCONS_00026095	Rpt5	19027	-2.739	-0.065	No
row_203	TCONS_00005734	RnrL	19032	-2.747	-0.063	No
row_204	TCONS_00028568	Rpt3R	19066	-2.800	-0.062	No
row_205	TCONS_00034756	REG	19167	-2.962	-0.064	No

row_206	TCONS_00005713	Ufd4	19299	-3.198	-0.067	No
row_207	TCONS_00038576	CG8974	19438	-3.482	-0.070	No
row_208	TCONS_00031855	Rpt6R	19477	-3.557	-0.069	No
row_209	TCONS_00006420	Cul3	19640	-3.983	-0.073	No
row_210	TCONS_00027117	Drice	19652	-4.004	-0.070	No
row_211	TCONS_00014217	hpo	19761	-4.255	-0.071	No
row_212	TCONS_00023723	skap	19779	-4.318	-0.067	No
row_213	TCONS_00031412	pll	19861	-4.638	-0.067	No
row_214	TCONS_00005547	Pka-C1	19878	-4.703	-0.063	No
row_215	TCONS_00033132	sgg	19904	-4.796	-0.060	No
row_216	TCONS_00003640	Cul2	19909	-4.816	-0.056	No
row_217	TCONS_00034359	Rpt3	20226	-6.255	-0.065	No
row_218	TCONS_00037077	Rpt4	20306	-6.733	-0.062	No
row_219	TCONS_00027428	sip3	20374	-7.289	-0.059	No
row_220	TCONS_00027652	Ubc6	20438	-7.733	-0.055	No
row_221	TCONS_00034671	Cklalpha	20476	-8.155	-0.049	No
row_222	TCONS_00005246	Rack1	20537	-8.743	-0.044	No
row_223	TCONS_00003430	Pomp	20545	-8.821	-0.036	No
row_224	TCONS_00032724	SkpA	20621	-9.665	-0.030	No
row_225	TCONS_00023719	skap	20814	-13.162	-0.027	No
row_226	TCONS_00002836	Cyt-c-p	20903	-16.089	-0.016	No
row_227	TCONS_00027925	CG11459	21266	-49.463	0.012	No
GO:0050821 Protein stabilization						
Sp/CyO; hsrω^{66} *vs* Oregon R+ (WT)						
NAME	**SYMBOL**	**TITLE**	**RANK IN GENE LIST**	**RANK METRIC SCORE**	**RUNNING ES**	**CORE ENRICHMENT**
row_0	TCONS_00035140	CG8206	490	24.025	0.015	No
row_1	TCONS_00008289	14-3-3zeta	545	20.533	0.044	No
row_2	TCONS_00000497	aph-1	951	9.438	0.040	No
row_3	TCONS_00002857	Mhc	1169	7.160	0.041	No
row_4	TCONS_00008285	14-3-3zeta	1407	5.596	0.039	No
row_5	TCONS_00002858	Mhc	1450	5.385	0.045	No
row_6	TCONS_00016322	Usp47	1594	4.754	0.046	No
row_7	TCONS_00002855	Mhc	1677	4.535	0.049	No
row_8	TCONS_00001918	da	1682	4.521	0.056	No
row_9	TCONS_00038070	fw	2083	3.517	0.043	No
row_10	TCONS_00031638	Cnx99A	2107	3.486	0.047	No
row_11	TCONS_00026218	crb	2263	3.202	0.045	No
row_12	TCONS_00016323	Usp47	2492	2.829	0.038	No
row_13	TCONS_00013586	Mlf	2502	2.815	0.042	No
row_14	TCONS_00020498	syd	2531	2.776	0.045	No
row_15	TCONS_00016320	Usp47	3032	2.191	0.026	No
row_16	TCONS_00017603	stv	3326	1.941	0.015	No
row_17	TCONS_00020503	syd	3344	1.922	0.017	No
row_18	TCONS_00015689	Cdc37	3462	1.840	0.014	No
row_19	TCONS_00028665	tws	3529	1.798	0.014	No
row_20	TCONS_00021621	CG7945	3540	1.792	0.017	No
row_21	TCONS_00017608	stv	3676	1.719	0.013	No
row_22	TCONS_00003914	lwr	3875	1.609	0.006	No
row_23	TCONS_00024929	CSN5	4232	1.420	-0.008	No
row_24	TCONS_00020493	syd	4642	1.245	-0.025	No
row_25	TCONS_00037201	Sxl	4901	1.155	-0.036	No
row_26	TCONS_00005490	alien	5011	1.122	-0.039	No
row_27	TCONS_00007869	CSN4	5129	1.084	-0.043	No
row_28	TCONS_00037200	Sxl	5245	1.045	-0.047	No
row_29	TCONS_00028666	tws	5299	1.030	-0.047	No
row_30	TCONS_00013585	Mlf	5398	0.999	-0.050	No
row_31	TCONS_00013587	Mlf	5421	0.992	-0.050	No
row_32	TCONS_00026222	crb	5681	0.926	-0.061	No
row_33	TCONS_00037211	Sxl	5760	0.904	-0.063	No
row_34	TCONS_00007940	CSN7	5832	0.888	-0.065	No
row_35	TCONS_00028669	tws	5882	0.875	-0.066	No
row_36	TCONS_00020125	DnaJ-1	6023	0.839	-0.071	No

row_37	TCONS_00015449	Hipk	6608	0.714	-0.097	No
row_38	TCONS_00035121	CG8134	7072	0.615	-0.118	No
row_39	TCONS_00029264	CG9922	7098	0.610	-0.118	No
row_40	TCONS_00034577	sicily	7301	0.576	-0.126	No
row_41	TCONS_00001920	da	7645	0.511	-0.142	No
row_42	TCONS_00038071	fw	7646	0.511	-0.141	No
row_43	TCONS_00020675	orb2	7711	0.499	-0.143	No
row_44	TCONS_00028670	tws	7882	0.472	-0.150	No
row_45	TCONS_00002853	Mhc	7906	0.467	-0.151	No
row_46	TCONS_00035141	CG8206	8476	0.369	-0.177	No
row_47	TCONS_00002866	Mhc	8501	0.364	-0.177	No
row_48	TCONS_00035120	CG8134	8538	0.356	-0.178	No
row_49	TCONS_00005488	alien	8719	0.321	-0.186	No
row_50	TCONS_00007617	Bap170	8829	0.304	-0.191	No
row_51	TCONS_00037144	shf	8958	0.285	-0.196	No
row_52	TCONS_00034145	ric8a	9030	0.274	-0.199	No
row_53	TCONS_00037146	shf	9385	0.219	-0.215	No
row_54	TCONS_00037147	shf	9693	0.169	-0.230	No
row_55	TCONS_00012401	Ccs	9765	0.157	-0.233	No
row_56	TCONS_00028661	tws	10069	0.107	-0.247	No
row_57	TCONS_00025953	CSN6	10242	0.075	-0.255	No
row_58	TCONS_00001525	CSN8	10310	0.064	-0.258	No
row_59	TCONS_00020672	orb2	10505	0.034	-0.267	No
row_60	TCONS_00038559	CG12379	10633	0.016	-0.272	No
row_61	TCONS_00015448	Hipk	10749	-0.005	-0.278	No
row_62	TCONS_00017607	stv	11477	-0.119	-0.312	No
row_63	TCONS_00020673	orb2	11964	-0.193	-0.334	No
row_64	TCONS_00031641	Cnx99A	12588	-0.295	-0.363	No
row_65	TCONS_00013588	Mlf	12682	-0.309	-0.367	No
row_66	TCONS_00003917	lwr	13310	-0.415	-0.395	No
row_67	TCONS_00037230	Sxl	13610	-0.465	-0.408	No
row_68	TCONS_00024268	Snx3	13734	-0.486	-0.413	No
row_69	TCONS_00013590	Mlf	13943	-0.519	-0.422	No
row_70	TCONS_00031642	Cnx99A	14000	-0.527	-0.424	No
row_71	TCONS_00034146	ric8a	14003	-0.528	-0.423	No
row_72	TCONS_00003915	lwr	14223	-0.564	-0.433	No
row_73	TCONS_00008292	14-3-3zeta	14345	-0.587	-0.437	No
row_74	TCONS_00017605	stv	14442	-0.605	-0.441	No
row_75	TCONS_00020499	syd	14520	-0.619	-0.444	No
row_76	TCONS_00015452	Hipk	14806	-0.679	-0.456	No
row_77	TCONS_00037221	Sxl	15348	-0.791	-0.480	No
row_78	TCONS_00017604	stv	15497	-0.825	-0.486	No
row_79	TCONS_00038681	Tob	15502	-0.827	-0.484	No
row_80	TCONS_00019776	ntc	15773	-0.891	-0.496	No
row_81	TCONS_00015957	Hsp83	16189	-0.999	-0.513	No
row_82	TCONS_00037231	Sxl	16704	-1.159	-0.536	No
row_83	TCONS_00013580	Mlf	16937	-1.237	-0.545	No
row_84	TCONS_00028659	tws	17245	-1.351	-0.557	No
row_85	TCONS_00017606	stv	17302	-1.376	-0.557	No
row_86	TCONS_00037199	Sxl	17332	-1.391	-0.556	No
row_87	TCONS_00038069	fw	17448	-1.439	-0.560	No
row_88	TCONS_00037145	shf	17460	-1.446	-0.558	No
row_89	TCONS_00028668	tws	17665	-1.553	-0.565	No
row_90	TCONS_00022188	CSN1b	18076	-1.785	-0.581	No
row_91	TCONS_00012402	Ccs	18085	-1.789	-0.579	No
row_92	TCONS_00028259	Sgt1	18212	-1.882	-0.582	No
row_93	TCONS_00020497	syd	18234	-1.904	-0.580	No
row_94	TCONS_00037225	Sxl	18310	-1.971	-0.580	No
row_95	TCONS_00037229	Sxl	18460	-2.093	-0.584	No
row_96	TCONS_00022560	CSN3	19210	-3.039	-0.614	No
row_97	TCONS_00012506	trsn	19450	-3.498	-0.620	No
row_98	TCONS_00005491	alien	19563	-3.740	-0.619	No
row_99	TCONS_00029263	CG9922	19820	-4.462	-0.624	Yes

row_100	TCONS_00020124	DnaJ-1	19895	-4.764	-0.620	Yes
row_101	TCONS_00021622	CG7945	19939	-4.922	-0.615	Yes
row_102	TCONS_00007870	CSN4	20006	-5.173	-0.610	Yes
row_103	TCONS_00013582	Mlf	20068	-5.418	-0.604	Yes
row_104	TCONS_00015688	Cdc37	20081	-5.478	-0.596	Yes
row_105	TCONS_00008286	14-3-3zeta	20179	-5.965	-0.591	Yes
row_106	TCONS_00002871	Mhc	20221	-6.216	-0.584	Yes
row_107	TCONS_00024928	CSN5	20371	-7.268	-0.579	Yes
row_108	TCONS_00024267	Snx3	20410	-7.531	-0.569	Yes
row_109	TCONS_00000496	aph-1	20490	-8.281	-0.560	Yes
row_110	TCONS_00002859	Mhc	20872	-14.872	-0.555	Yes
row_111	TCONS_00003916	lwr	20917	-16.472	-0.531	Yes
row_112	TCONS_00008282	14-3-3zeta	20975	-18.356	-0.505	Yes
row_113	TCONS_00008290	14-3-3zeta	21087	-24.432	-0.472	Yes
row_114	TCONS_00002852	Mhc	21131	-28.513	-0.430	Yes
row_115	TCONS_00002851	Mhc	21149	-30.745	-0.383	Yes
row_116	TCONS_00008288	14-3-3zeta	21212	-37.904	-0.326	Yes
row_117	TCONS_00002856	Mhc	21286	-56.731	-0.241	Yes
row_118	TCONS_00002854	Mhc	21321	-73.092	-0.129	Yes
row_119	TCONS_00015958	Hsp83	21348	-88.888	0.008	Yes
GO:0101031 Protein folding chaperone complex						
Sp/CyO; hsrω^{66} *vs* Oregon R+ (WT)						
NAME	**SYMBOL**	**TITLE**	**RANK IN GENE LIST**	**RANK METRIC SCORE**	**RUNNING ES**	**CORE ENRICHMENT**
row_0	TCONS_00024976	CCT3	3181	2.049	-0.135	No
row_1	TCONS_00027760	CG11999	3477	1.831	-0.138	No
row_2	TCONS_00017026	CG8336	4341	1.373	-0.169	No
row_3	TCONS_00010987	spag	6308	0.777	-0.256	No
row_4	TCONS_00030564	CCT1	6753	0.684	-0.272	No
row_5	TCONS_00017025	CG8336	11354	-0.103	-0.486	No
row_6	TCONS_00015957	Hsp83	16189	-0.999	-0.704	No
row_7	TCONS_00024975	CCT3	16313	-1.036	-0.704	No
row_8	TCONS_00017028	CG8336	16674	-1.148	-0.713	No
row_9	TCONS_00038000	Nrd1	18790	-2.442	-0.797	No
row_10	TCONS_00023705	CCT7	19690	-4.100	-0.813	Yes
row_11	TCONS_00024974	CCT3	20071	-5.435	-0.797	Yes
row_12	TCONS_00008642	CCT5	20125	-5.706	-0.765	Yes
row_13	TCONS_00012108	CCT8	20259	-6.470	-0.731	Yes
row_14	TCONS_00034096	CCT2	20395	-7.417	-0.692	Yes
row_15	TCONS_00006126	CCT4	20558	-9.016	-0.644	Yes
row_16	TCONS_00030565	CCT1	20561	-9.031	-0.588	Yes
row_17	TCONS_00035142	CCT6	20842	-14.050	-0.515	Yes
row_18	TCONS_00015958	Hsp83	21348	-88.888	0.008	Yes
GO: 0034605 Cellular response to heat						
Sp/CyO; hsrω^{66} *vs* Oregon R+ (WT)						
NAME	**SYMBOL**	**TITLE**	**RANK IN GENE LIST**	**RANK METRIC SCORE**	**RUNNING ES**	**CORE ENRICHMENT**
row_0	TCONS_00026060	Sec13	830	11.701	-0.027	No
row_1	TCONS_00017655	Hsc70Cb	1081	7.855	-0.030	No
row_2	TCONS_00021202	thoc6	1510	5.102	-0.045	No
row_3	TCONS_00004103	tho2	1858	4.047	-0.057	No
row_4	TCONS_00030795	Nup98-96	3207	2.033	-0.117	No
row_5	TCONS_00030035	Mekk1	3471	1.835	-0.128	No
row_6	TCONS_00019135	thoc7	5533	0.960	-0.222	No
row_7	TCONS_00017659	Hsc70Cb	5849	0.884	-0.236	No
row_8	TCONS_00030034	Mekk1	7313	0.573	-0.304	No
row_9	TCONS_00011391	Trap1	7987	0.452	-0.335	No
row_10	TCONS_00017657	Hsc70Cb	8085	0.435	-0.339	No
row_11	TCONS_00029932	Rpb4	8454	0.374	-0.355	No
row_12	TCONS_00030797	Nup98-96	8860	0.300	-0.374	No
row_13	TCONS_00011392	Trap1	10544	0.028	-0.452	No
row_14	TCONS_00010921	thoc5	11182	-0.078	-0.482	No
row_15	TCONS_00027479	Parp	11726	-0.159	-0.507	No

row_16	TCONS_00019136	thoc7	12622	-0.299	-0.548	No
row_17	TCONS_00017658	Hsc70Cb	13367	-0.423	-0.582	No
row_18	TCONS_00034357	Hsp60A	13554	-0.455	-0.591	No
row_19	TCONS_00017661	Hsc70Cb	15032	-0.727	-0.659	No
row_20	TCONS_00030796	Nup98-96	15506	-0.827	-0.680	No
row_21	TCONS_00011119	Atf-2	15888	-0.921	-0.696	No
row_22	TCONS_00017662	Hsc70Cb	16073	-0.965	-0.704	No
row_23	TCONS_00015957	Hsp83	16189	-0.999	-0.708	No
row_24	TCONS_00006081	CG5446	16555	-1.108	-0.724	No
row_25	TCONS_00034358	Hsp60A	16655	-1.140	-0.728	No
row_26	TCONS_00002506	RpII33	17467	-1.452	-0.764	No
row_27	TCONS_00006080	CG5446	17814	-1.635	-0.778	No
row_28	TCONS_00007905	Nup50	18353	-1.999	-0.801	No
row_29	TCONS_00027885	Hpr1	18379	-2.020	-0.800	No
row_30	TCONS_00004104	tho2	18539	-2.165	-0.805	No
row_31	TCONS_00017654	Hsc70Cb	19413	-3.405	-0.843	No
row_32	TCONS_00026867	Gp93	19509	-3.619	-0.843	No
row_33	TCONS_00007046	Victoria	20055	-5.382	-0.863	No
row_34	TCONS_00007045	TotF	20317	-6.793	-0.868	Yes
row_35	TCONS_00025594	TotB	20482	-8.231	-0.867	Yes
row_36	TCONS_00025593	TotC	21290	-58.630	-0.844	Yes
row_37	TCONS_00015958	Hsp83	21348	-88.888	-0.755	Yes
row_38	TCONS_00025592	TotA	21486	-737.050	0.002	Yes
GO: 0032543 Mitochondrial translation						
Sp/CyO; hsrω^{66} *vs* Oregon R+ (WT)						
NAME	**SYMBOL**	**TITLE**	**RANK IN GENE LIST**	**RANK METRIC SCORE**	**RUNNING ES**	**CORE ENRICHMENT**
row_0	TCONS_00035672	HisRS	945	9.561	-0.011	No
row_1	TCONS_00016174	mRpS6	2089	3.511	-0.052	No
row_2	TCONS_00017993	mRpS34	2126	3.444	-0.042	No
row_3	TCONS_00025828	mRpL35	2479	2.842	-0.049	No
row_4	TCONS_00035153	mRpS30	2589	2.692	-0.044	No
row_5	TCONS_00022244	mRpL21	2648	2.601	-0.038	No
row_6	TCONS_00018204	TrpRS-m	2745	2.493	-0.034	No
row_7	TCONS_00034698	mRpL49	2756	2.483	-0.026	No
row_8	TCONS_00008931	mEFTu1	2849	2.394	-0.022	No
row_9	TCONS_00001976	CG6094	2966	2.246	-0.020	No
row_10	TCONS_00006539	mRpL4	3097	2.123	-0.018	No
row_11	TCONS_00000860	mRpL28	3712	1.697	-0.041	No
row_12	TCONS_00023626	mRpL1	3754	1.672	-0.037	No
row_13	TCONS_00017764	GlyRS	3822	1.640	-0.035	No
row_14	TCONS_00011866	mRpL52	4246	1.414	-0.050	No
row_15	TCONS_00032960	mRpL16	4271	1.403	-0.046	No
row_16	TCONS_00010356	mRpL54	4346	1.369	-0.045	No
row_17	TCONS_00025968	mRpL45	4899	1.155	-0.066	No
row_18	TCONS_00014781	mRpS29	5177	1.066	-0.076	No
row_19	TCONS_00030606	CG17141	5770	0.902	-0.100	No
row_20	TCONS_00035675	HisRS	6015	0.840	-0.109	No
row_21	TCONS_00016236	LeuRS-m	6108	0.820	-0.110	No
row_22	TCONS_00027227	mRpS18C	6227	0.793	-0.113	No
row_23	TCONS_00035673	HisRS	6251	0.790	-0.111	No
row_24	TCONS_00000324	mRpL48	6338	0.772	-0.113	No
row_25	TCONS_00000323	mRpL48	6465	0.746	-0.116	No
row_26	TCONS_00008688	mIF3	6717	0.691	-0.125	No
row_27	TCONS_00031562	mIF2	6781	0.676	-0.126	No
row_28	TCONS_00035674	HisRS	7792	0.485	-0.171	No
row_29	TCONS_00004520	mRpL27	8007	0.449	-0.180	No
row_30	TCONS_00039339	mRpS14	8111	0.430	-0.183	No
row_31	TCONS_00039340	mRpS14	8456	0.373	-0.198	No
row_32	TCONS_00013434	mRpL41	8924	0.289	-0.219	No
row_33	TCONS_00024690	SerRS-m	9194	0.249	-0.230	No
row_34	TCONS_00002378	mRF1	9225	0.244	-0.231	No
row_35	TCONS_00023553	ArgRS-m	10257	0.072	-0.279	No

row_36	TCONS_00007076	mRpS18B	10314	0.064	-0.281	No
row_37	TCONS_00020334	mRpL50	10828	-0.019	-0.305	No
row_38	TCONS_00025012	mRpS11	10919	-0.035	-0.309	No
row_39	TCONS_00028285	mRpS18A	11444	-0.115	-0.333	No
row_40	TCONS_00023554	ArgRS-m	11582	-0.138	-0.339	No
row_41	TCONS_00007857	drosha	11676	-0.153	-0.343	No
row_42	TCONS_00008930	mEFTu1	11845	-0.177	-0.350	No
row_43	TCONS_00004519	mRpL27	11934	-0.189	-0.354	No
row_44	TCONS_00015398	mRpL17	11937	-0.189	-0.353	No
row_45	TCONS_00001917	mRpS7	12255	-0.239	-0.367	No
row_46	TCONS_00024625	mRpS10	12766	-0.322	-0.390	No
row_47	TCONS_00000859	mRpL28	13264	-0.409	-0.412	No
row_48	TCONS_00036630	tko	13349	-0.420	-0.414	No
row_49	TCONS_00017929	IleRS-m	13510	-0.447	-0.420	No
row_50	TCONS_00030887	Slimp	13516	-0.448	-0.419	No
row_51	TCONS_00011834	mEFTu2	13697	-0.479	-0.425	No
row_52	TCONS_00000095	mRpL10	15067	-0.733	-0.487	No
row_53	TCONS_00025964	mRRF2	15513	-0.828	-0.505	No
row_54	TCONS_00020525	mRpL36	15521	-0.831	-0.502	No
row_55	TCONS_00004603	mRpS2	15563	-0.844	-0.501	No
row_56	TCONS_00017889	mRpS31	15957	-0.937	-0.516	No
row_57	TCONS_00010852	mRpL43	16326	-1.040	-0.530	No
row_58	TCONS_00015685	mRpL46	16399	-1.062	-0.530	No
row_59	TCONS_00018223	mRpS26	16403	-1.063	-0.526	No
row_60	TCONS_00013041	CG4679	16963	-1.247	-0.548	No
row_61	TCONS_00030886	GatB	17088	-1.289	-0.549	No
row_62	TCONS_00038361	mRpS25	17259	-1.359	-0.552	Yes
row_63	TCONS_00028746	mRpL37	17351	-1.399	-0.552	Yes
row_64	TCONS_00015397	mRpL17	17399	-1.417	-0.549	Yes
row_65	TCONS_00005125	mEFG1	17412	-1.424	-0.545	Yes
row_66	TCONS_00036607	mRpL14	17458	-1.445	-0.542	Yes
row_67	TCONS_00030070	mRpL55	17603	-1.518	-0.543	Yes
row_68	TCONS_00021319	mRpL20	17631	-1.534	-0.539	Yes
row_69	TCONS_00016957	mRRF1	17736	-1.593	-0.539	Yes
row_70	TCONS_00030904	mRpS24	17785	-1.622	-0.535	Yes
row_71	TCONS_00021548	mRpL39	17831	-1.644	-0.532	Yes
row_72	TCONS_00029165	mRpS21	17871	-1.666	-0.528	Yes
row_73	TCONS_00024688	mRpL9	17935	-1.705	-0.525	Yes
row_74	TCONS_00036629	tko	18103	-1.801	-0.526	Yes
row_75	TCONS_00024093	mRpL40	18142	-1.830	-0.522	Yes
row_76	TCONS_00030065	GatA	18147	-1.835	-0.516	Yes
row_77	TCONS_00007077	mRpS18B	18177	-1.858	-0.511	Yes
row_78	TCONS_00008979	mRpL53	18219	-1.890	-0.506	Yes
row_79	TCONS_00028178	mRpS9	18240	-1.910	-0.500	Yes
row_80	TCONS_00034947	mRpL38	18348	-1.996	-0.498	Yes
row_81	TCONS_00024546	mRpL11	18406	-2.050	-0.494	Yes
row_82	TCONS_00023673	mRpL19	18473	-2.101	-0.490	Yes
row_83	TCONS_00015244	TyrRS-m	18567	-2.201	-0.486	Yes
row_84	TCONS_00022498	mRpL15	18666	-2.295	-0.483	Yes
row_85	TCONS_00019551	mRpL23	18720	-2.370	-0.477	Yes
row_86	TCONS_00008687	mIF3	18798	-2.452	-0.473	Yes
row_87	TCONS_00004628	mRpL24	18821	-2.486	-0.465	Yes
row_88	TCONS_00032959	mRpL16	18836	-2.501	-0.457	Yes
row_89	TCONS_00008810	mRpL18	18856	-2.518	-0.449	Yes
row_90	TCONS_00036606	mRpL14	18926	-2.589	-0.443	Yes
row_91	TCONS_00016175	mRpS6	18947	-2.619	-0.435	Yes
row_92	TCONS_00015832	mRpS35	18994	-2.690	-0.428	Yes
row_93	TCONS_00004521	mRpL27	19037	-2.757	-0.420	Yes
row_94	TCONS_00027352	mRpL32	19057	-2.782	-0.412	Yes
row_95	TCONS_00035152	mRpS30	19062	-2.796	-0.402	Yes
row_96	TCONS_00015229	CG12848	19067	-2.800	-0.393	Yes
row_97	TCONS_00035147	mRpL3	19075	-2.811	-0.383	Yes
row_98	TCONS_00035424	mRpL22	19086	-2.832	-0.374	Yes

row_99	TCONS_00017254	mRpL2	19101	-2.847	-0.365	Yes
row_100	TCONS_00009354	mRpL34	19116	-2.859	-0.356	Yes
row_101	TCONS_00027782	mRpL44	19174	-2.977	-0.348	Yes
row_102	TCONS_00026853	mRpS22	19260	-3.123	-0.341	Yes
row_103	TCONS_00029166	mRpS21	19315	-3.218	-0.332	Yes
row_104	TCONS_00017763	GlyRS	19398	-3.380	-0.325	Yes
row_105	TCONS_00018203	TrpRS-m	19429	-3.452	-0.314	Yes
row_106	TCONS_00006254	mRpS23	19492	-3.595	-0.305	Yes
row_107	TCONS_00001977	CG6094	19495	-3.598	-0.292	Yes
row_108	TCONS_00010637	bonsai	19516	-3.638	-0.281	Yes
row_109	TCONS_00006689	mEFTs	19620	-3.932	-0.272	Yes
row_110	TCONS_00028478	mRpL47	19656	-4.012	-0.259	Yes
row_111	TCONS_00022245	mRpL21	19868	-4.668	-0.253	Yes
row_112	TCONS_00006853	mRpL13	19910	-4.829	-0.238	Yes
row_113	TCONS_00001916	mRpS7	20107	-5.607	-0.228	Yes
row_114	TCONS_00008272	mRpL42	20129	-5.732	-0.209	Yes
row_115	TCONS_00015134	mRpS17	20178	-5.962	-0.191	Yes
row_116	TCONS_00024624	mRpS10	20214	-6.189	-0.171	Yes
row_117	TCONS_00033411	mRpL30	20440	-7.742	-0.155	Yes
row_118	TCONS_00029648	mRpS33	20441	-7.743	-0.128	Yes
row_119	TCONS_00005434	mRpL51	20484	-8.238	-0.101	Yes
row_120	TCONS_00013253	mRpS16	20488	-8.271	-0.073	Yes
row_121	TCONS_00014065	mRpS28	20673	-10.600	-0.045	Yes
row_122	TCONS_00016879	mRpL12	20739	-11.904	-0.007	Yes
row_123	TCONS_00036841	mRpL33	20782	-12.581	0.035	Yes

Table S2

				GO:0003735 structural constituent of ribosome									
S-hsruRNAi vs sev-GAL4 > UAS-GFP							sev-GAL4 > hsru^{EP2037} vs sev-GAL4 > UAS-GFP						
NAME	SYMBOL	TITLE	RANK IN GENE LIST	RANK METRIC SCORE	RUNNING ES	CORE ENRICHMENT	NAME	SYMBOL	TITLE	RANK IN GENE LIST	RANK METRIC SCORE	RUNNING ES	CORE ENRICHMENT
row_0	TCONS_00015256	RpL41	3	9224.600	0.171	Yes	row_0	TCONS_00015256	RpL41	3	12466.500	0.181	Yes
row_1	TCONS_00015113	RpL39	14	3218.570	0.230	Yes	row_1	TCONS_00015113	RpL39	11	4171.290	0.240	Yes
row_2	TCONS_00010698	RpL23	19	1998.640	0.266	Yes	row_2	TCONS_00010698	RpL23	18	2543.400	0.277	Yes
row_3	TCONS_00007367	RpL21	20	1910.540	0.302	Yes	row_3	TCONS_00028798	RpS25	23	1986.360	0.305	Yes
row_4	TCONS_00013256	RpS23	26	1674.880	0.332	Yes	row_4	TCONS_00009471	RpLP2	26	1887.790	0.332	Yes
row_5	TCONS_00009471	RpLP2	28	1568.520	0.361	Yes	row_5	TCONS_00007367	RpL21	27	1850.120	0.359	Yes
row_6	TCONS_00010414	RpL29	30	1409.480	0.387	Yes	row_6	TCONS_00023896	RpS29	28	1799.380	0.385	Yes
row_7	TCONS_00023896	RpS29	32	1362.440	0.412	Yes	row_7	TCONS_00010414	RpL29	30	1668.940	0.409	Yes
row_8	TCONS_00028798	RpS25	35	1286.380	0.436	Yes	row_8	TCONS_00013256	RpS23	31	1636.810	0.433	Yes
row_9	TCONS_00005288	RpL36A	37	1161.750	0.458	Yes	row_9	TCONS_00000138	RpLP1	33	1459.500	0.454	Yes
row_10	TCONS_00011250	RpL38	38	1157.880	0.479	Yes	row_10	TCONS_00019083	RpL15	34	1400.030	0.474	Yes
row_11	TCONS_00000138	RpLP1	39	1119.420	0.500	Yes	row_11	TCONS_00011250	RpL38	35	1354.810	0.494	Yes
row_12	TCONS_00019083	RpL15	40	1108.280	0.520	Yes	row_12	TCONS_00005288	RpL36A	39	1214.590	0.511	Yes
row_13	TCONS_00036282	RpL36	42	885.330	0.537	Yes	row_13	TCONS_00039004	RpS5a	40	1196.750	0.529	Yes
row_14	TCONS_00039004	RpS5a	44	836.530	0.552	Yes	row_14	TCONS_00036282	RpL36	44	1069.720	0.544	Yes
row_15	TCONS_00013710	RpS15	45	829.760	0.568	Yes	row_15	TCONS_00032363	RpS3A	45	1025.760	0.559	Yes
row_16	TCONS_00012798	RpS11	46	828.950	0.583	Yes	row_16	TCONS_00013710	RpS15	47	996.880	0.573	Yes
row_17	TCONS_00031758	RpL32	47	816.960	0.598	Yes	row_17	TCONS_00031168	RpL27	48	953.810	0.587	Yes
row_18	TCONS_00038209	RpS15Aa	49	808.980	0.613	Yes	row_18	TCONS_00012798	RpS11	49	945.910	0.601	Yes
row_19	TCONS_00015285	RpL19	50	773.370	0.627	Yes	row_19	TCONS_00038209	RpS15Aa	50	938.690	0.614	Yes
row_20	TCONS_00006882	RpL30	52	762.750	0.641	Yes	row_20	TCONS_00004515	RpL27A	51	930.100	0.628	Yes
row_21	TCONS_00022856	RpL10	54	739.550	0.655	Yes	row_21	TCONS_00025589	RpS30	52	917.290	0.641	Yes
row_22	TCONS_00005392	RpS13	55	736.200	0.669	Yes	row_22	TCONS_00031758	RpL32	53	914.520	0.654	Yes
row_23	TCONS_00017545	RpS4	57	700.580	0.682	Yes	row_23	TCONS_00006882	RpL30	55	902.100	0.667	Yes
row_24	TCONS_00032363	RpS3A	59	691.970	0.694	Yes	row_24	TCONS_00022856	RpL10	56	901.640	0.681	Yes
row_25	TCONS_00025589	RpS30	60	686.030	0.707	Yes	row_25	TCONS_00005392	RpS13	57	863.660	0.693	Yes
row_26	TCONS_00004515	RpL27A	61	680.290	0.720	Yes	row_26	TCONS_00026061	RpS3	59	831.220	0.705	Yes
row_27	TCONS_00031168	RpL27	62	674.920	0.732	Yes	row_27	TCONS_00020782	RpS17	61	759.770	0.716	Yes
row_28	TCONS_00013915	RpL18A	68	536.640	0.742	Yes	row_28	TCONS_00000510	RpS21	62	754.990	0.727	Yes
row_29	TCONS_00007372	RpL5	70	514.635	0.751	Yes	row_29	TCONS_00015285	RpL19	64	749.460	0.738	Yes
row_30	TCONS_00020782	RpS17	71	506.690	0.760	Yes	row_30	TCONS_00007372	RpL5	65	743.975	0.748	Yes
row_31	TCONS_00005864	RpL9	72	506.260	0.770	Yes	row_31	TCONS_00005864	RpL9	69	685.330	0.758	Yes
row_32	TCONS_00026061	RpS3	73	504.080	0.779	Yes	row_32	TCONS_00027129	RpS8	70	678.200	0.768	Yes
row_33	TCONS_00017367	RpL10Ab	75	481.210	0.788	Yes	row_33	TCONS_00013915	RpL18A	71	663.910	0.778	Yes
row_34	TCONS_00018297	RpL26	76	476.450	0.797	Yes	row_34	TCONS_00000745	RpL40	73	651.610	0.787	Yes
row_35	TCONS_00033538	RpL35	77	471.760	0.806	Yes	row_35	TCONS_00017367	RpL10Ab	74	642.960	0.796	Yes
row_36	TCONS_00000510	RpS21	79	464.780	0.814	Yes	row_36	TCONS_00017545	RpS4	75	640.690	0.806	Yes
row_37	TCONS_00000904	RpL37A	80	451.500	0.823	Yes	row_37	TCONS_00000904	RpL37A	76	573.250	0.814	Yes
row_38	TCONS_00031788	RpS7	81	441.750	0.831	Yes	row_38	TCONS_00010110	RpL11	77	569.910	0.822	Yes
row_39	TCONS_00000745	RpL40	85	424.950	0.838	Yes	row_39	TCONS_00010623	RpS16	79	563.340	0.830	Yes
row_40	TCONS_00027129	RpS8	86	421.900	0.846	Yes	row_40	TCONS_00034160	RpS28b	81	560.240	0.838	Yes
row_41	TCONS_00035388	RpS19a	87	421.440	0.854	Yes	row_41	TCONS_00010955	RpL12	83	527.590	0.846	Yes
row_42	TCONS_00033879	RpS14a	88	395.163	0.861	Yes	row_42	TCONS_00033538	RpL35	84	526.860	0.853	Yes
row_43	TCONS_00031090	RpS27	89	387.060	0.868	Yes	row_43	TCONS_00033879	RpS14a	85	526.758	0.861	Yes
row_44	TCONS_00006206	RpL24	90	375.150	0.875	Yes	row_44	TCONS_00035388	RpS19a	86	520.790	0.869	Yes
row_45	TCONS_00010955	RpL12	91	369.630	0.882	Yes	row_45	TCONS_00006777	RpS26	88	494.420	0.876	Yes
row_46	TCONS_00005600	RpS2	94	333.080	0.888	Yes	row_46	TCONS_00017540	RpS12	91	463.130	0.882	Yes
row_47	TCONS_00010110	RpL11	98	325.730	0.894	Yes	row_47	TCONS_00031090	RpS27	93	397.330	0.888	Yes
row_48	TCONS_00006777	RpS26	100	319.410	0.900	Yes	row_48	TCONS_00008187	RpL31	94	396.310	0.894	Yes
row_49	TCONS_00017540	RpS12	101	316.040	0.906	Yes	row_49	TCONS_00018297	RpL26	97	387.060	0.899	Yes
row_50	TCONS_00010623	RpS16	110	286.720	0.910	Yes	row_50	TCONS_00006206	RpL24	98	386.670	0.905	Yes
row_51	TCONS_00034160	RpS28b	111	283.590	0.915	Yes	row_51	TCONS_00031788	RpS7	99	380.700	0.910	Yes
row_52	TCONS_00018833	RpLP0	113	276.800	0.920	Yes	row_52	TCONS_00005600	RpS2	100	375.440	0.916	Yes
row_53	TCONS_00014803	RpS24	115	249.350	0.925	Yes	row_53	TCONS_00020804	RpS9	103	342.820	0.920	Yes
row_54	TCONS_00020804	RpS9	116	248.320	0.930	Yes	row_54	TCONS_00035831	RpS10b	104	325.178	0.925	Yes
row_55	TCONS_00028451	RpL34b	117	247.742	0.934	Yes	row_55	TCONS_00028451	RpL34b	106	306.012	0.929	Yes
row_56	TCONS_00035831	RpS10b	119	233.476	0.938	Yes	row_56	TCONS_00027781	RpL35A	108	304.977	0.934	Yes
row_57	TCONS_00001858	RpL7	123	217.560	0.942	Yes	row_57	TCONS_00018833	RpLP0	110	288.920	0.938	Yes
row_58	TCONS_00027781	RpL35A	128	201.177	0.945	Yes	row_58	TCONS_00020331	RpL18	111	287.550	0.942	Yes
row_59	TCONS_00016818	RpL14	134	180.550	0.948	Yes	row_59	TCONS_00037131	RpL17	114	273.930	0.946	Yes
row_60	TCONS_00037131	RpL17	148	156.530	0.950	Yes	row_60	TCONS_00001858	RpL7	118	246.630	0.949	Yes
row_61	TCONS_00033881	RpS14b	157	136.087	0.951	Yes	row_61	TCONS_00014803	RpS24	119	246.040	0.953	Yes
row_62	TCONS_00008187	RpL31	159	130.090	0.954	Yes	row_62	TCONS_00025578	RpS20	129	201.590	0.955	Yes
row_63	TCONS_00031254	RpL34a	177	108.386	0.954	Yes	row_63	TCONS_00016818	RpL14	136	181.360	0.957	Yes
row_64	TCONS_00020331	RpL18	187	101.040	0.955	Yes	row_64	TCONS_00033881	RpS14b	145	166.664	0.958	Yes
row_65	TCONS_00028826	RpL24-like	230	69.618	0.952	No	row_65	TCONS_00031254	RpL34a	166	137.613	0.958	No
row_66	TCONS_00019032	mRpS5	238	67.346	0.952	No	row_66	TCONS_00028826	RpL24-like	196	107.899	0.956	No
row_67	TCONS_00008473	RpS15Ab	375	31.381	0.938	No	row_67	TCONS_00019032	mRpS5	218	84.994	0.955	No
row_68	TCONS_00029165	mRpS21	406	28.261	0.936	No	row_68	TCONS_00008473	RpS15Ab	301	51.155	0.947	No
row_69	TCONS_00001833	RpL13	451	24.200	0.931	No	row_69	TCONS_00029165	mRpS21	306	50.111	0.948	No
row_70	TCONS_00004519	mRpL27	520	20.295	0.924	No	row_70	TCONS_00004519	mRpL27	462	28.241	0.932	No
row_71	TCONS_00009354	mRpL34	572	17.861	0.919	No	row_71	TCONS_00028285	mRpS18A	539	23.474	0.924	No
row_72	TCONS_00036841	mRpL33	603	16.610	0.916	No	row_72	TCONS_00001916	mRpS7	542	23.342	0.924	No
row_73	TCONS_00017993	mRpS34	638	15.535	0.913	No	row_73	TCONS_00009354	mRpL34	546	23.196	0.924	No
row_74	TCONS_00030070	mRpL55	655	15.021	0.912	No	row_74	TCONS_00036841	mRpL33	598	20.536	0.919	No
row_75	TCONS_00001916	mRpS7	716	13.289	0.906	No	row_75	TCONS_00038361	mRpS25	627	19.664	0.916	No
row_76	TCONS_00021319	mRpL20	726	13.033	0.905	No	row_76	TCONS_00015134	mRpS17	646	19.004	0.915	No
row_77	TCONS_00012400	RpLP0-like	746	12.493	0.903	No	row_77	TCONS_00030070	mRpL55	658	18.584	0.914	No
row_78	TCONS_00028285	mRpS18A	764	12.090	0.901	No	row_78	TCONS_00019551	mRpL23	665	18.384	0.913	No
row_79	TCONS_00024546	mRpL11	796	11.427	0.898	No	row_79	TCONS_00012400	RpLP0-like	682	17.853	0.912	No
row_80	TCONS_00015134	mRpS17	804	11.218	0.898	No	row_80	TCONS_00013253	mRpS16	685	17.656	0.912	No
row_81	TCONS_00038361	mRpS25	805	11.153	0.898	No	row_81	TCONS_00024624	mRpS10	699	17.299	0.911	No
row_82	TCONS_00024624	mRpS10	806	11.132	0.898	No	row_82	TCONS_00021548	mRpL39	716	16.719	0.909	No
row_83	TCONS_00013253	mRpS16	810	11.054	0.898	No	row_83	TCONS_00033411	mRpL30	754	15.764	0.906	No
row_84	TCONS_00011866	mRpL52	814	10.981	0.898	No	row_84	TCONS_00029648	mRpS33	758	15.711	0.905	No
row_85	TCONS_00029648	mRpS33	823	10.852	0.897	No	row_85	TCONS_00004628	mRpL24	793	14.211	0.902	No
row_86	TCONS_00036472	CG14817	832	10.745	0.897	No	row_86	TCONS_00011866	mRpL52	837	13.283	0.898	No
row_87	TCONS_00004628	mRpL24	862	10.242	0.894	No	row_87	TCONS_00034698	mRpL49	843	13.222	0.897	No
row_88	TCONS_00023673	mRpL19	904	9.465	0.890	No	row_88	TCONS_00017993	mRpS34	866	12.821	0.895	No
row_89	TCONS_00017254	mRpL2	999	8.013	0.880	No	row_89	TCONS_00006539	mRpL4	872	12.752	0.895	No
row_90	TCONS_00020525	mRpL36	1044	7.470	0.875	No	row_90	TCONS_00020525	mRpL36	889	12.285	0.893	No
row_91	TCONS_00028478	mRpL47	1071	7.130	0.873	No	row_91	TCONS_00015397	mRpL17	931	11.442	0.889	No
row_92	TCONS_00021548	mRpL39	1096	6.928	0.870	No	row_92	TCONS_00023673	mRpL19	945	11.253	0.888	No
row_93	TCONS_00008810	mRpL18	1116	6.787	0.868	No	row_93	TCONS_00024546	mRpL11	985	10.602	0.884	No
row_94	TCONS_00036606	mRpL14	1119	6.764	0.868	No	row_94	TCONS_00021319	mRpL20	1012	10.205	0.881	No
row_95	TCONS_00017889	mRpS31	1164	6.230	0.864	No	row_95	TCONS_00016175	mRpS6	1038	9.800	0.879	No
row_96	TCONS_00006539	mRpL4	1180	6.078	0.862	No	row_96	TCONS_00005434	mRpL51	1059	9.524	0.877	No
row_97	TCONS_00022244	mRpL21	1181	6.069	0.862	No	row_97	TCONS_00006254	mRpS23	1065	9.395	0.876	No
row_98	TCONS_00030904	mRpS24	1188	6.028	0.862	No	row_98	TCONS_00036472	CG14817	1071	9.282	0.876	No
row_99	TCONS_00019551	mRpL23	1190	6.004	0.862	No	row_99	TCONS_00001833	RpL13	1096	8.950	0.873	No
row_100	TCONS_00025968	mRpL45	1195	5.969	0.861	No	row_100	TCONS_00036606	mRpL14	1191	8.004	0.864	No
row_101	TCONS_00033411	mRpL30	1223	5.730	0.859	No	row_101	TCONS_00025828	mRpL35	1200	7.944	0.863	No
row_102	TCONS_00028178	mRpS9	1305	5.007	0.850	No	row_102	TCONS_00017254	mRpL2	1216	7.828	0.861	No
row_103	TCONS_00015397	mRpL17	1329	4.873	0.848	No	row_103	TCONS_00025968	mRpL45	1272	7.337	0.856	No
row_104	TCONS_00015832	mRpS35	1332	4.855	0.848	No	row_104	TCONS_00028478	mRpL47	1274	7.321	0.856	No
row_105	TCONS_00005434	mRpL51	1340	4.785	0.847	No	row_105	TCONS_00027782	mRpL44	1301	7.031	0.853	No
row_106	TCONS_00014065	mRpS28	1350	4.716	0.846	No	row_106	TCONS_00027227	mRpS18C	1334	6.782	0.850	No
row_107	TCONS_00032959	mRpL16	1358	4.664	0.845	No	row_107	TCONS_00032959	mRpL16	1337	6.765	0.850	No
row_108	TCONS_00022498	mRpL15	1407	4.347	0.840	No	row_108	TCONS_00022244	mRpL21	1345	6.736	0.849	No
row_109	TCONS_00034698	mRpL49	1530	3.799	0.827	No	row_109	TCONS_00035147	mRpL3	1385	6.404	0.845	No
row_110	TCONS_00026189	cav	1531	3.797	0.828	No	row_110	TCONS_00014065	mRpS28	1425	6.108	0.841	No
row_111	TCONS_00035147	mRpL3	1552	3.706	0.825	No	row_111	TCONS_00013434	mRpL41	1451	5.881	0.838	No
row_112	TCONS_00010356	mRpL54	1597	3.492	0.821	No	row_112	TCONS_00022498	mRpL15	1457	5.842	0.838	No
row_113	TCONS_00006254	mRpS23	1630	3.364	0.817	No	row_113	TCONS_00000859	mRpL28	1476	5.756	0.836	No
row_114	TCONS_00013434	mRpL41	1764	2.770	0.803	No	row_114	TCONS_00020334	mRpL50	1507	5.525	0.833	No
row_115	TCONS_00010852	mRpL43	1858	2.424	0.794	No	row_115	TCONS_00008272	mRpL42	1548	5.251	0.829	No
row_116	TCONS_00025578	RpS20	2083	1.820	0.770	No	row_116	TCONS_00010637	bonsai	1566	5.147	0.827	No
row_117	TCONS_00037074	CG11700	2121	1.745	0.766	No	row_117	TCONS_00010852	mRpL43	1579	5.095	0.826	No
row_118	TCONS_00010637	bonsai	2208	1.546	0.757	No	row_118	TCONS_00010356	mRpL54	1618	4.846	0.822	No
row_119	TCONS_00020334	mRpL50	2325	1.309	0.744	No	row_119	TCONS_00015832	mRpS35	1619	4.843	0.822	No
row_120	TCONS_00024093	mRpL40	2379	1.229	0.739	No	row_120	TCONS_00008810	mRpL18	1646	4.654	0.819	No
row_121	TCONS_00018223	mRpS26	2478	1.077	0.728	No	row_121	TCONS_00024093	mRpL40	1695	4.422	0.814	No
row_122	TCONS_00023626	mRpL1	2553	0.980	0.720	No	row_122	TCONS_00026189	cav	1709	4.342	0.813	No
row_123	TCONS_00030580	CG31156	2619	0.882	0.713	No	row_123	TCONS_00027352	mRpL32	1766	4.069	0.807	No
row_124	TCONS_00000859	mRpL28	2646	0.845	0.711	No	row_124	TCONS_00036629	tko	1779	3.999	0.806	No
row_125	TCONS_00024604	RpL10Aa	2741	0.742	0.701	No	row_125	TCONS_00017889	mRpS31	1823	3.854	0.801	No
row_126	TCONS_00028746	mRpL37	2820	0.658	0.692	No	row_126	TCONS_00028178	mRpS9	1914	3.498	0.791	No
row_127	TCONS_00030833	RpS19b	2980	0.492	0.675	No	row_127	TCONS_00018223	mRpS26	1970	3.297	0.786	No
row_128	TCONS_00014907	RpL22-like	3331	0.271	0.638	No	row_128	TCONS_00030904	mRpS24	1992	3.183	0.783	No
row_129	TCONS_00007076	mRpS18B	3611	0.147	0.608	No	row_129	TCONS_00000095	mRpL10	2146	2.647	0.767	No
row_130	TCONS_00025828	mRpL35	3867	0.083	0.581	No	row_130	TCONS_00025012	mRpS11	2159	2.603	0.766	No
row_131	TCONS_00027782	mRpL44	3933	0.071	0.574	No	row_131	TCONS_00007076	mRpS18B	2166	2.590	0.765	No
row_132	TCONS_00027227	mRpS18C	4044	0.049	0.563	No	row_132	TCONS_00037074	CG11700	2281	2.297	0.753	No
row_133	TCONS_00027352	mRpL32	4295	0.011	0.536	No	row_133	TCONS_00016879	mRpL12	2296	2.260	0.752	No
row_134	TCONS_00014892	RpL37b	4525	0.000	0.512	No	row_134	TCONS_00023626	mRpL1	2551	1.667	0.725	No
row_135	TCONS_00024688	mRpL9	5190	-0.088	0.441	No	row_135	TCONS_00026853	mRpS22	2731	1.313	0.706	No
row_136	TCONS_00000095	mRpL10	5201	-0.091	0.440	No	row_136	TCONS_00028746	mRpL37	3094	0.793	0.667	No
row_137	TCONS_00031991	RpL6	5291	-0.110	0.430	No	row_137	TCONS_00014781	mRpS29	3107	0.777	0.666	No
row_138	TCONS_00000323	mRpL48	5846	-0.324	0.371	No	row_138	TCONS_00015685	mRpL46	3177	0.705	0.659	No
row_139	TCONS_00026830	RpS10a	5939	-0.365	0.362	No	row_139	TCONS_00024688	mRpL9	3242	0.624	0.652	No
row_140	TCONS_00004603	mRpS2	6298	-0.563	0.323	No	row_140	TCONS_00000323	mRpL48	3277	0.589	0.648	No
row_141	TCONS_00029402	RpS5b	6761	-0.962	0.274	No	row_141	TCONS_00030833	RpS19b	3301	0.570	0.646	No

row_142	TCONS_00014781	mRpS29	6850	-1.035	0.265	No			row_142	TCONS_00030580	CG31156	3304	0.569	0.645	No
row_143	TCONS_00034947	mRpL38	7124	-1.415	0.236	No			row_143	TCONS_00029402	RpS5b	3830	0.226	0.590	No
row_144	TCONS_00015685	mRpL46	7225	-1.561	0.225	No			row_144	TCONS_00004603	mRpS2	4105	0.132	0.560	No
row_145	TCONS_00008272	mRpL42	7382	-1.802	0.209	No			row_145	TCONS_00014907	RpL22-like	4421	0.064	0.527	No
row_146	TCONS_00016175	mRpS6	7674	-2.571	0.178	No			row_146	TCONS_00024604	RpL10Aa	4798	0.006	0.487	No
row_147	TCONS_00016879	mRpL12	7686	-2.584	0.176	No			row_147	TCONS_00014892	RpL37b	4995	0.000	0.466	No
row_148	TCONS_00026853	mRpS22	7930	-3.298	0.151	No			row_148	TCONS_00026830	RpS10a	6138	-0.269	0.344	No
row_149	TCONS_00025012	mRpS11	8166	-4.228	0.126	No			row_149	TCONS_00034947	mRpL38	7040	-1.151	0.248	No
row_150	TCONS_00035424	mRpL22	8415	-5.606	0.099	No			row_150	TCONS_00035424	mRpL22	7947	-3.702	0.152	No
row_151	TCONS_00035152	mRpS30	8941	-11.256	0.044	No			row_151	TCONS_00035152	mRpS30	8772	-9.807	0.064	No
row_152	TCONS_00036629	tko	9103	-14.201	0.027	No			row_152	TCONS_00036392	sta	9516	-146.080	-0.013	No
row_153	TCONS_00037101	RpL7A	9523	-167.080	-0.015	No			row_153	TCONS_00037101	RpL7A	9519	-180.100	-0.011	No
row_154	TCONS_00036392	sta	9530	-248.560	-0.011	No			row_154	TCONS_00031991	RpL6	9525	-239.910	-0.008	No
row_155	TCONS_00026854	RpL4	9531	-267.559	-0.006	No			row_155	TCONS_00015800	RpL8	9529	-298.510	-0.004	No
row_156	TCONS_00015800	RpL8	9534	-371.450	0.001	No			row_156	TCONS_00026854	RpL4	9532	-336.339	0.001	No
						GO:0006412									
S-hsruRNAi vs sev-GAL4 > UAS-GFP								**sev-GAL4 > hsru[EP0001] vs sev-GAL4 > UAS-GFP**						
NAME	**SYMBOL**	**TITLE**	**RANK IN GENE LIST**	**RANK METRIC SCORE**	**RUNNING ES**	**CORE ENRICHMENT**			**NAME**	**SYMBOL**	**TITLE**	**RANK IN GENE LIST**	**RANK METRIC SCORE**	**RUNNING ES**	**CORE ENRICHMENT**
row_0	TCONS_00015256	RpL41	3	9224.600	0.170	Yes			row_0	TCONS_00015256	RpL41	3	12466.500	0.180	Yes
row_1	TCONS_00015113	RpL39	14	3218.570	0.229	Yes			row_1	TCONS_00015113	RpL39	11	4171.290	0.239	Yes
row_2	TCONS_00010698	RpL23	19	1998.640	0.265	Yes			row_2	TCONS_00010698	RpL23	18	2543.400	0.276	Yes
row_3	TCONS_00007367	RpL21	20	1910.540	0.301	Yes			row_3	TCONS_00028798	RpS25	23	1986.360	0.304	Yes
row_4	TCONS_00013256	RpS23	26	1674.880	0.331	Yes			row_4	TCONS_00009471	RpLP2	26	1887.790	0.331	Yes
row_5	TCONS_00009471	RpLP2	28	1568.520	0.360	Yes			row_5	TCONS_00007367	RpL21	27	1850.120	0.358	Yes
row_6	TCONS_00010414	RpL29	30	1409.480	0.386	Yes			row_6	TCONS_00023896	RpS29	28	1799.380	0.384	Yes
row_7	TCONS_00023896	RpS29	32	1362.440	0.411	Yes			row_7	TCONS_00010414	RpL29	30	1668.940	0.408	Yes
row_8	TCONS_00028798	RpS25	35	1286.380	0.434	Yes			row_8	TCONS_00013256	RpS23	31	1636.810	0.431	Yes
row_9	TCONS_00005288	RpL36A	37	1161.750	0.456	Yes			row_9	TCONS_00000138	RpLP1	33	1459.500	0.452	Yes
row_10	TCONS_00011250	RpL38	38	1157.880	0.477	Yes			row_10	TCONS_00019083	RpL15	34	1400.030	0.473	Yes
row_11	TCONS_00000138	RpLP1	39	1119.420	0.498	Yes			row_11	TCONS_00011250	RpL38	35	1354.810	0.492	Yes
row_12	TCONS_00019083	RpL15	40	1108.280	0.518	Yes			row_12	TCONS_00005288	RpL36A	39	1214.590	0.510	Yes
row_13	TCONS_00036282	RpL36	42	885.330	0.535	Yes			row_13	TCONS_00039004	RpS5a	40	1196.750	0.527	Yes
row_14	TCONS_00039004	RpS5a	44	836.530	0.550	Yes			row_14	TCONS_00036282	RpL36	44	1069.720	0.542	Yes
row_15	TCONS_00013710	RpS15	45	829.760	0.565	Yes			row_15	TCONS_00032363	RpS3A	45	1025.760	0.557	Yes
row_16	TCONS_00012798	RpS11	46	828.950	0.581	Yes			row_16	TCONS_00013710	RpS15	47	996.880	0.571	Yes
row_17	TCONS_00031758	RpL32	47	816.960	0.596	Yes			row_17	TCONS_00031168	RpL27	48	953.810	0.585	Yes
row_18	TCONS_00038209	RpS15Aa	49	808.980	0.611	Yes			row_18	TCONS_00012798	RpS11	49	945.910	0.599	Yes
row_19	TCONS_00015285	RpL19	50	773.370	0.625	Yes			row_19	TCONS_00038209	RpS15Aa	50	938.690	0.612	Yes
row_20	TCONS_00006882	RpL30	52	762.750	0.639	Yes			row_20	TCONS_00004515	RpL27A	51	930.100	0.626	Yes
row_21	TCONS_00022856	RpL10	54	739.550	0.653	Yes			row_21	TCONS_00025589	RpS30	52	917.290	0.639	Yes
row_22	TCONS_00005392	RpS13	55	736.200	0.666	Yes			row_22	TCONS_00031758	RpL32	53	914.520	0.652	Yes
row_23	TCONS_00017545	RpS4	57	700.580	0.679	Yes			row_23	TCONS_00006882	RpL30	55	902.100	0.665	Yes
row_24	TCONS_00032363	RpS3A	59	691.970	0.692	Yes			row_24	TCONS_00022856	RpL10	56	901.640	0.678	Yes
row_25	TCONS_00025589	RpS30	60	686.030	0.704	Yes			row_25	TCONS_00005392	RpS13	57	863.660	0.691	Yes
row_26	TCONS_00004515	RpL27A	61	680.290	0.717	Yes			row_26	TCONS_00026061	RpS3	59	831.220	0.702	Yes
row_27	TCONS_00031168	RpL27	62	674.920	0.729	Yes			row_27	TCONS_00020782	RpS17	61	759.770	0.713	Yes
row_28	TCONS_00013915	RpL18A	68	536.640	0.739	Yes			row_28	TCONS_00000510	RpS21	62	754.990	0.724	Yes
row_29	TCONS_00007372	RpL5	70	514.635	0.748	Yes			row_29	TCONS_00015285	RpL19	64	749.460	0.735	Yes
row_30	TCONS_00020782	RpS17	71	506.690	0.758	Yes			row_30	TCONS_00007372	RpL5	65	743.975	0.746	Yes
row_31	TCONS_00005864	RpL9	72	506.260	0.767	Yes			row_31	TCONS_00005864	RpL9	69	685.330	0.755	Yes
row_32	TCONS_00026061	RpS3	73	504.080	0.776	Yes			row_32	TCONS_00027129	RpS8	70	678.200	0.765	Yes
row_33	TCONS_00017367	RpL10Ab	75	481.210	0.785	Yes			row_33	TCONS_00013915	RpL18A	71	663.910	0.775	Yes
row_34	TCONS_00018297	RpL26	76	476.450	0.794	Yes			row_34	TCONS_00000745	RpL40	73	651.610	0.784	Yes
row_35	TCONS_00033538	RpL35	77	471.760	0.803	Yes			row_35	TCONS_00017367	RpL10Ab	74	642.960	0.793	Yes
row_36	TCONS_00000510	RpS21	79	464.780	0.811	Yes			row_36	TCONS_00017545	RpS4	75	640.690	0.803	Yes
row_37	TCONS_00000904	RpL37A	80	451.500	0.819	Yes			row_37	TCONS_00000904	RpL37A	76	573.250	0.811	Yes
row_38	TCONS_00031788	RpS7	81	441.750	0.828	Yes			row_38	TCONS_00010110	RpL11	77	569.910	0.819	Yes
row_39	TCONS_00000745	RpL40	85	424.950	0.835	Yes			row_39	TCONS_00010623	RpS16	79	563.340	0.827	Yes
row_40	TCONS_00027129	RpS8	86	421.900	0.843	Yes			row_40	TCONS_00034160	RpS28b	81	560.240	0.835	Yes
row_41	TCONS_00035388	RpS19a	87	421.440	0.851	Yes			row_41	TCONS_00010955	RpL12	83	527.590	0.843	Yes
row_42	TCONS_00033879	RpS14a	88	395.163	0.858	Yes			row_42	TCONS_00033538	RpL35	84	526.860	0.850	Yes
row_43	TCONS_00031090	RpS27	89	387.060	0.865	Yes			row_43	TCONS_00033879	RpS14a	85	526.758	0.858	Yes
row_44	TCONS_00006206	RpL24	90	375.150	0.872	Yes			row_44	TCONS_00035388	RpS19a	86	520.790	0.865	Yes
row_45	TCONS_00010955	RpL12	91	369.630	0.879	Yes			row_45	TCONS_00006777	RpS26	88	494.420	0.872	Yes
row_46	TCONS_00005600	RpS2	94	333.080	0.885	Yes			row_46	TCONS_00031090	RpS27	93	397.330	0.878	Yes
row_47	TCONS_00010110	RpL11	98	325.730	0.891	Yes			row_47	TCONS_00008187	RpL31	94	396.310	0.884	Yes
row_48	TCONS_00006777	RpS26	100	319.410	0.896	Yes			row_48	TCONS_00018297	RpL26	97	387.060	0.889	Yes
row_49	TCONS_00010623	RpS16	110	286.720	0.901	Yes			row_49	TCONS_00006206	RpL24	98	386.670	0.894	Yes
row_50	TCONS_00034160	RpS28b	111	283.590	0.906	Yes			row_50	TCONS_00031788	RpS7	99	380.700	0.900	Yes
row_51	TCONS_00018833	RpLP0	113	276.800	0.911	Yes			row_51	TCONS_00005600	RpS2	100	375.440	0.905	Yes
row_52	TCONS_00014803	RpS24	115	249.350	0.916	Yes			row_52	TCONS_00020804	RpS9	103	342.820	0.910	Yes
row_53	TCONS_00020804	RpS9	116	248.320	0.920	Yes			row_53	TCONS_00035831	RpS10b	104	325.178	0.915	Yes
row_54	TCONS_00028451	RpL34b	117	247.742	0.925	Yes			row_54	TCONS_00028451	RpL34b	106	306.012	0.919	Yes
row_55	TCONS_00035831	RpS10b	119	233.476	0.929	Yes			row_55	TCONS_00027781	RpL35A	108	304.977	0.923	Yes
row_56	TCONS_00001858	RpL7	123	217.560	0.933	Yes			row_56	TCONS_00018833	RpLP0	110	288.920	0.928	Yes
row_57	TCONS_00027781	RpL35A	128	201.177	0.936	Yes			row_57	TCONS_00020331	RpL18	111	287.550	0.932	Yes
row_58	TCONS_00016818	RpL14	134	180.550	0.939	Yes			row_58	TCONS_00037131	RpL17	114	273.930	0.935	Yes
row_59	TCONS_00001869	eEF1delta	143	162.760	0.941	Yes			row_59	TCONS_00001858	RpL7	118	246.630	0.939	Yes
row_60	TCONS_00037131	RpL17	148	156.530	0.943	Yes			row_60	TCONS_00014803	RpS24	119	246.040	0.942	Yes
row_61	TCONS_00033881	RpS14b	157	136.087	0.945	Yes			row_61	TCONS_00025578	RpS20	129	201.590	0.944	Yes
row_62	TCONS_00008187	RpL31	159	130.090	0.947	Yes			row_62	TCONS_00016818	RpL14	136	181.360	0.946	Yes
row_63	TCONS_00031254	RpL34a	177	108.386	0.947	Yes			row_63	TCONS_00001869	eEF1delta	141	177.248	0.948	Yes
row_64	TCONS_00020331	RpL18	187	101.040	0.948	Yes			row_64	TCONS_00033881	RpS14b	145	166.664	0.950	Yes
row_65	TCONS_00028826	RpL24-like	230	69.618	0.945	No			row_65	TCONS_00031254	RpL34a	166	137.613	0.950	No
row_66	TCONS_00008473	RpS15Ab	375	31.381	0.930	No			row_66	TCONS_00028826	RpL24-like	196	107.899	0.949	No
row_67	TCONS_00029165	mRpS21	406	28.261	0.928	No			row_67	TCONS_00008473	RpS15Ab	301	51.155	0.938	No
row_68	TCONS_00001833	RpL13	451	24.200	0.923	No			row_68	TCONS_00029165	mRpS21	306	50.111	0.939	No
row_69	TCONS_00038652	eIF5	496	21.317	0.919	No			row_69	TCONS_00004519	mRpL27	462	28.241	0.922	No
row_70	TCONS_00004519	mRpL27	520	20.295	0.917	No			row_70	TCONS_00030906	CG5515	532	23.687	0.915	No
row_71	TCONS_00009354	mRpL34	572	17.861	0.912	No			row_71	TCONS_00028285	mRpS18A	539	23.474	0.915	No
row_72	TCONS_00036841	mRpL33	603	16.610	0.909	No			row_72	TCONS_00001916	mRpS7	542	23.342	0.915	No
row_73	TCONS_00017993	mRpS34	638	15.535	0.906	No			row_73	TCONS_00009354	mRpL34	546	23.196	0.915	No
row_74	TCONS_00030070	mRpL55	655	15.021	0.904	No			row_74	TCONS_00038652	eIF5	584	21.142	0.912	No
row_75	TCONS_00030906	CG5515	705	13.468	0.899	No			row_75	TCONS_00036841	mRpL33	598	20.536	0.910	No
row_76	TCONS_00001916	mRpS7	716	13.289	0.898	No			row_76	TCONS_00038361	mRpS25	627	19.664	0.908	No
row_77	TCONS_00021319	mRpL20	726	13.033	0.898	No			row_77	TCONS_00015134	mRpS17	646	19.004	0.906	No
row_78	TCONS_00012400	RpLP0-like	746	12.493	0.896	No			row_78	TCONS_00030070	mRpL55	658	18.584	0.905	No
row_79	TCONS_00028285	mRpS18A	764	12.090	0.894	No			row_79	TCONS_00019551	mRpL23	665	18.384	0.905	No
row_80	TCONS_00020679	pix	795	11.452	0.891	No			row_80	TCONS_00012400	RpLP0-like	682	17.853	0.903	No
row_81	TCONS_00024546	mRpL11	796	11.427	0.892	No			row_81	TCONS_00013253	mRpS16	685	17.656	0.903	No
row_82	TCONS_00015134	mRpS17	804	11.218	0.891	No			row_82	TCONS_00024624	mRpS10	699	17.299	0.902	No
row_83	TCONS_00038361	mRpS25	805	11.153	0.891	No			row_83	TCONS_00021548	mRpL39	716	16.719	0.901	No
row_84	TCONS_00024624	mRpS10	806	11.132	0.891	No			row_84	TCONS_00033411	mRpL30	754	15.764	0.897	No
row_85	TCONS_00013253	mRpS16	810	11.054	0.891	No			row_85	TCONS_00029648	mRpS33	758	15.711	0.897	No
row_86	TCONS_00011866	mRpL52	814	10.981	0.891	No			row_86	TCONS_00004628	mRpL24	793	14.211	0.894	No
row_87	TCONS_00029648	mRpS33	823	10.852	0.890	No			row_87	TCONS_00011866	mRpL52	837	13.283	0.889	No
row_88	TCONS_00004628	mRpL24	862	10.242	0.887	No			row_88	TCONS_00034698	mRpL49	843	13.222	0.889	No
row_89	TCONS_00023673	mRpL19	904	9.465	0.882	No			row_89	TCONS_00017993	mRpS34	866	12.821	0.887	No
row_90	TCONS_00020616	GAPsec	917	9.266	0.881	No			row_90	TCONS_00006539	mRpL4	872	12.752	0.886	No
row_91	TCONS_00017254	mRpL2	999	8.013	0.873	No			row_91	TCONS_00008623	128up	874	12.704	0.886	No
row_92	TCONS_00030135	CG6195	1020	7.801	0.871	No			row_92	TCONS_00020525	mRpL36	889	12.285	0.885	No
row_93	TCONS_00020525	mRpL36	1044	7.470	0.868	No			row_93	TCONS_00015397	mRpL17	931	11.442	0.881	No
row_94	TCONS_00028478	mRpL47	1071	7.130	0.866	No			row_94	TCONS_00023673	mRpL19	945	11.253	0.880	No
row_95	TCONS_00025006	CG5220	1081	7.038	0.865	No			row_95	TCONS_00020679	pix	950	11.192	0.879	No
row_96	TCONS_00021548	mRpL39	1096	6.928	0.864	No			row_96	TCONS_00024546	mRpL11	985	10.602	0.876	No
row_97	TCONS_00008810	mRpL18	1116	6.787	0.862	No			row_97	TCONS_00021319	mRpL20	1012	10.205	0.873	No
row_98	TCONS_00036606	mRpL14	1119	6.764	0.862	No			row_98	TCONS_00025006	CG5220	1034	9.831	0.871	No
row_99	TCONS_00008623	128up	1129	6.623	0.861	No			row_99	TCONS_00016175	mRpS6	1038	9.800	0.871	No
row_100	TCONS_00017889	mRpS31	1164	6.230	0.857	No			row_100	TCONS_00001976	CG6094	1057	9.531	0.869	No
row_101	TCONS_00001976	CG6094	1173	6.155	0.857	No			row_101	TCONS_00005434	mRpL51	1059	9.524	0.869	No
row_102	TCONS_00006539	mRpL4	1180	6.078	0.856	No			row_102	TCONS_00006254	mRpS23	1065	9.395	0.869	No
row_103	TCONS_00022244	mRpL21	1181	6.069	0.856	No			row_103	TCONS_00001833	RpL13	1096	8.950	0.866	No
row_104	TCONS_00030904	mRpS24	1188	6.028	0.856	No			row_104	TCONS_00030135	CG6195	1131	8.591	0.862	No
row_105	TCONS_00019551	mRpL23	1190	6.004	0.856	No			row_105	TCONS_00036606	mRpL14	1191	8.004	0.856	No
row_106	TCONS_00025968	mRpL45	1195	5.969	0.855	No			row_106	TCONS_00025828	mRpL35	1200	7.944	0.855	No
row_107	TCONS_00033411	mRpL30	1223	5.730	0.852	No			row_107	TCONS_00017254	mRpL2	1216	7.828	0.854	No
row_108	TCONS_00012079	CG8635	1251	5.427	0.850	No			row_108	TCONS_00025968	mRpL45	1272	7.337	0.848	No
row_109	TCONS_00028178	mRpS9	1305	5.007	0.844	No			row_109	TCONS_00028478	mRpL47	1274	7.321	0.848	No
row_110	TCONS_00015397	mRpL17	1329	4.873	0.842	No			row_110	TCONS_00027782	mRpL44	1301	7.031	0.845	No
row_111	TCONS_00015832	mRpS35	1332	4.855	0.842	No			row_111	TCONS_00027227	mRpS18C	1334	6.782	0.842	No
row_112	TCONS_00005434	mRpL51	1340	4.785	0.841	No			row_112	TCONS_00032959	mRpL16	1337	6.765	0.842	No
row_113	TCONS_00014065	mRpS28	1350	4.716	0.840	No			row_113	TCONS_00022244	mRpL21	1345	6.736	0.841	No
row_114	TCONS_00032959	mRpL16	1358	4.664	0.839	No			row_114	TCONS_00035147	mRpL3	1385	6.404	0.837	No
row_115	TCONS_00022498	mRpL15	1407	4.347	0.834	No			row_115	TCONS_00023188	CG1427	1415	6.181	0.834	No
row_116	TCONS_00034698	mRpL49	1530	3.799	0.821	No			row_116	TCONS_00014065	mRpS28	1425	6.108	0.833	No
row_117	TCONS_00035147	mRpL3	1552	3.706	0.819	No			row_117	TCONS_00013434	mRpL41	1451	5.881	0.831	No
row_118	TCONS_00004448	CG31957	1586	3.557	0.816	No			row_118	TCONS_00022498	mRpL15	1457	5.842	0.830	No
row_119	TCONS_00010356	mRpL54	1597	3.492	0.815	No			row_119	TCONS_00000859	mRpL28	1476	5.756	0.828	No
row_120	TCONS_00006254	mRpS23	1630	3.364	0.811	No			row_120	TCONS_00020334	mRpL50	1507	5.525	0.825	No
row_121	TCONS_00013434	mRpL41	1764	2.770	0.797	No			row_121	TCONS_00008272	mRpL42	1548	5.251	0.821	No
row_122	TCONS_00030346	CG7009	1816	2.583	0.792	No			row_122	TCONS_00030346	CG7009	1562	5.157	0.820	No
row_123	TCONS_00030887	Slimp	1846	2.451	0.789	No			row_123	TCONS_00010637	bonsai	1566	5.147	0.819	No
row_124	TCONS_00010852	mRpL43	1858	2.424	0.788	No			row_124	TCONS_00010852	mRpL43	1579	5.095	0.818	No
row_125	TCONS_00026448	Cltn	1913	2.267	0.782	No			row_125	TCONS_00010356	mRpL54	1618	4.846	0.814	No
row_126	TCONS_00016736	Sbp2	1931	2.228	0.780	No			row_126	TCONS_00015832	mRpS35	1619	4.843	0.814	No
row_127	TCONS_00025578	RpS20	2083	1.820	0.764	No			row_127	TCONS_00020616	GAPsec	1645	4.658	0.812	No
row_128	TCONS_00010637	bonsai	2208	1.546	0.751	No			row_128	TCONS_00008810	mRpL18	1646	4.654	0.812	No
row_129	TCONS_00030606	CG17141	2250	1.465	0.746	No			row_129	TCONS_00024093	mRpL40	1695	4.422	0.807	No

row_130	TCONS_00020334	mRpL50	2325	1.309	0.739	No		row_130	TCONS_00015229	CG12848	1701	4.392	0.806	No
row_131	TCONS_00024093	mRpL40	2379	1.229	0.733	No		row_131	TCONS_00027352	mRpL32	1766	4.069	0.799	No
row_132	TCONS_00018223	mRpS26	2478	1.077	0.722	No		row_132	TCONS_00036629	tko	1779	3.999	0.798	No
row_133	TCONS_00023626	mRpL1	2553	0.980	0.715	No		row_133	TCONS_00017889	mRpS31	1823	3.854	0.794	No
row_134	TCONS_00030580	CG31156	2619	0.882	0.708	No		row_134	TCONS_00028178	mRpS9	1914	3.498	0.784	No
row_135	TCONS_00000859	mRpL28	2646	0.845	0.705	No		row_135	TCONS_00018223	mRpS26	1970	3.297	0.778	No
row_136	TCONS_00024604	RpL10Aa	2741	0.742	0.695	No		row_136	TCONS_00030904	mRpS24	1992	3.183	0.776	No
row_137	TCONS_00015229	CG12848	2777	0.709	0.691	No		row_137	TCONS_00044448	CG11957	2066	2.888	0.768	No
row_138	TCONS_00028746	mRpL37	2820	0.658	0.687	No		row_138	TCONS_00000095	mRpL10	2146	2.647	0.760	No
row_139	TCONS_00031973	CG1750	2926	0.540	0.675	No		row_139	TCONS_00025012	mRpS11	2159	2.603	0.759	No
row_140	TCONS_00030833	RpS19b	2980	0.492	0.670	No		row_140	TCONS_00007076	mRpS18B	2166	2.590	0.758	No
row_141	TCONS_00014907	RpL22-like	3331	0.271	0.632	No		row_141	TCONS_00035106	CG8097	2214	2.454	0.753	No
row_142	TCONS_00014017	Dgp-1	3432	0.228	0.622	No		row_142	TCONS_00031973	CG1750	2254	2.363	0.749	No
row_143	TCONS_00035106	CG8097	3487	0.198	0.616	No		row_143	TCONS_00016879	mRpL12	2296	2.260	0.745	No
row_144	TCONS_00007076	mRpS18B	3611	0.147	0.603	No		row_144	TCONS_00012079	CG8635	2390	2.042	0.735	No
row_145	TCONS_00025828	mRpL35	3867	0.083	0.575	No		row_145	TCONS_00034045	CG1789	2422	1.950	0.731	No
row_146	TCONS_00027782	mRpL44	3933	0.071	0.568	No		row_146	TCONS_00030606	CG17141	2536	1.692	0.719	No
row_147	TCONS_00027227	mRpS18C	4044	0.049	0.557	No		row_147	TCONS_00026448	Clbn	2546	1.675	0.718	No
row_148	TCONS_00027352	mRpL32	4295	0.011	0.530	No		row_148	TCONS_00023626	mRpL1	2551	1.667	0.718	No
row_149	TCONS_00013839	CG15605	4506	0.000	0.508	No		row_149	TCONS_00033227	CG10802	2641	1.481	0.709	No
row_150	TCONS_00014892	RpL37b	4525	0.000	0.506	No		row_150	TCONS_00016736	Sbp2	2653	1.458	0.707	No
row_151	TCONS_00024688	mRpL9	5190	-0.088	0.435	No		row_151	TCONS_00026853	mRpS22	2731	1.313	0.699	No
row_152	TCONS_00000095	mRpL10	5201	-0.091	0.434	No		row_152	TCONS_00030887	Slmp	2814	1.177	0.690	No
row_153	TCONS_00031991	RpL6	5291	-0.110	0.424	No		row_153	TCONS_00030065	gatA	2920	1.023	0.679	No
row_154	TCONS_00005630	CG13126	5422	-0.147	0.410	No		row_154	TCONS_00027891	CG2017	2950	0.987	0.676	No
row_155	TCONS_00030704	orb	5692	-0.249	0.381	No		row_155	TCONS_00028746	mRpL37	3094	0.793	0.661	No
row_156	TCONS_00000323	mRpL48	5846	-0.324	0.365	No		row_156	TCONS_00014781	mRpS29	3107	0.777	0.660	No
row_157	TCONS_00026830	RpS10a	5939	-0.365	0.355	No		row_157	TCONS_00015685	mRpL46	3177	0.705	0.652	No
row_158	TCONS_00033227	CG10802	5955	-0.373	0.354	No		row_158	TCONS_00024688	mRpL9	3242	0.624	0.645	No
row_159	TCONS_00030065	gatA	5958	-0.375	0.353	No		row_159	TCONS_00000323	mRpL48	3277	0.589	0.642	No
row_160	TCONS_00023188	CG1427	6168	-0.479	0.331	No		row_160	TCONS_00030833	RpS19b	3301	0.570	0.639	No
row_161	TCONS_00004603	mRpS2	6298	-0.563	0.317	No		row_161	TCONS_00030580	CG31156	3304	0.569	0.639	No
row_162	TCONS_00034045	CG1789	6419	-0.653	0.304	No		row_162	TCONS_00005630	CG13126	3705	0.282	0.596	No
row_163	TCONS_00013041	CG4679	6721	-0.926	0.272	No		row_163	TCONS_00029402	RpS5b	3830	0.226	0.583	No
row_164	TCONS_00029402	RpS5b	6761	-0.962	0.268	No		row_164	TCONS_00004603	mRpS2	4105	0.132	0.554	No
row_165	TCONS_00014781	mRpS29	6850	-1.035	0.259	No		row_165	TCONS_00014907	RpL22-like	4421	0.064	0.520	No
row_166	TCONS_00027891	CG2017	7067	-1.339	0.236	No		row_166	TCONS_00030704	orb	4701	0.022	0.490	No
row_167	TCONS_00034947	mRpL38	7124	-1.415	0.230	No		row_167	TCONS_00024604	RpL10Aa	4798	0.006	0.480	No
row_168	TCONS_00015685	mRpL46	7225	-1.561	0.219	No		row_168	TCONS_00013839	CG15605	4978	0.000	0.461	No
row_169	TCONS_00008272	mRpL42	7382	-1.802	0.202	No		row_169	TCONS_00014892	RpL37b	4995	0.000	0.459	No
row_170	TCONS_00016175	mRpS6	7674	-2.571	0.171	No		row_170	TCONS_00026830	RpS10a	6138	-0.269	0.337	No
row_171	TCONS_00016879	mRpL12	7686	-2.584	0.170	No		row_171	TCONS_00013041	CG4679	6386	-0.425	0.311	No
row_172	TCONS_00011066	CG11414	7922	-3.279	0.145	No		row_172	TCONS_00026870	CG4849	6580	-0.580	0.290	No
row_173	TCONS_00026853	mRpS22	7930	-3.298	0.144	No		row_173	TCONS_00034947	mRpL38	7040	-1.151	0.241	No
row_174	TCONS_00026870	CG4849	8042	-3.740	0.133	No		row_174	TCONS_00014017	Dgp-1	7529	-2.217	0.189	No
row_175	TCONS_00007857	drosha	8086	-3.943	0.128	No		row_175	TCONS_00035424	mRpL22	7947	-3.702	0.144	No
row_176	TCONS_00025012	mRpS11	8166	-4.228	0.120	No		row_176	TCONS_00007857	drosha	7998	-3.909	0.139	No
row_177	TCONS_00019739	eIF5B	8174	-4.269	0.119	No		row_177	TCONS_00004590	mxt	8408	-6.272	0.095	No
row_178	TCONS_00015017	eIF6	8276	-4.825	0.108	No		row_178	TCONS_00011066	CG11414	8429	-6.378	0.093	No
row_179	TCONS_00019460	HBS1	8288	-4.870	0.107	No		row_179	TCONS_00015017	eIF6	8470	-6.687	0.089	No
row_180	TCONS_00035424	mRpL22	8415	-5.606	0.094	No		row_180	TCONS_00019460	HBS1	8748	-9.465	0.060	No
row_181	TCONS_00004590	mxt	8494	-6.087	0.086	No		row_181	TCONS_00019739	eIF5B	8752	-9.495	0.059	No
row_182	TCONS_00035152	mRpS30	8941	-11.256	0.038	No		row_182	TCONS_00035152	mRpS30	8772	-9.807	0.057	No
row_183	TCONS_00018782	CG7414	8992	-12.015	0.033	No		row_183	TCONS_00018782	CG7414	9255	-21.627	0.006	No
row_184	TCONS_00008840	NAT1	9065	-13.422	0.026	No		row_184	TCONS_00008840	Nat1	9482	-69.609	-0.017	No
row_185	TCONS_00036629	tko	9103	-14.201	0.022	No		row_185	TCONS_00036392	sta	9516	-146.080	-0.018	No
row_186	TCONS_00037101	RpL7A	9523	-167.080	-0.020	No		row_186	TCONS_00037101	RpL7A	9519	-180.100	-0.016	No
row_187	TCONS_00036392	sta	9530	-248.560	-0.016	No		row_187	TCONS_00031991	RpL6	9525	-239.910	-0.013	No
row_188	TCONS_00026854	RpL4	9531	-267.559	-0.011	No		row_188	TCONS_00015800	RpL8	9529	-298.510	-0.009	No
row_189	TCONS_00005246	Rack1	9532	-269.820	-0.006	No		row_189	TCONS_00026854	RpL4	9532	-336.339	-0.004	No
row_190	TCONS_00015800	RpL8	9534	-371.450	0.001	No		row_190	TCONS_00005246	Rack1	9533	-367.240	0.001	No

GO 0043161 Proteosomal mediated ubiquitin-dependent protein catabolic process

S-hsruRNAi vs sev-GAL4 > UAS-GFP

NAME	SYMBOL	TITLE	RANK IN GENE LIST	RANK METRIC SCORE	RUNNING ES	CORE ENRICHMENT
row_0	TCONS_00001298	Sem1	114	261.508	0.100	Yes
row_1	TCONS_00019022	CG40045	152	142.502	0.157	Yes
row_2	TCONS_00009646	Prosalpha5	180	105.220	0.199	Yes
row_3	TCONS_00008471	Prosbeta5	193	96.776	0.239	Yes
row_4	TCONS_00006591	Prosbeta4	196	94.573	0.279	Yes
row_5	TCONS_00021867	Prosbeta6	205	85.412	0.315	Yes
row_6	TCONS_00032721	skpA	210	81.736	0.349	Yes
row_7	TCONS_00001866	Prosalpha6	215	77.225	0.382	Yes
row_8	TCONS_00035282	Prosalpha4	241	65.727	0.407	Yes
row_9	TCONS_00028382	Prosbeta3	259	60.372	0.431	Yes
row_10	TCONS_00003430	Pomp	260	59.860	0.457	Yes
row_11	TCONS_00032193	Rad23	266	58.553	0.481	Yes
row_12	TCONS_00012325	Prosalpha7	282	51.049	0.502	Yes
row_13	TCONS_00013327	Rpn6	300	48.172	0.520	Yes
row_14	TCONS_00017760	Prosbeta2	314	43.457	0.537	Yes
row_15	TCONS_00011274	gus	317	43.021	0.556	Yes
row_16	TCONS_00018020	Rpn12	320	41.709	0.573	Yes
row_17	TCONS_00024242	Prosalpha2	336	39.303	0.588	Yes
row_18	TCONS_00010323	Prosalpha3	345	37.677	0.604	Yes
row_19	TCONS_00023242	Rpn5	357	35.075	0.618	Yes
row_20	TCONS_00030781	Rpn9	359	34.997	0.632	Yes
row_21	TCONS_00013621	Prosbeta1	397	29.626	0.641	Yes
row_22	TCONS_00008253	TER94	401	29.088	0.653	Yes
row_23	TCONS_00018733	Rpn10	429	26.197	0.662	Yes
row_24	TCONS_00026095	Rpt5	538	19.436	0.658	Yes
row_25	TCONS_00027761	Prosbeta7	544	19.222	0.666	Yes
row_26	TCONS_00036015	Rpt6	557	18.472	0.673	Yes
row_27	TCONS_00034359	Rpt3	561	18.407	0.680	Yes
row_28	TCONS_00034753	CG32640	608	16.316	0.682	Yes
row_29	TCONS_00011035	Rpn8	631	15.759	0.687	Yes
row_30	TCONS_00003150	Rpn3	644	15.342	0.692	Yes
row_31	TCONS_00000356	Der-1	686	13.905	0.693	Yes
row_32	TCONS_00021015	Ufd1-like	695	13.713	0.698	Yes
row_33	TCONS_00004688	Rpn11	701	13.598	0.704	Yes
row_34	TCONS_00013035	Fsn	867	10.156	0.690	No
row_35	TCONS_00014541	CG3295	868	10.146	0.695	No
row_36	TCONS_00008457	CG7220	912	9.329	0.694	No
row_37	TCONS_00003640	Cul2	937	8.923	0.695	No
row_38	TCONS_00006146	CG9934	1049	7.416	0.687	No
row_39	TCONS_00017453	vih	1152	6.373	0.679	No
row_40	TCONS_00014080	SP2637	1193	5.992	0.677	No
row_41	TCONS_00000632	CG12795	1334	4.842	0.664	No
row_42	TCONS_00013881	APC10	1337	4.822	0.666	No
row_43	TCONS_00013207	Rpn13	1391	4.430	0.662	No
row_44	TCONS_00031855	Rpt6R	1397	4.392	0.663	No
row_45	TCONS_00004937	CG13766	1444	4.180	0.660	No
row_46	TCONS_00024499	CG3061	1500	3.948	0.656	No
row_47	TCONS_00030561	Rpn7	1526	3.831	0.655	No
row_48	TCONS_00010930	mr	1549	3.721	0.654	No
row_49	TCONS_00029814	CG5823	1702	3.066	0.639	No
row_50	TCONS_00021115	CG11658	1729	2.905	0.638	No
row_51	TCONS_00009307	CG30466	1739	2.873	0.638	No
row_52	TCONS_00033699	Pat1	1759	2.781	0.637	No
row_53	TCONS_00006035	CG6766	1806	2.630	0.634	No
row_54	TCONS_00020710	CG4911	1815	2.589	0.634	No
row_55	TCONS_00026448	Clbn	1913	2.267	0.624	No
row_56	TCONS_00008886	fsd	1925	2.240	0.624	No
row_57	TCONS_00024357	pic	2003	2.032	0.617	No
row_58	TCONS_00022542	CG4042	2012	2.002	0.617	No
row_59	TCONS_00030343	slmb	2098	1.779	0.609	No
row_60	TCONS_00037077	Rpt4	2158	1.661	0.603	No
row_61	TCONS_00029660	Der-2	2168	1.635	0.603	No
row_62	TCONS_00019548	CG1317	2169	1.634	0.603	No
row_63	TCONS_00004963	CG31633	2213	1.537	0.599	No
row_64	TCONS_00017876	CG10516	2218	1.533	0.600	No
row_65	TCONS_00006414	Cul3	2319	1.317	0.590	No
row_66	TCONS_00037940	CG2247	2324	1.315	0.590	No
row_67	TCONS_00022749	CG7148	2450	1.117	0.577	No
row_68	TCONS_00014435	Ate1	2461	1.103	0.576	No
row_69	TCONS_00029046	CG5961	2482	1.071	0.575	No
row_70	TCONS_00031604	alpha-Man-Ib	2661	0.828	0.556	No
row_71	TCONS_00020795	pall	2682	0.795	0.554	No
row_72	TCONS_00010277	CG9945	2698	0.779	0.553	No
row_73	TCONS_00016062	CG43089	2968	0.503	0.524	No
row_74	TCONS_00001582	CG13088	3145	0.383	0.506	No
row_75	TCONS_00016092	ida	3226	0.334	0.497	No
row_76	TCONS_00022487	CG33969	3229	0.332	0.497	No
row_77	TCONS_00012774	skpB	3262	0.310	0.494	No
row_78	TCONS_00024948	CG14891	3345	0.261	0.485	No
row_79	TCONS_00035887	skpC	3399	0.240	0.480	No
row_80	TCONS_00029270	CG12402	3749	0.111	0.442	No
row_81	TCONS_00038353	Fbxl4	3804	0.099	0.437	No
row_82	TCONS_00018171	Nedd4	3855	0.087	0.431	No
row_83	TCONS_00010564	CG6758	3863	0.084	0.431	No

sev-GAL4 > hsru^{EP3027} vs sev-GAL4 > UAS-GFP

NAME	SYMBOL	TITLE	RANK IN GENE LIST	RANK METRIC SCORE	RUNNING ES	CORE ENRICHMENT
row_0	TCONS_00001298	Sem1	117	263.788	0.080	Yes
row_1	TCONS_00006591	Prosbeta4	170	133.392	0.121	Yes
row_2	TCONS_00009646	Prosalpha5	177	125.267	0.164	Yes
row_3	TCONS_00021867	Prosbeta6	178	123.631	0.207	Yes
row_4	TCONS_00028382	Prosbeta3	179	122.468	0.249	Yes
row_5	TCONS_00008471	Prosbeta5	181	120.372	0.291	Yes
row_6	TCONS_00032721	skpA	182	118.086	0.333	Yes
row_7	TCONS_00019022	CG40045	191	110.154	0.370	Yes
row_8	TCONS_00035282	Prosalpha4	211	90.672	0.400	Yes
row_9	TCONS_00012325	Prosalpha7	225	80.962	0.427	Yes
row_10	TCONS_00011274	gus	249	67.193	0.448	Yes
row_11	TCONS_00001866	Prosalpha6	262	63.822	0.469	Yes
row_12	TCONS_00032193	Rad23	277	58.476	0.487	Yes
row_13	TCONS_00003430	Pomp	279	58.000	0.508	Yes
row_14	TCONS_00013621	Prosbeta1	298	52.070	0.524	Yes
row_15	TCONS_00017760	Prosbeta2	314	49.001	0.539	Yes
row_16	TCONS_00024242	Prosalpha2	334	44.247	0.553	Yes
row_17	TCONS_00030781	Rpn9	355	41.310	0.565	Yes
row_18	TCONS_00018020	Rpn12	412	32.859	0.570	Yes
row_19	TCONS_00010323	Prosalpha3	425	31.699	0.580	Yes
row_20	TCONS_00020793	Uch-L5	431	30.923	0.590	Yes
row_21	TCONS_00030561	Rpn7	461	28.250	0.597	Yes
row_22	TCONS_00013327	Rpn6	496	25.837	0.603	Yes
row_23	TCONS_00026095	Rpt5	558	22.490	0.604	Yes
row_24	TCONS_00023242	Rpn5	609	20.253	0.606	Yes
row_25	TCONS_00036015	Rpt6	617	19.942	0.612	Yes
row_26	TCONS_00004688	Rpn11	619	19.880	0.619	Yes
row_27	TCONS_00021015	Ufd1-like	743	15.927	0.611	Yes
row_28	TCONS_00003640	Cul2	838	13.277	0.606	Yes
row_29	TCONS_00008253	TER94	841	13.245	0.610	Yes
row_30	TCONS_00003150	Rpn3	892	12.205	0.609	Yes
row_31	TCONS_00018733	Rpn10	903	11.981	0.612	Yes
row_32	TCONS_00000356	Der-1	910	11.798	0.616	Yes
row_33	TCONS_00010565	CG11275	943	11.281	0.616	Yes
row_34	TCONS_00017453	vih	972	10.786	0.617	Yes
row_35	TCONS_00027761	Prosbeta7	1008	10.235	0.617	Yes
row_36	TCONS_00014541	CG3295	1019	10.097	0.619	Yes
row_37	TCONS_00034359	Rpt3	1100	8.917	0.614	No
row_38	TCONS_00013035	Fsn	1114	8.714	0.615	No
row_39	TCONS_00013881	APC10	1258	7.509	0.603	No
row_40	TCONS_00014080	SP2637	1395	6.352	0.590	No
row_41	TCONS_00010930	mr	1455	5.850	0.586	No
row_42	TCONS_00000632	CG12795	1528	5.365	0.580	No
row_43	TCONS_00008457	CG7220	1679	4.484	0.566	No
row_44	TCONS_00004937	CG13766	1694	4.428	0.566	No
row_45	TCONS_00024357	pic	1700	4.393	0.567	No
row_46	TCONS_00009307	CG30466	1740	4.182	0.564	No
row_47	TCONS_00022749	CG7148	1752	4.132	0.565	No
row_48	TCONS_00011035	Rpn8	1799	3.935	0.561	No
row_49	TCONS_00022487	CG33969	1821	3.865	0.560	No
row_50	TCONS_00024499	CG3061	1828	3.807	0.561	No
row_51	TCONS_00033699	Pat1	1847	3.731	0.560	No
row_52	TCONS_00022542	CG4042	1905	3.540	0.555	No
row_53	TCONS_00006035	CG6766	1920	3.457	0.555	No
row_54	TCONS_00019548	CG1317	1925	3.444	0.556	No
row_55	TCONS_00034753	CG32640	1951	3.357	0.554	No
row_56	TCONS_00021115	CG11658	1964	3.310	0.554	No
row_57	TCONS_00008886	fsd	1974	3.281	0.554	No
row_58	TCONS_00017876	CG10516	2005	3.121	0.552	No
row_59	TCONS_00004963	CG31633	2059	2.940	0.548	No
row_60	TCONS_00001582	CG13088	2114	2.708	0.543	No
row_61	TCONS_00029046	CG5961	2135	2.662	0.542	No
row_62	TCONS_00021317	CG11261	2388	2.049	0.515	No
row_63	TCONS_00031604	alpha-Man-Ib	2431	1.930	0.512	No
row_64	TCONS_00029814	CG5823	2531	1.703	0.502	No
row_65	TCONS_00026448	Clbn	2546	1.675	0.501	No
row_66	TCONS_00020795	pall	2603	1.552	0.495	No
row_67	TCONS_00016092	ida	2625	1.517	0.494	No
row_68	TCONS_00010277	CG9945	2640	1.485	0.493	No
row_69	TCONS_00032023	CG2126	2643	1.479	0.493	No
row_70	TCONS_00018394	CG32221	2670	1.421	0.491	No
row_71	TCONS_00029660	Der-2	2756	1.268	0.482	No
row_72	TCONS_00014435	Ate1	2910	1.041	0.466	No
row_73	TCONS_00012774	skpB	3004	0.908	0.456	No
row_74	TCONS_00004629	jet	3103	0.779	0.446	No
row_75	TCONS_00004354	CG15412	3110	0.774	0.446	No
row_76	TCONS_00039099	CG15814	3112	0.772	0.446	No
row_77	TCONS_00007999	gcl	3252	0.612	0.431	No
row_78	TCONS_00015005	CG15800	3267	0.600	0.430	No
row_79	TCONS_00024948	CG14891	3289	0.582	0.428	No
row_80	TCONS_00002785	fzy	3355	0.524	0.421	No
row_81	TCONS_00011980	Cul4	3380	0.510	0.419	No
row_82	TCONS_00027063	CG2010	3716	0.279	0.383	No
row_83	TCONS_00016062	CG43089	3774	0.249	0.377	No

row_84	TCONS_00039450	skpE	3940	0.069	0.423	No		row_84	TCONS_00029270	CG12402	3961	0.174	0.357	No
row_85	TCONS_00028981	CG14739	4031	0.051	0.413	No		row_85	TCONS_00001724	Cks30A	4015	0.157	0.352	No
row_86	TCONS_00033564	Prosbeta2R1	4053	0.047	0.411	No		row_86	TCONS_00007132	CG9316	4261	0.095	0.326	No
row_87	TCONS_00035886	skpD	4388	0.000	0.375	No		row_87	TCONS_00003010	Prosbeta5R2	4308	0.084	0.321	No
row_88	TCONS_00031940	Prosalpha3T	4479	0.000	0.366	No		row_88	TCONS_00035887	skpC	4333	0.079	0.318	No
row_89	TCONS_00014914	Prosbeta5R1	4565	0.000	0.356	No		row_89	TCONS_00035886	skpD	4358	0.075	0.316	No
row_90	TCONS_00018129	CG7707	4670	0.000	0.345	No		row_90	TCONS_00010207	CG11044	4465	0.056	0.304	No
row_91	TCONS_00038086	CG1924	4763	-0.004	0.336	No		row_91	TCONS_00021553	Rpn12R	4477	0.054	0.303	No
row_92	TCONS_00039090	CG8188	4830	-0.016	0.329	No		row_92	TCONS_00026795	CG14260	4516	0.048	0.299	No
row_93	TCONS_00003010	Prosbeta5R2	4863	-0.022	0.325	No		row_93	TCONS_00034091	APC4	4754	0.012	0.274	No
row_94	TCONS_00004354	CG15412	4960	-0.041	0.315	No		row_94	TCONS_00031940	Prosalpha3T	4954	0.000	0.253	No
row_95	TCONS_00027428	sip3	4978	-0.044	0.313	No		row_95	TCONS_00014914	Prosbeta5R1	5028	0.000	0.245	No
row_96	TCONS_00021553	Rpn12R	5021	-0.053	0.309	No		row_96	TCONS_00033564	Prosbeta2R1	5107	0.000	0.237	No
row_97	TCONS_00014948	skpF	5060	-0.063	0.305	No		row_97	TCONS_00018129	CG7707	5124	0.000	0.235	No
row_98	TCONS_00015171	CG42383	5146	-0.079	0.296	No		row_98	TCONS_00028981	CG14739	5177	0.000	0.229	No
row_99	TCONS_00001199	CG11070	5165	-0.082	0.294	No		row_99	TCONS_00038353	Fbxl4	5197	-0.002	0.227	No
row_100	TCONS_00007132	CG9316	5174	-0.086	0.293	No		row_100	TCONS_00038086	CG1924	5198	-0.002	0.227	No
row_101	TCONS_00027692	Prosbeta2R2	5222	-0.096	0.288	No		row_101	TCONS_00010564	CG6758	5424	-0.037	0.203	No
row_102	TCONS_00015178	Prosalpha4T2	5308	-0.116	0.279	No		row_102	TCONS_00015171	CG42383	5426	-0.037	0.203	No
row_103	TCONS_00021106	CG32085	5340	-0.123	0.276	No		row_103	TCONS_00027428	sip3	5472	-0.044	0.198	No
row_104	TCONS_00010207	CG11044	5373	-0.131	0.272	No		row_104	TCONS_00014948	skpF	5556	-0.063	0.189	No
row_105	TCONS_00018068	sina	5377	-0.133	0.272	No		row_105	TCONS_00015178	Prosalpha4T2	5638	-0.085	0.181	No
row_106	TCONS_00017384	Rpt4R	5382	-0.134	0.272	No		row_106	TCONS_00018071	sinah	5734	-0.111	0.171	No
row_107	TCONS_00026795	CG14260	5445	-0.156	0.265	No		row_107	TCONS_00009655	CG18467	5890	-0.157	0.154	No
row_108	TCONS_00021317	CG11261	5519	-0.178	0.257	No		row_108	TCONS_00017384	Rpt4R	5965	-0.184	0.146	No
row_109	TCONS_00014794	dnr1	5704	-0.255	0.238	No		row_109	TCONS_00012103	CG8272	6022	-0.207	0.141	No
row_110	TCONS_00030294	Prosalpha4T1	5752	-0.277	0.233	No		row_110	TCONS_00037940	CG2247	6037	-0.219	0.139	No
row_111	TCONS_00029138	CG8476	5806	-0.300	0.227	No		row_111	TCONS_00030294	Prosalpha4T1	6155	-0.280	0.127	No
row_112	TCONS_00000368	CG4238	5854	-0.326	0.222	No		row_112	TCONS_00039450	skpE	6202	-0.309	0.122	No
row_113	TCONS_00018394	CG32221	5930	-0.360	0.215	No		row_113	TCONS_00027692	Prosbeta2R2	6240	-0.334	0.118	No
row_114	TCONS_00012713	CG9003	5941	-0.365	0.214	No		row_114	TCONS_00029138	CG8476	6346	-0.398	0.107	No
row_115	TCONS_00018071	sinah	5944	-0.368	0.214	No		row_115	TCONS_00004874	Fbw5	6391	-0.432	0.102	No
row_116	TCONS_00027063	CG2010	6002	-0.395	0.208	No		row_116	TCONS_00026166	CG10694	6415	-0.453	0.100	No
row_117	TCONS_00015005	CG15800	6111	-0.451	0.196	No		row_117	TCONS_00020710	CG4911	6557	-0.560	0.085	No
row_118	TCONS_00009655	CG18467	6206	-0.500	0.187	No		row_118	TCONS_00000368	CG4238	6593	-0.587	0.082	No
row_119	TCONS_00026166	CG10694	6240	-0.519	0.183	No		row_119	TCONS_00001199	CG11070	6623	-0.625	0.079	No
row_120	TCONS_00002371	Edem2	6382	-0.630	0.168	No		row_120	TCONS_00033145	CG2681	6630	-0.633	0.078	No
row_121	TCONS_00033145	CG2681	6390	-0.639	0.168	No		row_121	TCONS_00027512	Skp2	6688	-0.686	0.073	No
row_122	TCONS_00004874	Fbw5	6480	-0.710	0.159	No		row_122	TCONS_00031855	Rpt6R	6760	-0.744	0.065	No
row_123	TCONS_00012103	CG8272	6535	-0.754	0.153	No		row_123	TCONS_00021106	CG32085	6903	-0.946	0.050	No
row_124	TCONS_00011980	Cul4	6543	-0.764	0.153	No		row_124	TCONS_00014794	dnr1	6979	-1.061	0.043	No
row_125	TCONS_00004629	jet	6563	-0.780	0.151	No		row_125	TCONS_00006414	Cul3	7024	-1.128	0.039	No
row_126	TCONS_00003368	Cdc23	6659	-0.862	0.141	No		row_126	TCONS_00018171	Nedd4	7083	-1.228	0.033	No
row_127	TCONS_00001988	Trim9	6838	-1.024	0.123	No		row_127	TCONS_00004509	morgue	7212	-1.473	0.020	No
row_128	TCONS_00034091	APC4	6878	-1.065	0.119	No		row_128	TCONS_00002371	Edem2	7220	-1.487	0.019	No
row_129	TCONS_00037169	CG14435	6883	-1.071	0.119	No		row_129	TCONS_00000137	ebi	7224	-1.489	0.020	No
row_130	TCONS_00032023	CG2126	6933	-1.138	0.114	No		row_130	TCONS_00001228	Rca1	7304	-1.664	0.012	No
row_131	TCONS_00007999	gcl	6964	-1.184	0.112	No		row_131	TCONS_00012965	CG17019	7349	-1.766	0.008	No
row_132	TCONS_00030831	Rpt2	7153	-1.461	0.092	No		row_132	TCONS_00037169	CG14435	7533	-2.224	-0.011	No
row_133	TCONS_00002785	fzy	7247	-1.594	0.083	No		row_133	TCONS_00003368	Cdc23	7573	-2.355	-0.014	No
row_134	TCONS_00018720	CG7611	7278	-1.636	0.081	No		row_134	TCONS_00001988	Trim9	7630	-2.551	-0.020	No
row_135	TCONS_00031603	Cul5	7330	-1.703	0.076	No		row_135	TCONS_00039090	CG8188	7697	-2.763	-0.026	No
row_136	TCONS_00004509	morgue	7331	-1.707	0.077	No		row_136	TCONS_00004644	CG8892	7736	-2.929	-0.029	No
row_137	TCONS_00036492	Edem1	7353	-1.741	0.075	No		row_137	TCONS_00031514	CG5003	7774	-3.055	-0.032	No
row_138	TCONS_00039099	CG15814	7387	-1.816	0.072	No		row_138	TCONS_00012796	CG8858	7806	-3.166	-0.034	No
row_139	TCONS_00004644	CG8892	7432	-1.941	0.068	No		row_139	TCONS_00020505	CG8042	7852	-3.340	-0.037	No
row_140	TCONS_00012965	CG17019	7441	-1.958	0.068	No		row_140	TCONS_00036492	Edem1	7909	-3.542	-0.042	No
row_141	TCONS_00022501	CG5199	7481	-2.069	0.065	No		row_141	TCONS_00022501	CG5199	7914	-3.556	-0.041	No
row_142	TCONS_00020505	CG8042	7502	-2.123	0.064	No		row_142	TCONS_00010811	mi	7919	-3.570	-0.041	No
row_143	TCONS_00000137	ebi	7509	-2.133	0.064	No		row_143	TCONS_00031603	Cul5	7952	-3.723	-0.043	No
row_144	TCONS_00009992	tn	7656	-2.520	0.050	No		row_144	TCONS_00018068	sina	7963	-3.770	-0.042	No
row_145	TCONS_00012796	CG8858	7683	-2.578	0.048	No		row_145	TCONS_00013285	phyl	7986	-3.846	-0.043	No
row_146	TCONS_00001228	Rca1	7691	-2.595	0.048	No		row_146	TCONS_00030343	slmb	8000	-3.912	-0.043	No
row_147	TCONS_00010811	mi	7812	-2.940	0.037	No		row_147	TCONS_00008307	dmpd	8116	-4.518	-0.054	No
row_148	TCONS_00013623	casp	7846	-3.063	0.035	No		row_148	TCONS_00018720	CG7611	8187	-4.961	-0.060	No
row_149	TCONS_00027512	Skp2	7925	-3.288	0.028	No		row_149	TCONS_00023748	Kdm2	8201	-5.033	-0.060	No
row_150	TCONS_00008307	dmpd	7958	-3.389	0.026	No		row_150	TCONS_00010853	l(2)dtl	8202	-5.034	-0.058	No
row_151	TCONS_00011799	p47	8023	-3.675	0.020	No		row_151	TCONS_00013623	casp	8220	-5.131	-0.058	No
row_152	TCONS_00013285	phyl	8034	-3.715	0.021	No		row_152	TCONS_00034167	CG42797	8241	-5.250	-0.058	No
row_153	TCONS_00034167	CG42797	8064	-3.843	0.019	No		row_153	TCONS_00038518	shtd	8300	-5.584	-0.062	No
row_154	TCONS_00003998	Plap	8106	-4.006	0.017	No		row_154	TCONS_00012713	CG9003	8419	-6.324	-0.073	No
row_155	TCONS_00010853	l(2)dtl	8139	-4.109	0.015	No		row_155	TCONS_00021030	Ube3a	8420	-6.329	-0.071	No
row_156	TCONS_00001724	Cks30A	8163	-4.224	0.015	No		row_156	TCONS_00037077	Rpt4	8509	-7.038	-0.077	No
row_157	TCONS_00038518	shtd	8175	-4.281	0.015	No		row_157	TCONS_00006146	CG9934	8536	-7.213	-0.078	No
row_158	TCONS_00023748	Kdm2	8198	-4.401	0.015	No		row_158	TCONS_00011799	p47	8554	-7.420	-0.077	No
row_159	TCONS_00031514	CG5003	8229	-4.584	0.013	No		row_159	TCONS_00009992	tn	8588	-7.761	-0.078	No
row_160	TCONS_00020793	Uch-L5	8305	-5.028	0.008	No		row_160	TCONS_00000377	Su(dx)	8618	-8.097	-0.078	No
row_161	TCONS_00007847	Cul1	8323	-5.121	0.008	No		row_161	TCONS_00005436	lmgA	8702	-8.918	-0.084	No
row_162	TCONS_00000377	Su(dx)	8344	-5.182	0.008	No		row_162	TCONS_00003998	Plap	8754	-9.519	-0.086	No
row_163	TCONS_00021030	Ube3a	8437	-5.723	0.001	No		row_163	TCONS_00030831	Rpt2	8776	-9.831	-0.085	No
row_164	TCONS_00029255	rdx	8443	-5.757	0.003	No		row_164	TCONS_00020335	Cdc27	8796	-10.135	-0.083	No
row_165	TCONS_00005436	lmgA	8640	-7.447	-0.015	No		row_165	TCONS_00032873	inc	8887	-11.511	-0.089	No
row_166	TCONS_00032873	inc	8703	-7.946	-0.018	No		row_166	TCONS_00029255	rdx	8939	-12.339	-0.090	No
row_167	TCONS_00020335	Cdc27	8736	-8.324	-0.018	No		row_167	TCONS_00013207	Spn13	9014	-13.806	-0.093	No
row_168	TCONS_00031638	Cnx99A	8786	-9.046	-0.020	No		row_168	TCONS_00016598	CG7546	9037	-14.386	-0.090	No
row_169	TCONS_00010565	CG11275	8890	-10.280	-0.026	No		row_169	TCONS_00007847	Cul1	9113	-16.200	-0.093	No
row_170	TCONS_00018413	Rpn1	8924	-10.929	-0.025	No		row_170	TCONS_00018413	Rpn1	9177	-18.158	-0.093	No
row_171	TCONS_00016598	CG7546	8969	-11.614	-0.025	No		row_171	TCONS_00019904	ago	9192	-18.581	-0.088	No
row_172	TCONS_00019904	ago	9131	-14.942	-0.036	No		row_172	TCONS_00031638	Cnx99A	9234	-20.445	-0.085	No
row_173	TCONS_00037984	Hsc70-3	9244	-19.387	-0.039	No		row_173	TCONS_00027030	Rpn2	9304	-25.297	-0.084	No
row_174	TCONS_00027030	Rpn2	9283	-21.621	-0.034	No		row_174	TCONS_00035126	CG8184	9348	-29.091	-0.078	No
row_175	TCONS_00029371	eff	9291	-22.046	-0.025	No		row_175	TCONS_00014821	ppa	9357	-30.176	-0.069	No
row_176	TCONS_00014821	ppa	9361	-26.854	-0.021	No		row_176	TCONS_00029371	eff	9488	-73.508	-0.057	No
row_177	TCONS_00035126	CG8184	9375	-28.306	-0.011	No		row_177	TCONS_00026867	Gp93	9491	-77.620	-0.030	No
row_178	TCONS_00026867	Gp93	9488	-66.207	0.006	No		row_178	TCONS_00037984	Hsc70-3	9502	-101.550	0.004	No

GO:0050821 Protein stabalization

S-hsruRNAi vs sev-GAL4 > UAS-GFP

NAME	SYMBOL	TITLE	RANK IN GENE LIST	RANK METRIC SCORE	RUNNING ES	CORE ENRICHMENT
row_0	TCONS_00015957	Hsp83	107	293.051	0.335	Yes
row_1	TCONS_00008282	14-3-3zeta	197	93.382	0.436	Yes
row_2	TCONS_00020124	DnaJ-1	337	39.079	0.467	Yes
row_3	TCONS_00001525	CSN8	368	32.789	0.503	Yes
row_4	TCONS_00029263	CG9922	511	20.548	0.512	Yes
row_5	TCONS_00028259	Sgt1	556	18.478	0.530	Yes
row_6	TCONS_00012506	trsn	729	12.991	0.527	Yes
row_7	TCONS_00024267	Snx3	835	10.666	0.528	Yes
row_8	TCONS_00024928	CSN5	882	9.806	0.535	Yes
row_9	TCONS_00000496	aph-1	946	8.742	0.539	Yes
row_10	TCONS_00005488	alien	1185	6.052	0.521	No
row_11	TCONS_00007869	CSN4	1480	4.006	0.495	No
row_12	TCONS_00013580	Mlf	1509	3.907	0.496	No
row_13	TCONS_00021621	CG7945	1756	2.794	0.474	No
row_14	TCONS_00022560	CSN3	1881	2.353	0.464	No
row_15	TCONS_00022188	CSN1b	1907	2.295	0.464	No
row_16	TCONS_00034577	sicily	1966	2.128	0.460	No
row_17	TCONS_00012401	Ccs	1976	2.110	0.462	No
row_18	TCONS_00025953	CSN6	2366	1.253	0.422	No
row_19	TCONS_00038559	CG12379	5518	-0.176	0.091	No
row_20	TCONS_00034145	ric8a	6799	-0.993	-0.043	No
row_21	TCONS_00007940	CSN7	7144	-1.448	-0.077	No
row_22	TCONS_00020493	syd	7326	-1.698	-0.094	No
row_23	TCONS_00035120	CG8134	8067	-3.863	-0.167	No
row_24	TCONS_00038069	fw	8673	-7.701	-0.222	No
row_25	TCONS_00031638	Cnx99A	8786	-9.046	-0.223	No
row_26	TCONS_00017603	stv	8896	-10.355	-0.222	No
row_27	TCONS_00035140	CG8206	8901	-10.496	-0.210	No
row_28	TCONS_00003914	lwr	8911	-10.651	-0.199	No
row_29	TCONS_00001918	da	9035	-12.712	-0.196	No
row_30	TCONS_00028659	tws	9062	-13.372	-0.183	No
row_31	TCONS_00007617	Bap170	9081	-13.756	-0.169	No
row_32	TCONS_00026218	crb	9095	-14.013	-0.154	No
row_33	TCONS_00037144	shf	9155	-15.596	-0.142	No
row_34	TCONS_00015448	hipk	9331	-24.265	-0.131	No
row_35	TCONS_00002851	Mhc	9515	-129.922	0.003	No

sev-GAL4 > hsru^{EP3037} vs sev-GAL4 > UAS-GFP

NAME	SYMBOL	TITLE	RANK IN GENE LIST	RANK METRIC SCORE	RUNNING ES	CORE ENRICHMENT
row_0	TCONS_00015957	Hsp83	116	265.342	0.345	Yes
row_1	TCONS_00008282	14-3-3zeta	313	49.017	0.390	Yes
row_2	TCONS_00001525	CSN8	315	48.917	0.456	Yes
row_3	TCONS_00029263	CG9922	356	40.938	0.507	Yes
row_4	TCONS_00020124	DnaJ-1	437	30.449	0.540	Yes
row_5	TCONS_00012506	trsn	536	23.627	0.561	Yes
row_6	TCONS_00028259	Sgt1	697	17.324	0.568	Yes
row_7	TCONS_00024928	CSN5	900	12.112	0.563	Yes
row_8	TCONS_00005488	alien	934	11.398	0.574	Yes
row_9	TCONS_00000496	aph-1	1133	8.539	0.565	Yes
row_10	TCONS_00024267	Snx3	1149	8.345	0.575	Yes
row_11	TCONS_00007869	CSN4	1187	8.018	0.582	Yes
row_12	TCONS_00012401	Ccs	1412	6.187	0.566	No
row_13	TCONS_00021621	CG7945	1685	4.470	0.544	No
row_14	TCONS_00013580	Mlf	1760	4.101	0.542	No
row_15	TCONS_00002851	Mhc	1825	3.843	0.540	No
row_16	TCONS_00034577	sicily	2040	3.008	0.522	No
row_17	TCONS_00022560	CSN3	2138	2.656	0.515	No
row_18	TCONS_00022188	CSN1b	2182	2.542	0.514	No
row_19	TCONS_00038559	CG12379	2356	2.131	0.499	No
row_20	TCONS_00034145	ric8a	7495	-2.133	-0.039	No
row_21	TCONS_00025953	CSN6	7769	-3.042	-0.064	No
row_22	TCONS_00020493	syd	7787	-3.091	-0.061	No
row_23	TCONS_00035120	CG8134	7807	-3.172	-0.059	No
row_24	TCONS_00007940	CSN7	8019	-4.041	-0.076	No
row_25	TCONS_00035140	CG8206	8392	-6.193	-0.107	No
row_26	TCONS_00038069	fw	8654	-8.478	-0.123	No
row_27	TCONS_00017603	stv	8911	-11.894	-0.134	No
row_28	TCONS_00003914	lwr	8929	-12.171	-0.119	No
row_29	TCONS_00028659	tws	9057	-14.856	-0.112	No
row_30	TCONS_00007617	Bap170	9104	-15.999	-0.096	No
row_31	TCONS_00001918	da	9112	-16.181	-0.075	No
row_32	TCONS_00037144	shf	9204	-19.129	-0.058	No
row_33	TCONS_00031638	Cnx99A	9234	-20.445	-0.034	No
row_34	TCONS_00026218	crb	9276	-23.311	-0.007	No
row_35	TCONS_00015448	hipk	9310	-25.761	0.024	No

GO:006417 Regulation of translation

S-hsruRNAi vs sev-GAL4 > UAS-GFP

NAME	SYMBOL	TITLE	RANK IN GENE LIST	RANK METRIC SCORE	RUNNING ES	CORE ENRICHMENT
row_0	TCONS_00001869	eEF1delta	143	162.760	0.063	No
row_1	TCONS_00027810	kra	178	107.882	0.111	No
row_2	TCONS_00001871	me31B	209	83.155	0.147	No
row_3	TCONS_00020751	Hsp67Bc	262	59.651	0.170	No
row_4	TCONS_00020693	smg	263	59.376	0.199	No
row_5	TCONS_00016657	Srp9	380	31.066	0.201	No
row_6	TCONS_00038652	eIF5	496	21.317	0.199	No
row_7	TCONS_00014569	LSm1	605	16.422	0.196	No
row_8	TCONS_00024318	Paip2	815	10.972	0.179	No

sev-GAL4 > hsru^{EP3037} vs sev-GAL4 > UAS-GFP

NAME	SYMBOL	TITLE	RANK IN GENE LIST	RANK METRIC SCORE	RUNNING ES	CORE ENRICHMENT
row_0	TCONS_00001869	eEF1delta	141	172.248	0.056	No
row_1	TCONS_00020693	smg	199	106.450	0.093	No
row_2	TCONS_00001871	me31B	210	91.224	0.130	No
row_3	TCONS_00027810	kra	238	72.213	0.157	No
row_4	TCONS_00016657	Srp9	428	31.455	0.149	No
row_5	TCONS_00014569	LSm1	509	24.869	0.151	No
row_6	TCONS_00038652	eIF5	584	21.142	0.152	No
row_7	TCONS_00029459	Rpb7	696	17.352	0.147	No
row_8	TCONS_00014983	l(2)efl	725	16.477	0.151	No

row_9	TCONS_00029459	Rpb7	842	10.477	0.181	No			row_9	TCONS_00034698	mRpL49	843	13.222	0.144	No
row_10	TCONS_00022694	Mkrn1	844	10.443	0.186	No			row_10	TCONS_00022694	Mkrn1	994	10.387	0.132	No
row_11	TCONS_00020616	GAPsec	917	9.266	0.183	No			row_11	TCONS_00001976	CG6094	1057	9.531	0.130	No
row_12	TCONS_00032524	4E-T	1076	7.078	0.169	No			row_12	TCONS_00027854	CG2091	1076	9.232	0.132	No
row_13	TCONS_00000325	Rrp40	1172	6.155	0.162	No			row_13	TCONS_00000325	Rrp40	1156	8.271	0.127	No
row_14	TCONS_00001976	CG6094	1173	6.155	0.165	No			row_14	TCONS_00032524	4E-T	1195	7.976	0.126	No
row_15	TCONS_00027854	CG2091	1184	6.055	0.167	No			row_15	TCONS_00024070	CG14701	1271	7.348	0.121	No
row_16	TCONS_00023178	Rheb	1313	4.952	0.156	No			row_16	TCONS_00023178	Rheb	1296	7.095	0.121	No
row_17	TCONS_00021110	CG11652	1474	4.026	0.141	No			row_17	TCONS_00014964	Rrp4	1329	6.826	0.121	No
row_18	TCONS_00034698	mRpL49	1530	3.799	0.137	No			row_18	TCONS_00023188	CG1427	1415	6.181	0.114	No
row_19	TCONS_00004448	CG31957	1586	3.557	0.133	No			row_19	TCONS_00009345	Rrp42	1450	5.895	0.113	No
row_20	TCONS_00015584	312	1616	3.421	0.131	No			row_20	TCONS_00030577	Dph5	1470	5.775	0.113	No
row_21	TCONS_00003951	CG3862	1648	3.285	0.129	No			row_21	TCONS_00015584	312	1484	5.686	0.114	No
row_22	TCONS_00007089	La	1867	2.411	0.107	No			row_22	TCONS_00021110	CG11652	1525	5.382	0.112	No
row_23	TCONS_00022521	mTerf3	1870	2.398	0.108	No			row_23	TCONS_00024318	Paip2	1527	5.368	0.114	No
row_24	TCONS_00016736	Sbp2	1931	2.228	0.103	No			row_24	TCONS_00029399	CG7265	1582	5.088	0.111	No
row_25	TCONS_00009345	Rrp42	1950	2.163	0.102	No			row_25	TCONS_00020616	GAPsec	1645	4.658	0.106	No
row_26	TCONS_00030577	Dph5	2161	1.655	0.081	No			row_26	TCONS_00022521	mTerf3	1724	4.277	0.100	No
row_27	TCONS_00007092	CG10947	2244	1.477	0.073	No			row_27	TCONS_00007089	La	1969	3.298	0.075	No
row_28	TCONS_00037115	CG3184	2365	1.254	0.061	No			row_28	TCONS_00003951	CG3862	1993	3.182	0.074	No
row_29	TCONS_00021817	roq	2388	1.216	0.059	No			row_29	TCONS_00004448	CG31957	2066	2.888	0.067	No
row_30	TCONS_00014964	Rrp4	2516	1.026	0.046	No			row_30	TCONS_00010982	Zfrp8	2449	1.880	0.028	No
row_31	TCONS_00002243	CG31759	2605	0.905	0.037	No			row_31	TCONS_00002243	CG31759	2635	1.494	0.009	No
row_32	TCONS_00010982	Zfrp8	2706	0.771	0.027	No			row_32	TCONS_00005863	aub	2651	1.462	0.008	No
row_33	TCONS_00038561	CG11679	2763	0.727	0.021	No			row_33	TCONS_00016736	Sbp2	2653	1.458	0.008	No
row_34	TCONS_00027464	CG2053	3014	0.470	-0.005	No			row_34	TCONS_00033726	Pink1	2777	1.232	-0.004	No
row_35	TCONS_00005863	aub	3299	0.290	-0.035	No			row_35	TCONS_00003495	CG9253	2794	1.210	-0.006	No
row_36	TCONS_00004284	okr	3387	0.245	-0.044	No			row_36	TCONS_00038561	CG11679	2825	1.167	-0.008	No
row_37	TCONS_00014017	Dgp-1	3432	0.228	-0.049	No			row_37	TCONS_00027891	CG2017	2950	0.987	-0.021	No
row_38	TCONS_00016855	CG6576	3697	0.123	-0.077	No			row_38	TCONS_00024689	Sra-1	3081	0.808	-0.035	No
row_39	TCONS_00013670	krimp	3936	0.069	-0.102	No			row_39	TCONS_00024542	spn-B	3187	0.696	-0.045	No
row_40	TCONS_00024070	CG14701	4104	0.038	-0.120	No			row_40	TCONS_00037115	CG3184	3268	0.600	-0.054	No
row_41	TCONS_00002680	CG15262	4593	0.000	-0.172	No			row_41	TCONS_00031089	bam	3312	0.564	-0.058	No
row_42	TCONS_00005492	Rcd-1r	4832	-0.016	-0.197	No			row_42	TCONS_00024269	Not10	3430	0.460	-0.070	No
row_43	TCONS_00027428	sip3	4978	-0.044	-0.212	No			row_43	TCONS_00026425	PQBP1	3440	0.452	-0.071	No
row_44	TCONS_00002645	vas	5213	-0.094	-0.237	No			row_44	TCONS_00010825	apt	3625	0.321	-0.090	No
row_45	TCONS_00024542	spn-B	5296	-0.111	-0.246	No			row_45	TCONS_00016855	CG6576	4314	0.083	-0.163	No
row_46	TCONS_00024269	Not10	5458	-0.158	-0.263	No			row_46	TCONS_00030704	orb	4701	0.022	-0.204	No
row_47	TCONS_00031089	bam	5503	-0.172	-0.267	No			row_47	TCONS_00005492	Rcd-1r	4765	0.010	-0.211	No
row_48	TCONS_00030704	orb	5692	-0.249	-0.287	No			row_48	TCONS_00002680	CG15262	5056	0.000	-0.242	No
row_49	TCONS_00026425	PQBP1	5839	-0.320	-0.302	No			row_49	TCONS_00013670	krimp	5304	-0.017	-0.268	No
row_50	TCONS_00023188	CG1427	6168	-0.479	-0.337	No			row_50	TCONS_00002645	vas	5318	-0.019	-0.269	No
row_51	TCONS_00038945	Rrp45	6384	-0.631	-0.360	No			row_51	TCONS_00004284	okr	5334	-0.022	-0.271	No
row_52	TCONS_00006783	bsf	6620	-0.824	-0.384	No			row_52	TCONS_00038945	Rrp45	5410	-0.035	-0.279	No
row_53	TCONS_00029399	CG7265	6892	-1.078	-0.412	No			row_53	TCONS_00027428	sip3	5472	-0.044	-0.285	No
row_54	TCONS_00010825	apt	7042	-1.290	-0.428	No			row_54	TCONS_00007092	CG10947	5762	-0.118	-0.316	No
row_55	TCONS_00027891	CG2017	7067	-1.339	-0.430	No			row_55	TCONS_00020718	bol	6384	-0.425	-0.382	No
row_56	TCONS_00019372	CG13928	7244	-1.593	-0.447	No			row_56	TCONS_00005605	CG13124	6397	-0.434	-0.383	No
row_57	TCONS_00016699	mus301	7320	-1.696	-0.455	No			row_57	TCONS_00026870	CG4849	6580	-0.580	-0.402	No
row_58	TCONS_00033726	Pink1	7346	-1.728	-0.456	No			row_58	TCONS_00016699	mus301	6712	-0.701	-0.416	No
row_59	TCONS_00027369	Gcn2	7410	-1.866	-0.462	No			row_59	TCONS_00027464	CG2053	6720	-0.706	-0.416	No
row_60	TCONS_00003495	CG9253	7494	-2.105	-0.470	No			row_60	TCONS_00020751	Hsp67Bc	6974	-1.053	-0.442	No
row_61	TCONS_00024689	Sra-1	7589	-2.366	-0.479	No			row_61	TCONS_00027369	Gcn2	7102	-1.263	-0.455	No
row_62	TCONS_00035148	CG17209	7615	-2.435	-0.480	No			row_62	TCONS_00035148	CG17209	7494	-2.131	-0.496	No
row_63	TCONS_00009992	tn	7656	-2.520	-0.483	No			row_63	TCONS_00014017	Dgp-1	7529	-2.217	-0.499	No
row_64	TCONS_00005605	CG13124	7758	-2.803	-0.493	No			row_64	TCONS_00006783	bsf	7618	-2.503	-0.507	No
row_65	TCONS_00020718	bol	7855	-3.096	-0.501	No			row_65	TCONS_00011324	mle	7738	-2.940	-0.518	No
row_66	TCONS_00027827	Rga	7869	-3.156	-0.501	No			row_66	TCONS_00015102	Not11	7876	-3.428	-0.532	No
row_67	TCONS_00011324	mle	7903	-3.231	-0.503	No			row_67	TCONS_00019372	CG13928	8021	-4.047	-0.545	No
row_68	TCONS_00026870	CG4849	8042	-3.740	-0.516	No			row_68	TCONS_00033067	fs(1)K10	8179	-4.898	-0.560	No
row_69	TCONS_00033067	fs(1)K10	8065	-3.855	-0.517	No			row_69	TCONS_00037989	CG15578	8253	-5.320	-0.565	No
row_70	TCONS_00015102	Not11	8090	-3.957	-0.517	No			row_70	TCONS_00015039	Upf3	8264	-5.397	-0.564	No
row_71	TCONS_00015039	Upf3	8138	-4.104	-0.520	No			row_71	TCONS_00032474	gw	8307	-5.623	-0.566	No
row_72	TCONS_00019739	eIF5B	8174	-4.269	-0.522	No			row_72	TCONS_00004590	mxt	8408	-6.272	-0.574	No
row_73	TCONS_00015017	eIF6	8276	-4.825	-0.530	No			row_73	TCONS_00027827	Rga	8423	-6.354	-0.573	No
row_74	TCONS_00037989	CG1578	8338	-5.164	-0.534	No			row_74	TCONS_00021170	Pop2	8467	-6.626	-0.575	No
row_75	TCONS_00004590	mxt	8494	-6.087	-0.548	No			row_75	TCONS_00015017	eIF6	8470	-6.687	-0.573	No
row_76	TCONS_00014019	CG5726	8543	-6.450	-0.550	Yes			row_76	TCONS_00021963	Rbp6	8520	-7.128	-0.575	No
row_77	TCONS_00030277	Pi3K92E	8554	-6.504	-0.548	Yes			row_77	TCONS_00014019	CG5726	8524	-7.159	-0.572	No
row_78	TCONS_00032474	gw	8557	-6.507	-0.545	Yes			row_78	TCONS_00009992	tn	8588	-7.761	-0.576	No
row_79	TCONS_00025007	Patr-1	8563	-6.617	-0.542	Yes			row_79	TCONS_00030277	Pi3K92E	8615	-8.077	-0.575	No
row_80	TCONS_00021963	Rbp6	8578	-6.755	-0.541	Yes			row_80	TCONS_00007593	bin3	8662	-8.533	-0.577	No
row_81	TCONS_00021170	Pop2	8595	-6.900	-0.539	Yes			row_81	TCONS_00008040	PAN2	8684	-8.745	-0.575	No
row_82	TCONS_00007593	bin3	8710	-7.996	-0.547	Yes			row_82	TCONS_00014996	egl	8747	-9.464	-0.578	Yes
row_83	TCONS_00014996	egl	8730	-8.232	-0.545	Yes			row_83	TCONS_00019739	eIF5B	8752	-9.495	-0.575	Yes
row_84	TCONS_00036944	spoon	8749	-8.526	-0.543	Yes			row_84	TCONS_00025007	Patr-1	8767	-9.745	-0.572	Yes
row_85	TCONS_00008040	PAN2	8838	-9.660	-0.548	Yes			row_85	TCONS_00030911	twin	8838	-10.721	-0.575	Yes
row_86	TCONS_00030911	twin	8875	-10.144	-0.547	Yes			row_86	TCONS_00021817	roq	8859	-11.065	-0.573	Yes
row_87	TCONS_00025837	how	8923	-10.917	-0.547	Yes			row_87	TCONS_00007907	Pabp2	8904	-11.708	-0.572	Yes
row_88	TCONS_00007907	Pabp2	8928	-11.027	-0.542	Yes			row_88	TCONS_00036944	spoon	8953	-12.712	-0.572	Yes
row_89	TCONS_00020600	Unr	8930	-11.056	-0.537	Yes			row_89	TCONS_00015037	Dcp1	8955	-12.767	-0.567	Yes
row_90	TCONS_00015037	Dcp1	8970	-11.634	-0.535	Yes			row_90	TCONS_00020600	Unr	8968	-12.935	-0.563	Yes
row_91	TCONS_00018782	CG7414	8992	-12.015	-0.532	Yes			row_91	TCONS_00013996	stau	9047	-14.566	-0.565	Yes
row_92	TCONS_00013801	CG8963	9025	-12.591	-0.529	Yes			row_92	TCONS_00025837	how	9058	-14.937	-0.560	Yes
row_93	TCONS_00008840	NAT1	9065	-13.422	-0.527	Yes			row_93	TCONS_00036258	elav	9079	-15.435	-0.556	Yes
row_94	TCONS_00015183	CG4612	9071	-13.503	-0.521	Yes			row_94	TCONS_00035850	Rcd-1	9107	-16.074	-0.552	Yes
row_95	TCONS_00036258	elav	9085	-13.804	-0.516	Yes			row_95	TCONS_00028926	glo	9129	-16.554	-0.548	Yes
row_96	TCONS_00013996	stau	9087	-13.851	-0.509	Yes			row_96	TCONS_00005879	Ge-1	9134	-16.609	-0.542	Yes
row_97	TCONS_00005879	Ge-1	9105	-14.223	-0.504	Yes			row_97	TCONS_00021662	Dcp2	9139	-16.779	-0.535	Yes
row_98	TCONS_00021662	Dcp2	9108	-14.306	-0.497	Yes			row_98	TCONS_00013801	CG8963	9144	-16.951	-0.529	Yes
row_99	TCONS_00028926	glo	9168	-16.036	-0.496	Yes			row_99	TCONS_00000643	Thor	9148	-17.051	-0.522	Yes
row_100	TCONS_00033347	tyf	9220	-18.081	-0.493	Yes			row_100	TCONS_00015183	CG4612	9184	-18.314	-0.518	Yes
row_101	TCONS_00035850	Rcd-1	9245	-19.526	-0.486	Yes			row_101	TCONS_00033347	tyf	9222	-19.746	-0.514	Yes
row_102	TCONS_00010377	Xbp1	9268	-20.867	-0.478	Yes			row_102	TCONS_00018782	CG7414	9255	-21.627	-0.508	Yes
row_103	TCONS_00011300	Not3	9289	-21.964	-0.470	Yes			row_103	TCONS_00011300	Not3	9307	-25.609	-0.503	Yes
row_104	TCONS_00000643	Thor	9321	-23.637	-0.462	Yes			row_104	TCONS_00015962	CG11505	9318	-26.275	-0.494	Yes
row_105	TCONS_00015962	CG11505	9345	-25.179	-0.452	Yes			row_105	TCONS_00015874	CG11486	9367	-31.199	-0.486	Yes
row_106	TCONS_00028405	pum	9364	-27.094	-0.441	Yes			row_106	TCONS_00028405	pum	9369	-31.395	-0.473	Yes
row_107	TCONS_00016552	lark	9370	-27.801	-0.428	Yes			row_107	TCONS_00012280	Not1	9378	-32.471	-0.461	Yes
row_108	TCONS_00015874	CG11486	9373	-28.042	-0.415	Yes			row_108	TCONS_00024719	Atx2	9402	-34.962	-0.449	Yes
row_109	TCONS_00009878	Dp1	9379	-28.876	-0.402	Yes			row_109	TCONS_00026905	Hrb98DE	9410	-36.693	-0.434	Yes
row_110	TCONS_00026905	Hrb98DE	9395	-30.295	-0.389	Yes			row_110	TCONS_00016552	lark	9413	-37.505	-0.419	Yes
row_111	TCONS_00028645	Fmr1	9406	-32.410	-0.375	Yes			row_111	TCONS_00026508	msi	9414	-38.239	-0.403	Yes
row_112	TCONS_00024719	Atx2	9407	-32.681	-0.359	Yes			row_112	TCONS_00028645	Fmr1	9416	-38.684	-0.388	Yes
row_113	TCONS_00012280	Not1	9410	-34.141	-0.343	Yes			row_113	TCONS_00031543	larp	9423	-41.638	-0.371	Yes
row_114	TCONS_00026508	msi	9411	-34.529	-0.326	Yes			row_114	TCONS_00010377	Xbp1	9432	-44.890	-0.354	Yes
row_115	TCONS_00031543	larp	9434	-39.071	-0.310	Yes			row_115	TCONS_00009878	Dp1	9445	-48.251	-0.335	Yes
row_116	TCONS_00003165	brat	9441	-41.831	-0.291	Yes			row_116	TCONS_00003165	brat	9474	-59.582	-0.314	Yes
row_117	TCONS_00025556	Syp	9477	-57.690	-0.267	Yes			row_117	TCONS_00008840	Nat1	9482	-69.609	-0.286	Yes
row_118	TCONS_00029198	sqd	9483	-61.899	-0.238	Yes			row_118	TCONS_00029198	sqd	9487	-73.264	-0.256	Yes
row_119	TCONS_00014983	l(2)efl	9496	-76.654	-0.202	Yes			row_119	TCONS_00025556	Syp	9496	-84.662	-0.222	Yes
row_120	TCONS_00032110	heph	9504	-95.304	-0.157	Yes			row_120	TCONS_00032110	heph	9501	-99.340	-0.182	Yes
row_121	TCONS_00001238	Hrb27C	9517	-134.372	-0.094	Yes			row_121	TCONS_00001238	Hrb27C	9520	-180.743	-0.110	Yes
row_122	TCONS_00009815	pAbp	9527	-202.088	0.002	Yes			row_122	TCONS_00009815	pAbp	9527	-272.233	0.002	Yes
					GO:0006986 Response to unfolded protein										
S-hsruRNAi vs sev-GAL4 > UAS-GFP							sev-GAL4 > hsrω^{EP3027} vs sev-GAL4 > UAS-GFP								
NAME	SYMBOL	TITLE	RANK IN GENE LIST	RANK METRIC SCORE	RUNNING ES	CORE ENRICHMENT		NAME	SYMBOL	TITLE	RANK IN GENE LIST	RANK METRIC SCORE	RUNNING ES	CORE ENRICHMENT	
row_0	TCONS_00019696	CG32276	140	169.591	0.128	No		row_0	TCONS_00019696	CG32276	171	133.369	0.080	No	
row_1	TCONS_00030872	Hsp68	327	39.900	0.142	No		row_1	TCONS_00020560	Bi-1	510	24.860	0.062	No	
row_2	TCONS_00020560	Bi-1	535	19.638	0.137	No		row_2	TCONS_00030872	Hsp68	713	16.887	0.054	No	
row_3	TCONS_00000356	Der-1	686	13.905	0.132	No		row_3	TCONS_00000356	Der-1	910	11.798	0.042	No	
row_4	TCONS_00007487	Atf6	735	12.769	0.138	No		row_4	TCONS_00007487	Atf6	935	11.394	0.048	No	
row_5	TCONS_00006035	CG6766	1806	2.630	0.028	No		row_5	TCONS_00006035	CG6766	1920	3.457	-0.053	No	
row_6	TCONS_00029660	Der-2	2168	1.635	-0.009	No		row_6	TCONS_00013268	Hsc70-5	2504	1.753	-0.113	No	
row_7	TCONS_00024354	Hsc70-2	2433	1.135	-0.035	No		row_7	TCONS_00030588	wfs1	2516	1.730	-0.113	No	
row_8	TCONS_00006219	Hsp60D	3779	0.103	-0.177	No		row_8	TCONS_00024694	CG5038	2558	1.651	-0.116	No	
row_9	TCONS_00000179	Hsp60B	4122	0.034	-0.213	No		row_9	TCONS_00032023	CG2126	2643	1.479	-0.124	No	
row_10	TCONS_00030588	wfs1	4753	-0.003	-0.279	No		row_10	TCONS_00029660	Der-2	2756	1.268	-0.135	No	
row_11	TCONS_00001028	Hsp60C	4878	-0.025	-0.292	No		row_11	TCONS_00024354	Hsc70-2	2892	1.063	-0.148	No	
row_12	TCONS_00027428	sip3	4978	-0.044	-0.302	No		row_12	TCONS_00011391	Trap1	5227	-0.005	-0.394	No	
row_13	TCONS_00017640	Hsc70-1	5454	-0.157	-0.352	No		row_13	TCONS_00000179	Hsp60B	5239	-0.007	-0.395	No	
row_14	TCONS_00024694	CG5038	5617	-0.218	-0.369	No		row_14	TCONS_00001028	Hsp60C	5352	-0.025	-0.407	No	
row_15	TCONS_00013268	Hsc70-5	5964	-0.376	-0.405	No		row_15	TCONS_00006219	Hsp60D	5398	-0.032	-0.411	No	
row_16	TCONS_00005236	Herp	6181	-0.484	-0.427	No		row_16	TCONS_00027428	sip3	5472	-0.044	-0.419	No	
row_17	TCONS_00002371	Edem2	6382	-0.630	-0.448	No		row_17	TCONS_00017640	Hsc70-1	5714	-0.105	-0.444	No	
row_18	TCONS_00011391	Trap1	6510	-0.736	-0.460	No		row_18	TCONS_00030150	Ire1	6605	-0.603	-0.537	No	
row_19	TCONS_00032023	CG2126	6933	-1.138	-0.504	No		row_19	TCONS_00002371	Edem2	7220	-1.487	-0.601	No	
row_20	TCONS_00030150	Ire1	7122	-1.411	-0.522	No		row_20	TCONS_00005236	Herp	7406	-1.907	-0.619	No	
row_21	TCONS_00036492	Edem1	7353	-1.741	-0.545	No		row_21	TCONS_00027779	PEK	7490	-2.121	-0.626	No	
row_22	TCONS_00027779	PEK	7553	-2.260	-0.564	No		row_22	TCONS_00036492	Edem1	7909	-3.542	-0.667	No	
row_23	TCONS_00003918	Spp	7675	-2.571	-0.575	No		row_23	TCONS_00020568	CG7182	8117	-4.521	-0.686	No	
row_24	TCONS_00020568	CG7182	8326	-5.130	-0.639	No		row_24	TCONS_00003918	Spp	8798	-10.158	-0.750	No	
row_25	TCONS_00037984	Hsc70-3	9244	-19.387	-0.719	Yes		row_25	TCONS_00010377	Xbp1	9432	-44.890	-0.783	Yes	
row_26	TCONS_00010377	Xbp1	9268	-20.867	-0.704	Yes		row_26	TCONS_00037984	Hsc70-3	9502	-101.550	-0.716	Yes	
row_27	TCONS_00003542	crc	9510	-102.838	-0.643	Yes		row_27	TCONS_00003542	crc	9507	-110.005	-0.636	Yes	
row_28	TCONS_00024627	Hsc70-4	9540	-768.470	0.000	Yes		row_28	TCONS_00024627	Hsc70-4	9540	-872.570	0.000	Yes	

Table S3

						hnRNP: HRB57A								
	sev Gal4>hsr ω RNAi vs sev Gal4>UAS GFP								*sev Gal4>hsr ω^{EP3037} vs sev Gal4>UAS GFP*					
NAME	PROBE	DESCRIPTION (from dataset)	RANK IN GENE LIST	RANK METRIC SCORE	RUNNING ES	CORE ENRICHMENT		NAME	PROBE	DESCRIPTION (from dataset)	RANK IN GENE LIST	RANK METRIC SCORE	RUNNING ES	CORE ENRICHMENT
row_0	FBgn0027788	Hey	504	2.263	0.045	No		row_0	TCONS_00005693	Pten	1693	0.914	-0.155	No
row_1	FBgn0004132	boca	2631	0.742	-0.089	No		row_1	TCONS_00011848	boca	2114	0.763	-0.171	No
row_2	FBgn0026379	Pten	2787	0.697	-0.075	No		row_2	TCONS_00000846	CG3008	3956	0.212	-0.371	No
row_3	FBgn0031643	CG3008	5371	0.135	-0.266	No		row_3	TCONS_00028475	rump	6302	-0.690	-0.609	Yes
row_4	FBgn0038197	foxo	8389	-0.456	-0.478	No		row_4	TCONS_00015023	TBPH	6446	-0.778	-0.593	Yes
row_5	FBgn0015278	Pi3K68D	8423	-0.464	-0.464	No		row_5	TCONS_00021128	Pi3K68D	6637	-0.882	-0.579	Yes
row_6	FBgn0267790	rump	8798	-0.552	-0.472	No		row_6	TCONS_00015350	Pdk1	6864	-1.023	-0.563	Yes
row_7	FBgn0264491	how	9230	-0.698	-0.479	No		row_7	TCONS_00001617	Glt	7696	-1.688	-0.589	Yes
row_8	FBgn0025790	TBPH	9268	-0.708	-0.455	No		row_8	TCONS_00018440	gig	7878	-1.872	-0.534	Yes
row_9	FBgn0020386	Pdk1	9653	-0.833	-0.454	No		row_9	TCONS_00023801	ps	7960	-1.976	-0.463	Yes
row_10	FBgn0259139	glo	10172	-1.045	-0.455	No		row_10	TCONS_00022030	Pep	7986	-2.007	-0.385	Yes
row_11	FBgn0004401	Pep	11276	-1.547	-0.481	Yes		row_11	TCONS_00033191	N	8246	-2.340	-0.319	Yes
row_12	FBgn0001114	Glt	11779	-1.854	-0.451	Yes		row_12	TCONS_00029205	Hrb87F	8475	-2.666	-0.237	Yes
row_13	FBgn0004647	N	11805	-1.866	-0.384	Yes		row_13	TCONS_00035326	nonA	8643	-3.026	-0.134	Yes
row_14	FBgn0005198	gig	11897	-1.931	-0.320	Yes		row_14	TCONS_00037615	nej	8823	-3.871	0.003	Yes
row_15	FBgn0004237	Hrb87F	11954	-1.976	-0.251	Yes								
row_16	FBgn0261552	ps	12444	-2.409	-0.200	Yes								
row_17	FBgn0004227	nonA	12924	-3.093	-0.122	Yes								
row_18	FBgn0261617	nej	13148	-3.865	0.003	Yes								
						hnRNP: HRB87F								
	sev Gal4>hsr ω RNAi vs sev Gal4>UAS GFP								*sev Gal4>hsr ω^{EP3037} vs sev Gal4>UAS GFP*					
NAME	PROBE	DESCRIPTION (from dataset)	RANK IN GENE LIST	RANK METRIC SCORE	RUNNING ES	CORE ENRICHMENT		NAME	PROBE	DESCRIPTION (from dataset)	RANK IN GENE LIST	RANK METRIC SCORE	RUNNING ES	CORE ENRICHMENT
row_0	FBgn0034483	CG16894	598	2.087	0.051	No		row_0	TCONS_00005319	Su(var)205	1498	0.993	-0.125	No
row_1	FBgn0003607	Su(var)205	2752	0.709	-0.080	No		row_1	TCONS_00014427	CG16894	1934	0.829	-0.137	No
row_2	FBgn0036579	CG5027	4457	0.312	-0.195	No		row_2	TCONS_00017956	CG5027	3148	0.449	-0.254	No
row_3	FBgn0030624	CG9106	5193	0.170	-0.242	No		row_3	TCONS_00027693	CG2604	3227	0.428	-0.244	No
row_4	FBgn0264959	Src42A	7067	-0.139	-0.378	No		row_4	TCONS_00007562	Src42A	5164	-0.182	-0.455	No
row_5	FBgn0037298	CG2604	7482	-0.227	-0.399	No		row_5	TCONS_00031081	lobo	5333	-0.238	-0.463	No
row_6	FBgn0025790	TBPH	9268	-0.708	-0.502	No		row_6	TCONS_00015023	TBPH	6446	-0.778	-0.554	Yes
row_7	FBgn0259139	glo	10172	-1.045	-0.522	Yes		row_7	TCONS_00011324	mle	6792	-0.977	-0.550	Yes
row_8	FBgn0039229	Saf-B	10247	-1.075	-0.478	Yes		row_8	TCONS_00028926	glo	6946	-1.086	-0.518	Yes
row_9	FBgn0002774	mle	10293	-1.095	-0.431	Yes		row_9	TCONS_00026361	Saf-B	7283	-1.341	-0.496	Yes
row_10	FBgn0263396	sqd	10707	-1.283	-0.403	Yes		row_10	TCONS_00029198	sqd	7597	-1.594	-0.460	Yes
row_11	FBgn0001215	Hrb98DE	10713	-1.286	-0.344	Yes		row_11	TCONS_00026905	Hrb98DE	7652	-1.647	-0.392	Yes
row_12	FBgn0004838	Hrb27C	10818	-1.336	-0.290	Yes		row_12	TCONS_00001238	Hrb27C	7963	-1.979	-0.338	Yes
row_13	FBgn0013756	Mtor	11102	-1.452	-0.245	Yes		row_13	TCONS_00008592	Mtor	8144	-2.187	-0.261	Yes
row_14	FBgn0083946	lobo	11435	-1.649	-0.194	Yes		row_14	TCONS_00024081	pros	8806	-3.707	-0.169	Yes
row_15	FBgn0004595	pros	12975	-3.213	-0.162	Yes		row_15	TCONS_00037615	nej	8823	-3.871	0.003	Yes
row_16	FBgn0261617	nej	13148	-3.865	0.003	Yes								
						hnRNP: HRP38								
	sev Gal4>hsr ω RNAi vs sev Gal4>UAS GFP								*sev Gal4>hsr ω^{EP3037} vs sev Gal4>UAS GFP*					
NAME	PROBE	DESCRIPTION (from dataset)	RANK IN GENE LIST	RANK METRIC SCORE	RUNNING ES	CORE ENRICHMENT		NAME	PROBE	DESCRIPTION (from dataset)	RANK IN GENE LIST	RANK METRIC SCORE	RUNNING ES	CORE ENRICHMENT
row_0	FBgn0003015	osk	121	3.555	0.090	No		row_0	TCONS_00027479	Parp	1259	1.108	-0.105	No
row_1	FBgn0051431	CG31431	855	1.795	0.085	No		row_1	TCONS_00005319	Su(var)205	1498	0.993	-0.098	No
row_2	FBgn0003607	Su(var)205	2752	0.709	-0.040	No		row_2	TCONS_00015013	shu	2198	0.734	-0.152	No
row_3	FBgn0010348	Arf79F	2768	0.704	-0.021	No		row_3	TCONS_00025801	CG31431	2264	0.714	-0.135	No
row_4	FBgn0010247	Parp	2905	0.665	-0.013	No		row_4	TCONS_00006920	CG17568	2416	0.667	-0.129	No
row_5	FBgn0011207	pelo	3387	0.548	-0.034	No		row_5	TCONS_00001786	pelo	2714	0.575	-0.143	No
row_6	FBgn0032763	CG17568	3792	0.455	-0.052	No		row_6	TCONS_00022835	Arf79F	3021	0.485	-0.161	No
row_7	FBgn0003401	shu	4059	0.399	-0.061	No		row_7	TCONS_00036769	Parg	4136	0.153	-0.282	No
row_8	FBgn0041191	Rheb	4189	0.370	-0.061	No		row_8	TCONS_00013649	mrj	4233	0.122	-0.289	No
row_9	FBgn0030624	CG9106	5193	0.170	-0.132	No		row_9	TCONS_00010825	apt	4477	0.045	-0.315	No
row_10	FBgn0053113	Rtnl1	5462	0.116	-0.149	No		row_10	TCONS_00034910	Nup93-1	4760	-0.045	-0.345	No
row_11	FBgn0034091	mrj	5604	0.090	-0.157	No		row_11	TCONS_00000113	Pi3K21B	4895	-0.092	-0.357	No
row_12	FBgn0283652	Rpp30	5714	0.069	-0.164	No		row_12	TCONS_00036130	S6kII	6126	-0.597	-0.476	Yes
row_13	FBgn0001137	grk	6584	-0.035	-0.229	No		row_13	TCONS_00024502	foxo	6251	-0.662	-0.468	Yes
row_14	FBgn0020622	Pi3K21B	6923	-0.109	-0.251	No		row_14	TCONS_00028475	rump	6302	-0.690	-0.450	Yes
row_15	FBgn0027537	Nup93-1	7216	-0.170	-0.269	No		row_15	TCONS_00015023	TBPH	6446	-0.778	-0.439	Yes
row_16	FBgn0015903	apt	7327	-0.191	-0.272	No		row_16	TCONS_00025837	how	6840	-1.006	-0.449	Yes
row_17	FBgn0023216	Parg	7472	-0.224	-0.277	No		row_17	TCONS_00030452	InR	6903	-1.053	-0.420	Yes
row_18	FBgn0262866	S6kII	7655	-0.269	-0.283	No		row_18	TCONS_00028926	glo	6946	-1.086	-0.388	Yes
row_19	FBgn0283499	InR	7706	-0.279	-0.279	No		row_19	TCONS_00028841	PGRP-LB	7563	-1.555	-0.404	Yes
row_20	FBgn0038197	foxo	8389	-0.456	-0.318	No		row_20	TCONS_00014543	shg	7595	-1.592	-0.353	Yes
row_21	FBgn0003023	otu	8599	-0.508	-0.320	No		row_21	TCONS_00029198	sqd	7597	-1.594	-0.299	Yes
row_22	FBgn0267790	rump	8798	-0.552	-0.319	No		row_22	TCONS_00018440	gig	7878	-1.872	-0.266	Yes
row_23	FBgn0025790	TBPH	9268	-0.708	-0.335	No		row_23	TCONS_00001238	Hrb27C	7963	-1.979	-0.208	Yes
row_24	FBgn0002962	Nos	9402	-0.751	-0.324	No		row_24	TCONS_00028405	pum	8430	-2.604	-0.171	Yes
row_25	FBgn0265297	pAbp	9896	-0.929	-0.336	Yes		row_25	TCONS_00029205	Hrb87F	8475	-2.666	-0.085	Yes
row_26	FBgn0283472	S6k	9984	-0.968	-0.315	Yes		row_26	TCONS_00024081	pros	8806	-3.707	0.005	Yes
row_27	FBgn0037906	PGRP-LB	10201	-1.055	-0.302	Yes								
row_28	FBgn0003391	shg	10224	-1.064	-0.274	Yes								
row_29	FBgn0263396	sqd	10707	-1.283	-0.275	Yes								
row_30	FBgn0015799	Rbf	10769	-1.313	-0.243	Yes								
row_31	FBgn0004838	Hrb27C	10818	-1.336	-0.209	Yes								
row_32	FBgn0000810	fs(1)K10	10888	-1.370	-0.176	Yes								
row_33	FBgn0286070	cnk	10928	-1.394	-0.140	Yes								
row_34	FBgn0005198	gig	11897	-1.931	-0.160	Yes								
row_35	FBgn0031006	rictor	11907	-1.940	-0.106	Yes								
row_36	FBgn0004237	Hrb87F	11954	-1.976	-0.054	Yes								
row_37	FBgn0003165	pum	12107	-2.097	-0.007	Yes								
row_38	FBgn0004595	pros	12975	-3.213	0.017	Yes								
						hnRNP: HRBP59								
	sev Gal4>hsr ω RNAi vs sev Gal4>UAS GFP								*sev Gal4>EP3037 vs sev Gal4>UAS GFP*					
NAME	PROBE	DESCRIPTION (from dataset)	RANK IN GENE LIST	RANK METRIC SCORE	RUNNING ES	CORE ENRICHMENT		NAME	PROBE	DESCRIPTION (from dataset)	RANK IN GENE LIST	RANK METRIC SCORE	RUNNING ES	CORE ENRICHMENT

row_0	FBgn0039380	CG5890	1612	1.137	-0.070	No		row_0	TCONS_00026061	RpS3	861	1.349	-0.061	No
row_1	FBgn0000229	bsk	2580	0.758	-0.108	No		row_1	TCONS_00005863	aub	1005	1.248	-0.043	No
row_2	FBgn0000146	aub	4468	0.310	-0.237	No		row_2	TCONS_00005689	bsk	1652	0.931	-0.091	No
row_3	FBgn0038252	BigH1	4831	0.243	-0.254	No		row_3	TCONS_00014964	Rrp4	2204	0.732	-0.133	No
row_4	FBgn0038877	CG3308	4838	0.240	-0.243	No		row_4	TCONS_00013915	RpL18A	2880	0.526	-0.195	No
row_5	FBgn0034879	Rrp4	5412	0.126	-0.281	No		row_5	TCONS_00030359	CG3308	2892	0.522	-0.182	No
row_6	FBgn0010235	Klc	5460	0.117	-0.279	No		row_6	TCONS_00023045	lost	3592	0.316	-0.253	No
row_7	FBgn0031631	CG3225	5781	0.056	-0.301	No		row_7	TCONS_00024573	BigH1	4221	0.125	-0.321	No
row_8	FBgn0029729	CG12682	6233	0.000	-0.335	No		row_8	TCONS_00021286	Klc	4245	0.119	-0.320	No
row_9	FBgn0030620	CG5662	6283	0.000	-0.338	No		row_9	TCONS_00027005	CG11876	4252	0.117	-0.318	No
row_10	FBgn0033539	Git	6473	-0.010	-0.352	No		row_10	TCONS_00004577	CG3225	4328	0.090	-0.324	No
row_11	FBgn0039635	CG11876	7277	-0.182	-0.405	No		row_11	TCONS_00000113	Pi3K21B	4895	-0.092	-0.386	No
row_12	FBgn0262866	S6kII	7655	-0.269	-0.421	No		row_12	TCONS_00029314	su(Hw)	5062	-0.143	-0.400	No
row_13	FBgn0037084	Syx6	7801	-0.305	-0.418	No		row_13	TCONS_00012542	Git	5271	-0.214	-0.418	No
row_14	FBgn0025790	TBPH	9268	-0.708	-0.497	Yes		row_14	TCONS_00008506	Syx6	5376	-0.256	-0.423	No
row_15	FBgn0020386	Pdk1	9653	-0.833	-0.487	Yes		row_15	TCONS_00010388	tud	5443	-0.284	-0.423	No
row_16	FBgn0003567	su(Hw)	9680	-0.840	-0.451	Yes		row_16	TCONS_00020626	Prm	6079	-0.566	-0.479	Yes
row_17	FBgn0039749	CG11498	9983	-0.968	-0.429	Yes		row_17	TCONS_00036130	S6kII	6126	-0.597	-0.468	Yes
row_18	FBgn0000283	Cp190	10041	-0.992	-0.387	Yes		row_18	TCONS_00024502	foxo	6251	-0.662	-0.464	Yes
row_19	FBgn0001215	Hrb98DE	10713	-1.286	-0.379	Yes		row_19	TCONS_00028475	rump	6302	-0.690	-0.451	Yes
row_20	FBgn0286070	cnk	10928	-1.394	-0.331	Yes		row_20	TCONS_00015023	TBPH	6446	-0.778	-0.446	Yes
row_21	FBgn0031052	CG14215	11584	-1.747	-0.300	Yes		row_21	TCONS_00013525	Zasp52	6498	-0.801	-0.430	Yes
row_22	FBgn0265991	Zasp52	11951	-1.974	-0.236	Yes		row_22	TCONS_00015350	Pdk1	6864	-1.023	-0.443	Yes
row_23	FBgn0263934	esn	12209	-2.173	-0.155	Yes		row_23	TCONS_00028926	glo	6946	-1.086	-0.423	Yes
row_24	FBgn0050122	CG30122	12238	-2.202	-0.056	Yes		row_24	TCONS_00029472	Cp190	7468	-1.477	-0.442	Yes
row_25	FBgn0026317	Tsc1	12751	-2.771	0.034	Yes		row_25	TCONS_00030277	Pi3K92E	7568	-1.563	-0.410	Yes
								row_26	TCONS_00026905	Hrb98DE	7652	-1.647	-0.375	Yes
								row_27	TCONS_00013864	cnk	7750	-1.745	-0.338	Yes
								row_28	TCONS_00018440	gig	7878	-1.872	-0.301	Yes
								row_29	TCONS_00026174	Tsc1	8207	-2.282	-0.276	Yes
								row_30	TCONS_00039316	rictor	8238	-2.323	-0.216	Yes
								row_31	TCONS_00014076	CG30122	8367	-2.504	-0.162	Yes
								row_32	TCONS_00035856	CG14215	8398	-2.549	-0.096	Yes
								row_33	TCONS_00027191	sima	8431	-2.605	-0.028	Yes
								row_34	TCONS_00007712	esn	8516	-2.748	0.038	Yes
						hnRNP:SQUID								
	sev Gal4>hsr ω RNAi vs sev Gal4>UAS GFP								***sev Gal4>EP3037 vs sev Gal4>UAS GFP***					
NAME	**PROBE**	**DESCRIPTION (from dataset)**	**RANK IN GENE LIST**	**RANK METRIC SCORE**	**RUNNING ES**	**CORE ENRICHMENT**		**NAME**	**PROBE**	**DESCRIPTION (from dataset)**	**RANK IN GENE LIST**	**RANK METRIC SCORE**	**RUNNING ES**	**CORE ENRICHMENT**
row_0	FBgn0003015	osk	121	3.555	0.070	No		row_0	TCONS_00027479	Parp	1259	1.108	-0.115	No
row_1	FBgn0039038	CG6688	360	2.634	0.110	No		row_1	TCONS_00023178	Rheb	2923	0.514	-0.291	No
row_2	FBgn0002622	RpS3	2129	0.915	-0.004	No		row_2	TCONS_00003862	Rpp30	3117	0.457	-0.301	No
row_3	FBgn0010247	Parp	2905	0.665	-0.048	No		row_3	TCONS_00028747	Art1	3395	0.378	-0.323	No
row_4	FBgn0263594	lost	3116	0.609	-0.051	No		row_4	TCONS_00005417	grk	4680	-0.020	-0.468	No
row_5	FBgn0010409	RpL18A	3889	0.434	-0.100	No		row_5	TCONS_00025888	CG7069	4697	-0.025	-0.469	No
row_6	FBgn0037834	Art1	5009	0.207	-0.180	No		row_6	TCONS_00004651	Rtnl1	4727	-0.033	-0.472	No
row_7	FBgn0020622	Pi3K21B	6923	-0.109	-0.323	No		row_7	TCONS_00000113	Pi3K21B	4895	-0.092	-0.488	No
row_8	FBgn0037770	Art4	6961	-0.116	-0.324	No		row_8	TCONS_00034134	Dsor1	5660	-0.372	-0.566	No
row_9	FBgn0038952	CG7069	7154	-0.156	-0.335	No		row_9	TCONS_00024837	Akt1	5682	-0.382	-0.558	No
row_10	FBgn0010379	Akt1	7488	-0.229	-0.355	No		row_10	TCONS_00028602	Art4	5858	-0.471	-0.566	No
row_11	FBgn0262866	S6kII	7655	-0.269	-0.362	No		row_11	TCONS_00036130	S6kII	6126	-0.597	-0.582	No
row_12	FBgn0010269	Dsor1	7914	-0.331	-0.374	No		row_12	TCONS_00024502	foxo	6251	-0.662	-0.579	No
row_13	FBgn0038197	foxo	8389	-0.456	-0.400	No		row_13	TCONS_00015023	TBPH	6446	-0.778	-0.581	No
row_14	FBgn0039213	atl	8683	-0.527	-0.410	No		row_14	TCONS_00026277	atl	6547	-0.827	-0.572	No
row_15	FBgn0267790	rump	8798	-0.552	-0.407	No		row_15	TCONS_00015350	Pdk1	6864	-1.023	-0.582	Yes
row_16	FBgn0003731	Egfr	9171	-0.674	-0.420	Yes		row_16	TCONS_00020146	S6k	7051	-1.161	-0.574	Yes
row_17	FBgn0025790	TBPH	9268	-0.708	-0.412	Yes		row_17	TCONS_00010475	Egfr	7137	-1.223	-0.553	Yes
row_18	FBgn0002962	Nos	9402	-0.751	-0.405	Yes		row_18	TCONS_00022068	MED19	7221	-1.287	-0.530	Yes
row_19	FBgn0036761	MED19	9419	-0.757	-0.390	Yes		row_19	TCONS_00009815	pAbp	7281	-1.337	-0.503	Yes
row_20	FBgn0020386	Pdk1	9653	-0.833	-0.389	Yes		row_20	TCONS_00025556	Syp	7477	-1.485	-0.487	Yes
row_21	FBgn0038826	Syp	9888	-0.924	-0.386	Yes		row_21	TCONS_00000643	Thor	7521	-1.518	-0.454	Yes
row_22	FBgn0259139	glo	10172	-1.045	-0.385	Yes		row_22	TCONS_00036302	Rbf	7588	-1.586	-0.421	Yes
row_23	FBgn0000166	bcd	10217	-1.060	-0.364	Yes		row_23	TCONS_00026905	Hrb98DE	7652	-1.647	-0.387	Yes
row_24	FBgn0004390	RasGAP1	10499	-1.184	-0.360	Yes		row_24	TCONS_00020872	RasGAP1	7653	-1.647	-0.345	Yes
row_25	FBgn0015279	Pi3K92E	10509	-1.187	-0.334	Yes		row_25	TCONS_00013864	cnk	7750	-1.745	-0.312	Yes
row_26	FBgn0000826	png	10538	-1.196	-0.310	Yes		row_26	TCONS_00018440	gig	7878	-1.872	-0.279	Yes
row_27	FBgn0001215	Hrb98DE	10713	-1.286	-0.294	Yes		row_27	TCONS_00033067	fs(1)K10	7884	-1.880	-0.233	Yes
row_28	FBgn0004838	Hrb27C	10818	-1.336	-0.273	Yes		row_28	TCONS_00001238	Hrb27C	7963	-1.979	-0.192	Yes
row_29	FBgn0002781	4)-E,pre-mc	10939	-1.397	-0.251	Yes		row_29	TCONS_00022030	Pep	7986	-2.007	-0.143	Yes
row_30	FBgn0004401	Pep	11276	-1.547	-0.242	Yes		row_30	TCONS_00020600	Unr	8197	-2.273	-0.110	Yes
row_31	FBgn0263352	Unr	11737	-1.823	-0.237	Yes		row_31	TCONS_00026174	Tsc1	8207	-2.282	-0.053	Yes
row_32	FBgn0005198	gig	11897	-1.931	-0.206	Yes		row_32	TCONS_00039316	rictor	8238	-2.323	0.002	Yes
row_33	FBgn0031006	rictor	11907	-1.940	-0.164	Yes		row_33	TCONS_00029205	Hrb87F	8475	-2.666	0.042	Yes
row_34	FBgn0004237	Hrb87F	11954	-1.976	-0.123	Yes								
row_35	FBgn0003149	Prm	12348	-2.310	-0.102	Yes								
row_36	FBgn0266411	sima	12384	-2.334	-0.053	Yes								
row_37	FBgn0261560	Thor	12426	-2.384	-0.003	Yes								
row_38	FBgn0026317	Tsc1	12751	-2.771	0.034	Yes								